National Park Service
U.S. Department of the Interior

Natural Resource Stewardship and Science

Landscape Phenology, Vegetation Condition, and Relations with Climate at Canyonlands National Park, 2000–2019

Natural Resource Report NPS/NCPN/NRR—2023/2535



ON THE COVER

The “blue marble” image is the most detailed true-color image of Earth to date. Much of the information contained in this image came from a single remote-sensing device: NASA’s Moderate Resolution Imaging Spectroradiometer, or MODIS. Flying more than 700 kilometers above Earth onboard the Terra satellite, MODIS provides an integrated tool for observing a variety of terrestrial, oceanic, and atmospheric features of the Earth. Credit: NASA Goddard Space Flight Center.

Landscape Phenology, Vegetation Condition, and Relations with Climate at Canyonlands National Park, 2000–2019

Natural Resource Report NPS/NCPN/NRR—2023/2535

Prepared by
David Thoma
Northern Colorado Plateau Network
National Park Service
P.O. Box 848
Moab, UT 84532

Editing and Design
Alice Wondrak Biel
Northern Colorado Plateau Network
National Park Service
P.O. Box 848
Moab, UT 84532

June 2023

U.S. Department of the Interior
National Park Service
Natural Resource Stewardship and Science
Fort Collins, Colorado

The National Park Service, Natural Resource Stewardship and Science office in Fort Collins, Colorado, publishes a range of reports that address natural resource topics. These reports are of interest and applicability to a broad audience in the National Park Service and others in natural resource management, including scientists, conservation and environmental constituencies, and the public.

The Natural Resource Report Series is used to disseminate comprehensive information and analysis about natural resources and related topics concerning lands managed by the National Park Service. The series supports the advancement of science, informed decision-making, and the achievement of the National Park Service mission. The series also provides a forum for presenting more lengthy results that may not be accepted by publications with page limitations.

All manuscripts in the series receive the appropriate level of peer review to ensure the information is scientifically credible and technically accurate.

Views, statements, findings, conclusions, recommendations, and data in this report do not necessarily reflect views and policies of the National Park Service, U.S. Department of the Interior. Mention of trade names or commercial products does not constitute endorsement or recommendation for use by the U.S. Government.

This report is available from the Northern Colorado Plateau Network website, as well as at the Natural Resource Publications Management website. If you have difficulty accessing information in this publication, particularly if using assistive technology, please email irma@nps.gov.

Please cite this publication as:

Thoma, D. 2023. Landscape phenology, vegetation condition, and relations with climate at Canyonlands National Park, 2000–2019. Natural Resource Report NPS/NCPN/NRR—2023/2535. National Park Service, Fort Collins, Colorado. https://doi.org/10.36967/2299619.

NPS 164/189628, June 2023

Contents

Figures v
Tables vii
Acronyms and Abbreviations xi
Executive Summary xiii
Acknowledgements xv

1 Introduction 1
1.1 The importance of primary production 1
1.2 Satellite monitoring of primary production 1
1.3 Vegetation condition and vulnerability 2
1.4 Pivot points and responses 2
1.5 Phenology 3

2 Methods 5
2.1 Overview 5
2.2 Remote-sensing targets 5
2.3 Satellite imagery 6
2.4 Soil Adjusted Vegetation Index 9
2.5 Pixel timeseries extraction and smoothing 9
2.6 Water-balance model 9
2.7 Measures of vegetation production 11
2.8 Calculating the measures 11
2.9 Climate correlates with annual production 13
2.10 Conceptual basis of climate pivot points and responses 14
2.11 Phenology metrics and climate drivers 16

3 Results and Discussion 19
3.1 Completeness of satellite observations 19
3.2 Timeseries 19
3.3 Trends in indicators of annual production 19
3.4 Trends in indicators of growing-season production 22
3.5 Climate relations 23
3.6 Pivot points 29
3.7 Vegetation response 33
3.8 Multi-variable indicators of annual vegetation production 39
3.9 Land-surface phenology trends at Canyonlands National Park 39
3.10 Drivers of green-up 44
3.11 Climate patterns 48

4 How to Use this Report in Climate Smart Conservation Planning 51
4.1 Identifying management goals 51
4.2 Vulnerability assessment 51
4.3 Using pivot points and responses in climate-adaptation planning 52
4.4 Example vulnerability assessment 52
4.5 Identify and implement management actions 54
4.6 Tools to inform near-term management 54

5 Conclusions 55

6 Literature Cited 57

Appendix A. Supplemental Figures for Landscape Phenology, Vegetation Condition, and Relations with Climate at Canyonlands National Park, 2000–2019 ..63

Figures

Main Report

Figure 2-1. NCPN alliance groups analyzed for trends in production, phenology, and climate relations at Canyonlands National Park 8

Figure 2-2. Measures of annual production from a timeseries of 16-day soil adjusted vegetation index (SAVI) derived from MODIS imagery 12

Figure 2-3. Conceptual diagram of soil-moisture pivot point and response of a single vegetation-alliance map unit to variation in annual average soil moisture 13

Figure 2-4. Integrated area under the growing-season curve (shaded area) for one polygon over two calendar years 16

Figure 3-1. Soil-adjusted vegetation index timeseries by alliance group for 2,168 polygons analyzed for 2000–2019 20

Figure 3-2. Trends in mean growing-season iSAVI by alliance group, determined via simple linear regression 22

Figure 3-3. Spatial pattern of trends in mean annual iSAVI 24

Figure 3-4. Covariation in growing-season production, estimated as the iSAVI between March and October and water-year cumulative precipitation averaged within alliance groups, demonstrating the link between climate and vegetation production in the park at the annual scale 25

Figure 3-5. Three components of the Riparian alliance group in Figure 3-4 show differential impacts of tamarisk beetle 26

Figure 3-6. Significant (p-value <0.05) relationships between water-year climate variables and first difference of growing season iSAVI, 2000–2019 28

Figure 3-7. The mean precipitation pivot-point values shown here represent critical water needs for the different alliance groups 30

Figure 3-8. Precipitation pivot points for polygons with a significant relationship (p-value <0.05) between water-year annual precipitation and change in annual vegetation production, assessed as the interannual difference in iSAVI 31

Figure 3-9. A patch of dying junipers with the Abajo Mountains in the background, Cedar Mesa, Utah, 2019 32

Figure 3-10. Significant (p <0.05) water-related pivot points by alliance group 33

Figure 3-11. Sensitivity of growing-season vegetation production to annual water-year precipitation 34

Figure 3-12. Responses of different vegetation alliance groups to precipitation 35

Figure 3-13. Maps of percentage sand and clay content in top meter of soil, and depth to restrictive layer in alliance groups 37

Figure 3-14. Graphical depiction of the relationship between pivot points and responses in polygons that showed a significant relationship (p-value <0.05) between iSAVI and water-year precipitation (e.g., critical water need vs. rate of growing-season iSAVI change per mm precipitation) 38

Figure 3-15. Vegetation response to summed water-flux variables (regression slopes from iSAVI versus annual climate-variable sum) 40

Figure 3-16. Top models in multi-model comparison of climate correlates with interannual differences in growing-season iSAVI across all alliance groups 41

Figure 3-17. Top models of growing-season production by alliance group in multi-model comparisons of climate correlates with interannual differences in growing-season iSAVI 42

Figure 3-18. Top models in multi-model comparisons of climate correlates with start-of-season at the whole-park scale 44

Figure 3-19. Top models in multi-model comparisons of climate correlates with start-of-season at the alliance-group scale 45
Figure 3-20. Variable importance in the random-forest model of climate drivers of SOS 45
Figure 3-21. Predicted SOS date versus observed SOS date in the holdout dataset used for validation of the random-forests model for all polygons in Canyonlands NP 46
Figure 3-22. Predicted SOS date versus observed SOS date in the holdout dataset used for validation of the random-forests model for alliance groups 47
Figure 3-23. Long-term temporal patterns in precipitation in vegetation alliance groups 49
Figure 3-24. Annual precipitation trend over time, 2000–2019 50
Figure 4-1. The Climate Smart Conservation framework 51
Figure 4-2. Quantitative vulnerability analysis for a single Pinyon-Juniper polygon 53

Appendix A

Figure A-1. Spatial pattern of trends in maximum annual iSAVI 63
Figure A-2a. Pivot points for polygons where climate variables were significantly related to interannual variation in production (p-value < 0.05) 64
Figure A-2b. Pivot points for polygons where climate variables were significantly related to interannual variation in production (p-value < 0.05) 65
Figure A-2c. Pivot points for polygons where climate variables were significantly related to interannual variation in production (p-value < 0.05) 66
Figure A-2d. Pivot points for polygons where climate variables were significantly related to interannual variation in production (p-value < 0.05) 67
Figure A-2e. Pivot points for polygons where climate variables were significantly related to interannual variation in production (p-value < 0.05) 68
Figure A-2f. Pivot points for polygons where climate variables were significantly related to interannual variation in production (p-value < 0.05) 69
Figure A-2g. Pivot points for polygons where climate variables were significantly related to interannual variation in production (p-value < 0.05) 70
Figure A-2h. Pivot points for polygons where climate variables were significantly related to interannual variation in production (p-value < 0.05) 71
Figure A-2i. Pivot points for polygons where climate variables were significantly related to interannual variation in production (p-value < 0.05) 72
Figure A-2j. Pivot points for polygons where climate variables were significantly related to interannual variation in production (p-value < 0.05) 73
Figure A-2k. Pivot points for polygons where climate variables were significantly related to interannual variation in production (p-value < 0.05) 74
Figure A-2l. Pivot points for polygons where climate variables were significantly related to interannual variation in production (p-value < 0.05) 75
Figure A-3a. Sensitivity of growing season vegetation production to climate variables, where the relationship was significant (p-value < 0.05) 76
Figure A-3b. Sensitivity of growing season vegetation production to climate variables, where the relationship was significant (p-value < 0.05) 77
Figure A-3c. Sensitivity of growing season vegetation production to climate variables, where the relationship was significant (p-value < 0.05) 78
Figure A-3d. Sensitivity of growing season vegetation production to climate variables, where the relationship was significant (p-value < 0.05) 79
Figure A-3e. Sensitivity of growing season vegetation production to soil moisture where the relationship was significant (p-value < 0.05) 80
Figure A-3f. Sensitivity of growing season vegetation production to soil moisture where the relationship was significant (p-value < 0.05) 81

Figure A-3g. Sensitivity of growing season vegetation production to soil moisture where the relationship was significant (p-value < 0.05) 82
Figure A-3h. Sensitivity of growing season vegetation production to soil moisture where the relationship was significant (p-value < 0.05) 83
Figure A-3i. Sensitivity of growing season vegetation production to soil moisture where the relationship was significant (p-value < 0.05) 84
Figure A-3j. Sensitivity of growing season vegetation production to soil moisture where the relationship was significant (p-value < 0.05) 85
Figure A-3k. Sensitivity of growing season vegetation production to soil moisture where the relationship was significant (p-value < 0.05) 86
Figure A-3l. Sensitivity of growing season vegetation production to soil moisture where the relationship was significant (p-value < 0.05) 87
Figure A-4. Variation in a) precipitation pivot points and b) responses to precipitation as related to soil and site characteristics 88
Figure A-5. (a) Direction and magnitude of change rate in land surface phenology metrics determined as +/-days per year for start of season (Slope SOS), end of season (Slope EOS), length of season (Slope LOS) and timing of peak SAVI (Slope POP). (b) rates of change in phenology metrics by alliance group 89
Figure A-6a. Cumulative annual water balance variables over time in vegetation alliance groups 90
Figure A-6b. Cumulative annual water balance variables over time in vegetation alliance groups 91
Figure A-6c. Cumulative annual water balance variables over time in vegetation alliance groups 92
Figure A-6d. Cumulative annual water balance variables over time in vegetation alliance groups 93
Figure A-6e. Cumulative annual water balance variables over time in vegetation alliance groups 94

Tables

Table 2-1. NCPN alliance groups and corresponding National Vegetation Classification alliances, Canyonlands National Park.....7

Table 2-2. Climate and water-balance variables used to identify correlations with vegetation production and phenology. 11

Table 2-3. A priori models of climate influence on vegetation production competed via generalized linear mixed-effects modeling to identify best correlates with production. 14

Table 2-4. A priori models of climate influence on timing of green-up (start of the growing season). 18

Table 3-1. Amount of park area with increasing (pos) or decreasing (neg) trends in mean annual or maximum annual SAVI by alliance group. 21

Table 3-2. Changes in land-surface phenology in days averaged by alliance group during the 20-year study. 43

Acronyms and Abbreviations

Acronyms and abbreviations used in this report.

Acronym	Meaning
AET	actual evapotranspiration
D	climatic water deficit
EOS	end of season
GDD	growing degree days
LOS	length of season
Meltd	date of complete snowmelt
P	annual precipitation
PACK	snowpack water equivalent
PET	potential evapotranspiration
POP	period of peak
RAIN	rain
SNOW	snow
SOIL	soil moisture
SOS	start of season/green-up
SRAD	solar radiation
T	temperature (annual average)
Tmax	temperature (maximum)
Tmin	temperature (minimum)
VP	vapor pressure
VPD	vapor-pressure deficit
W	water as rain plus snowmelt

Executive Summary

Quantitatively linking satellite observations of vegetation condition and climate data over time provides insight to climate influences on primary production, phenology (timing of growth), and sensitivity of vegetation to weather and longer-term patterns of weather referred to as climate. This in turn provides a basis for understanding potential climate impacts to vegetation—and the potential to anticipate cascading ecological effects—such as impacts to forage, habitat, fire potential, and erosion—as climate changes in the future.

This report provides baseline information about vegetation production and condition over time at Canyonlands National Park (NP), as derived from satellite remote sensing. Its objective is to demonstrate methods of analysis, share findings, and document historic climate exposure and sensitivity of vegetation to weather and climate as a driver of vegetation change.

This report represents a quantitative foundation of vegetation–climate relationships on an annual timestep. The methods can be modified to finer temporal resolution and other spatial scales if further analyses are needed to inform park planning and management. The knowledge provided in this report can inform vulnerability assessments for Climate Smart Conservation planning by park managers. Patterns of pivot points and responses can serve as a guide to anticipate what, where, when, and why vegetation change may occur.

For this analysis, vegetation alliance groups were derived from vegetation-map polygons (Von Loh et al. 2007) by lumping vegetation types expected to respond similarly to climate. Relationships between vegetation production and phenology were evaluated for each alliance map unit larger than a satellite pixel (~300 × 300 m). We used a water-balance model to characterize the climate experienced by plants. Water balance translates temperature and precipitation into more biophysically relevant climate metrics, such as soil moisture and drought stress, that are often more strongly correlated with vegetation condition than temperature or precipitation are. By accounting for the interactions between temperature, precipitation, and site characteristics, water balance helps make regional climate assessments relevant to local scales.

The results provide a foundation for interpreting weather and climate as a driver of changes in primary production over a 20-year period at the polygon and alliance-group scale. Additionally, they demonstrate how vegetation type and site characteristics, such as soil properties, slope, and aspect, interact with climate at local scales to determine trends in vegetation condition. This report quantitatively defines critical water needs of vegetation and identifies which alliance types, in which locations, may be most susceptible to climate-change impacts in the future. Finally, this report explains how findings can be used in the Climate Smart Conservation framework, with scenario planning, to help manage park resources through transitions imposed by climate change.

Key findings:

- The patterns of pivot points and responses can serve as a guide to anticipate what, where, when, and why vegetation change may occur.
- Multiple indicators suggest annual trends in vegetation production increased in 58% and decreased in 2% of the area analyzed in and near Canyonlands NP between 2000 and 2019. *(see Table 3-1)*
- The largest area of increase occurred in the Pinyon-Juniper and Sparsely Vegetated alliance groups, representing 44 and 7.6% of the study area, respectively. *(see Table 3-1)*
- Small areas that decreased in annual production included Blackbrush, Dry Shrubland, Juniper, Dry Wash, Pinyon-Juniper, and Sparsely Vegetated alliance groups, representing only 1.5% of the study area. *(see Table 3-1)*

- Growing-season production increased in the Blackbrush, Douglas-fir, Dry Wash, Geology, Juniper, Pinyon-Juniper, Ponderosa Pine, Dry Shrubland, Mixed Montane Shrubland, and Sparsely Vegetated alliance groups. No downward growing-season trends were observed. *(see Figure 3-2)*
- Annual growing-season production was most strongly correlated with annual precipitation and soil moisture, suggesting that increases in annual precipitation may have caused some of the increase in production over the study period. *(see Figure 3-6)*
- The Douglas-fir, Mixed Montane Shrubland, and Disturbed alliance groups required the most precipitation to maintain production, whereas Water, Alkaline Wet and Ponderosa Pine required the least precipitation to maintain production. *(see Figure 3-7)*
- The Wet Shrubland, C3/C4 Grassland, and Annual Exotic Grassland alliance groups were most sensitive to water deficit and drought. *(see Figure 3-12)*
- Two to three years of soil moisture was the best indicator of annual production at the park scale. This was also generally true at the alliance-group scale. *(see Figures 3-16, 3-17)*
- By the end of the study period, the growing season was starting 12.6 days earlier on average across all alliance groups and ending 11.2 days later. The length of growing season was 23.8 days longer on average. *(see Table S-7 of Thoma 2023a)*
- Growing degree days and precipitation were the most important determinants of start of growing season. *(see Figure 3-18)*

This report provides a foundation for interpreting weather and climate as a driver of changes in primary production over a 20-year period at the polygon, alliance-group and park scales at Canyonlands National Park. It can be used to determine what, when, where and why future climate change may impact vegetation. This is achieved by incorporating information in this report with Planning for a Changing Climate (NPS 2021), which is intended to help park managers strategize and plan to conserve park resources through transitions imposed by climate change (see Section 4.4).

Acknowledgements

Thoughtful reviews from Matt Van Scoyoc (Southeast Utah Group) and Dustin Perkins (Northern Colorado Plateau Network) improved this report.

1 Introduction

This report provides baseline information about vegetation production and condition over time as derived from satellite remote sensing at three scales: park, vegetation-alliance group, and vegetation-alliance polygon. The objective is to demonstrate the methods of analysis, share standardized findings, and document historic climate exposure and sensitivity to weather and climate as a driver of vegetation change at Canyonlands National Park.

This study quantitatively defines critical water needs of vegetation and demonstrates how vegetation type and site characteristics interact with climate at local scales to determine change in vegetation condition. It provides a foundation for interpreting weather and climate as a driver of changes in primary production over a 20-year period at local scales and can be used to quantitatively determine which alliance types, in which locations, may be most susceptible to climate-change impacts in the future, providing a basis for vulnerability assessments in Climate Smart Conservation planning (see Chapter 4).

1.1 The importance of primary production

Photosynthesis is the process in plants that converts sunlight, CO_2, water, and minerals into the chemical forms of energy (carbohydrates, and sugars) essential to life. All terrestrial life depends on photosynthesis, also called "primary production" because it is the foundation of food webs. As the first step in creating food and habitat for wildlife, vegetation production is an important indicator, or "vital sign" of ecosystem health that can be tracked over time to assess conditions that support higher life forms in parks. The complex temporal and spatial patterns of primary production are influenced by many factors, including disturbances, such as wildfire and drought; differences in precipitation across space or over time; vegetation assemblages that differ in response to change; topography and soil properties; land use; and invasive species (Kariyeva and van Leeuwen 2011).

Sunlight provides the energy used to synthesize organic compounds from CO_2 and water. In semi-arid environments like the Colorado Plateau, sunlight and CO_2 are abundant and rarely limit production. But primary production is controlled by different environmental variables in different places. In tropical forests, primary production may be controlled by availability of sunlight (due to cloud cover and dense canopy) or soil nutrients. In deserts, primary production is mostly controlled by water availability. At the highest elevations on the Colorado Plateau, it may be controlled by cold temperatures and a short growing season. Changes in primary production may indicate changes in ecological structure (e.g., change in vegetation assemblage) or ecological function (e.g., loss of vegetation cover, resulting in erosion and loss of soil nutrients).

1.2 Satellite monitoring of primary production

Assessing the rate of photosynthesis and the condition of vegetation at broad landscape scales provides insight to the cycles of energy, nutrients, and water that sustain life in parks. Sunlight reflected from vegetation provides information about photosynthetic rates, leaf area, and biomass accumulation, as well as conditions of habitat and forage for animals. High-frequency satellite remote sensing of vegetation condition provides a broad-scale view of spatial patterns in vegetation condition, production, and change in response to climate, disturbance, and management actions over time.

The Northern Colorado Plateau Network (NCPN) monitors landscape-scale vegetation condition and trends using satellite imagery collected more frequently than ground-based data (which are also collected). The high frequency of observations and complete spatial coverage of satellite images is ideal for assessing seasonal as well as annual conditions and trends. The imagery also provides insight on the response of vegetation to climate patterns and disturbance (e.g., fire and forest disease, often mediated by climate) that cannot be obtained at broad scales in any other cost-effective way.

Quantitatively linking satellite observations of vegetation condition and climate data over time provides insight to climate influences on primary production, phenology (timing of growth), and sensitivity of vegetation to weather and long-term weather patterns referred to as climate. This in turn provides a basis for understanding potential climate impacts to vegetation and the potential to anticipate cascading ecological effects, such as impacts to forage, habitat, fire potential, and erosion, as climate changes in the future.

Primary production assessed via satellite remote sensing does not indicate which species are present, or which species are performing well or poorly. It is also not a "good" or "bad" judgement (i.e., increased or decreased production is not inherently good or bad). Monitoring primary production is analogous to monitoring river flow. Flow monitoring measures the timing and abundance of water that provides habitat for animals and other essential ecological functions. It does not indicate which organisms are present, or how different species are faring.

1.3 Vegetation condition and vulnerability

Vegetation condition and trend are monitored as changes in vegetation production, or the cumulative green biomass of leaves that grow via photosynthesis. Green biomass is strongly correlated with near-infrared and red wavelengths of solar energy reflecting off vegetation measured by satellites (Thoma et al. 2002). The satellite imagery reveals repeating seasonal fluctuations in growth and senescence, as well as annual trends or abrupt changes due to disturbances. Although disturbances can be detected, it is beyond the scope of this analysis to do so, because it requires different methods than those used here. However, all the data used to detect disturbance can be made available by the author.

Climate is a strong driver of vegetation distributions (Stephenson 1998). Variation in weather strongly affects vegetation condition through stress (e.g., drought) and disturbance (e.g., wildfire). Linking changes in vegetation production to climate provides important information about resistance to disturbance (resilient or susceptible) and recovery from disturbance (fast or slow).

Vegetation that is susceptible to disturbance and slow to recover is considered the most vulnerable to change (Kariyeva and van Leeuwen 2011). This kind of information can be used to assess vulnerability of vegetation assemblages to climate change.

1.4 Pivot points and responses

In semi-arid environments, vegetation persists when there is a positive balance between growth and resistance to drought (Noy-Meir 1973). Vegetation traits, such as rooting depth, xylem diameter, and stomatal density and resistance, interact with climate and site conditions to determine how vegetation responds to climate. Understanding these interactions provides insight to potential changes in vegetation condition and composition as the climate changes. When coupled with climate data, two important ecological characteristics, pivot points and responses, can be derived from measuring change in vegetation condition over time (Munson 2013).

A pivot point is the value of a climate variable at which annual vegetation production teeters between above- or below-average condition. For water variables, pivot points determine whether vegetation production increases or decreases given the water available for growth. A pivot point is analogous to the recommended eight glasses of water per day for adults: Except in extreme cases, more water is generally not bad—but less can have detrimental effects, even when unmet needs are slight. Semi-arid plants generally respond more positively than humans to water that exceeds minimum needs. But as with people, receiving less than the minimum can cause deterioration in condition. As such, the pivot point can be considered a critical water need as well as an indicator of drought tolerance. A species' basic water needs, and the rate of change when those needs are unmet or exceeded, are important ecological variables that determine how plants respond to weather and climate.

Plant traits determine how much water vegetation needs to maintain production. How much water is available depends on climate, weather, soil, and site properties. These interactions can cause variation in the magnitude of pivot points for the same climate variable across vegetation types. Some types may be more tolerant of drought conditions than others.

Vegetation response is the sensitivity of vegetation to a climate variable or, more specifically, the amount of change in vegetation production per unit change in a climate variable. This rate of change is a quantitative measure of vegetation sensitivity to climate. Cumulative annual vegetation production and phenology are indicators of vegetation response to a suite of environmental conditions. Some conditions, such as slope, aspect, and soil properties, are spatially variable but stable over time. Others, such as climate, vary both temporally and spatially. The vegetation growing at any location reflects adaptations suited to the environment where it persists. If conditions change, either abruptly or gradually, plants respond. The change can be spatial, due to differences in soil type or elevation. It can also be temporal, as weather and climate change over time.

Differences in vegetation response rates, or sensitivity, to water availability reflect survival strategies for persisting through drought or responding rapidly when water is available, making species more competitive if water needs are met. The survival strategies are a consequence of vegetation traits, including rooting depth, stomatal density, leaf area, and perennial versus annual growth forms that confer competitive advantage under different climate conditions. Generally, plant traits that favor one strategy preclude the others (Noy-Meir 1973; Thoma et al. 2019).

Individual plant responses to environmental conditions cumulatively scale up, resulting in spatial and temporal landscape patterns that can be detected in satellite imagery (Thoma et al. 2019). Because vegetation production and phenological responses are interrelated, it is useful to measure and report the two simultaneously. It is not always possible to know what caused a change noted in satellite imagery, but communication with park staff and ground-based monitoring can help interpret findings in this report.

1.5 Phenology

The annual cycle of vegetation growth and senescence, and reoccurring biological phenomena, such as seasonal migrations, are collectively known as phenology. Commonly known measures of vegetation phenology include timing of bud burst, first leaf, and spring bloom, all observed from the ground (de Beurs and Henebry 2010). The high-frequency observations from satellites make it possible to track vegetation phenology (Dunn and de Beurs 2011) at broad spatial scales that include an assemblage of different vegetation species, referred to as "land-surface phenology." Land-surface phenology is an indicator of ecosystem health because it regulates dependent ecological functions, such as pollination and onset of forage production (Dunn and de Beurs 2011). On the Colorado Plateau, springtime vegetation growth is preceded by warming temperatures and snowmelt. In drier regions, onset of springtime growth may be limited if there was insufficient accumulation of fall and winter soil moisture (Workie and Debella 2018).

Changes in land-surface phenology can provide an early indication of cascading climate-change impacts that may result in changing species assemblages and shifting range boundaries (Workie and Debella 2018). These may affect pollinators, as well as bird and mammal migrations. Determining the drivers of phenology, and changes in phenology over time, provides insights to cascading effects on pollinators and migrating animals that depend on growth initiation, forage production, and the length of growing season.

2 Methods

2.1 Overview

At a vegetation-mapping scoping meeting in February 2003, network and park staff delineated a project area consisting of the park plus a strip approximately 1.6 kilometers (1 mile) wide around its boundary. Although the Orange Cliffs section of Glen Canyon National Recreation Area was included in the project boundary for plot collection, only a one-half-mile-wide strip adjacent to the Canyonlands NP boundary was mapped and included in the final project boundary.

Wider environs were chosen along the park's southern boundary (the Beef Basin, Cross Canyon, and Butler Wash areas), because there is a research area within and surrounding this part of the park. The project boundary included the watershed boundary of this research area. Plot collection occurred throughout these wider southern environs, but mapping only occurred in the one-mile-wide strip adjacent to the park boundary. The total project mapping area was 170,618 hectares (421,605 acres). Of this area, 135,204 hectares (334,096 acres) were within the Canyonlands NP boundary and 35,414 hectares (87,509 acres) were in the environs. The environs were delineated to provide data to support management coordination on adjacent private, state, and BLM-managed lands.

This report was compiled by comparing climate data with variation in land-surface greenness over time, as measured in satellite imagery of the park's vegetation-mapping project area (Von Loh et al. 2007). A large archive of (460) remotely sensed satellite images was downloaded and processed in the statistical analysis software "R." A large amount of gridded climate data for the same area was downloaded and processed in Excel to estimate water-balance variables, such as soil moisture, evapotranspiration, and water deficit from temperature and precipitation (see Section 2.6). The imagery and water-balance/climate data were merged in R separately for each vegetation-alliance polygon (see Section 2.2) and analyzed statistically for spatial patterns across park landscapes and over time for trends.

2.2 Remote-sensing targets

Three scales of analysis are presented in this report: vegetation-alliance polygon, vegetation-alliance group, and parkwide. Vegetation-alliance polygons were derived from vegetation-map polygons by lumping together vegetation types expected to respond similarly to ecological disturbances, such as climate change (Von Loh et al. 2007; Jennings et al. 2009). The polygon scale features finer spatial resolution—but with higher resolution comes more complexity in interpretation. The group scale lumps similar alliances together for broader-scale interpretations, but is not always as accurate as the polygon scale, because lumping even slightly dissimilar objects introduces variation. The park-scale analysis is achieved by lumping all alliance polygons into a single analysis or by averaging analysis results across alliances to the park scale.

It is important to note that satellite-based proxies for primary production reflect production from all vegetation within a sampling unit, regardless of the alliance name (which identifies the dominant or diagnostic vegetation types). For example, a forested alliance type may include shrub or graminoid understory that influences the satellite signal. Untangling the proportional influence of the named alliance components from background components is beyond the scope of this report.

2.2.1 Alliance polygons

The National Vegetation Classification Standard (NVCS) identifies eight hierarchical levels of classification, ranging from Formation Class (Level 1, the broadest scale) to Association (Level 8, the finest scale). The finest scale used in this report was the vegetation Alliance (Level 7). The NVCS defines a vegetation alliance as "A characteristic range of species composition, habitat conditions, physiognomy, and diagnostic species, typically at least one of which is found in the uppermost or dominant stratum of the vegetation layer, and reflecting regional to subregional climate, substrates, hydrology, moisture/nutrient factors and disturbance regimes" (FGDC 2008).

Vegetation alliances are useful targets for tracking production and phenology because they are spatially repeating, relatively homogenous in type composition, and share similar affinities and responses to environmental conditions, such as climate. They are also mapped consistently across park units, making them an ideal classification level for cross-park analysis. Polygon boundaries for the alliances were obtained from park vegetation maps (Von Loh et al. 2007).

Analysis at the alliance, rather than association level, resulted in larger and fewer polygon targets that contained a larger number of satellite pixels. This helped ensure that satellite-image pixels fell mostly within target polygons and improved the signal-to-noise ratio necessary for tracking change in response to climate. Improving the signal-to-noise ratio in remote sensing of sparsely vegetated environments is achieved by spatially averaging pixels within relatively homogenous areas (Thoma et al. 2017). For this reason, the analysis in this report relies primarily on aggregated pixel means across the spatial extent of each target polygon, rather than per-pixel analysis. More detail on pixel screening to exclude low-quality observations and outliers can be found in Sections 2.3 and 2.5, below.

2.2.2 NCPN alliance groups

For purposes of this study, alliances that respond similarly to climate based on structure and life-history traits were further grouped by NCPN ecologist Dana Witwicki (personal comm.) to simplify interpretations and reporting.[1] We created our own grouping system to simplify the alliance naming conventions and reduce the large number of alliances, which were too numerous for meaningful reporting.

Beginning with 98 different National Vegetation Classification (NVC) alliances mapped consistently across NCPN park units, we created 32 alliance groups based on floristics, canopy structure, and local environmental conditions. Of those, 18 occurred in Canyonlands NP (Table 2-1, Figure 2-1). The alliance-group names are shortened representations of the dominant alliance(s) in each group. Hereafter, we refer to the grouped alliance categories as "NCPN alliance groups" or "alliance groups," but it should be noted that these groups are similar to, but different than, Level 6 of the NVC. A key that links each NCPN alliance group to vegetation-mapping units familiar to NCPN managers can be found in Table S-1 of Thoma (2023a). The image-analysis targets were the ungrouped alliance polygons, so while results reported in the body of this report are for NCPN alliance groups, results are also available by polygon for ungrouped alliances in the supplemental tables (Thoma 2023a).

2.3 Satellite imagery

Since early 2000, the moderate resolution imaging sensor (MODIS) on the Terra satellite, operated by NASA, has collected daily imagery of Earth at a spatial resolution of 250 meters (820 ft). Because cloud cover, cloud shadows, aerosols, smoke, and water vapor can interfere with clear views of Earth's surfaces, daily images are composited into a single image for 16-day time windows (product MOD13Q1). The 16-day composite images are created from values obtained from the clearest view during the 16-day window. They are generally the best-quality observations for every pixel during the 16-day window.

Even so, during extended periods of poor atmospheric viewing conditions, some pixel values are unreliable. For this reason, each pixel in the composite image is tagged with a quality rating that can be used to screen out unreliable values influenced by poor viewing conditions. Sophisticated algorithms are used to assess the quality of every pixel value based on measurements of atmospheric conditions made by the satellite during image acquisition (Didan et al. 2015).

There are 23 fixed, 16-day window periods in a year (with a few overlapping days at year's end to account for leap years). Thus, there were 457 viewing opportunities and 23 observations per year for every pixel in the NCPN during the period of record covered

1 Although there is an NVC Group level (6), the "NCPN alliance groups" discussed in this report were developed independently from the NVC for purposes of this study.

Table 2-1. NCPN alliance groups and corresponding National Vegetation Classification alliances, Canyonlands National Park.

NCPN alliance group	National Vegetation Classification alliance(s)[1]
Alkaline Wet	Mojave Seablite - Red Swampfire - Alkali Goldenbush Alkaline Wet Scrub Alliance
Blackbrush	Blackbrush Colorado Plateau Shrubland Alliance
Disturbed	[Chained and Seeded Pinyon-Juniper Woodland] Sagebrush Shrubland
	Non-natural
Douglas-fir	Douglas-fir Southern Rocky Mountain Forest & Woodland Alliance
Dry Wash	Fourwing Saltbush - Rubber Rabbitbrush Desert Wash Alliance
	Skunkbush Sumac - River Hawthorn - Stretchberry Shrubland Alliance
Geology	Geology
Annual Exotic Grassland	Cheatgrass - Medusa-head Ruderal Annual Grassland Alliance
C3/C4 Grassland	Indian Ricegrass - Bluebunch Wheatgrass - Sandhill Muhly Grassland Alliance
	Mormon-tea Colorado Plateau Shrubland Alliance
	Winterfat Steppe & Dwarf-shrubland Alliance
Juniper	Utah Juniper / Shrub Understory Woodland Alliance
	Utah Juniper / Herbaceous Understory Open Woodland Alliance
Pinyon-Juniper	Two-needle Pinyon - Utah Juniper / Shrub Understory Foothill & Lower Montane Dry-Mesic Woodland Alliance
	Two-needle Pinyon - Utah Juniper / Shrub Understory Colorado Plateau Woodland & Scrub Alliance
Ponderosa Pine	Ponderosa Pine - Littleleaf Mountain-mahogany Bedrock Cliff & Canyon Wooded Scrub Alliance
Riparian	Fremont Cottonwood Great Basin Riparian Forest Alliance
	Narrowleaf Willow - Dewystem Willow Shrubland Alliance
	Tamarisk species Ruderal Riparian Scrub Alliance
Dry Sagebrush	Sand Sagebrush Colorado Plateau Shrubland Alliance
	Wyoming Big Sagebrush Dry Steppe & Shrubland Alliance
	Basin Big Sagebrush - Foothill Big Sagebrush Dry Steppe & Shrubland Alliance
Dry Shrubland	Frosted Mint Shrubland Alliance
	Fourwing Saltbush Scrub Alliance
	Mormon-tea - Yellow Rabbitbrush - Skunkbush Sumac Talus Sparse Scrub Alliance
	Torrey's Joint-fir Shrubland Alliance
Mixed Montane Shrubland	Gambel Oak - Mountain Snowberry Shrubland Alliance
Wet Shrubland	Greasewood Intermountain Wet Shrubland Alliance
Sparsely Vegetated	Singleleaf Ash - Skunkbush Sumac - Cliff Fendlerbush Talus & Rock Outcrop Shrubland Alliance
	Joint-fir species - Saline Wildrye - Crispleaf Buckwheat Badlands Cold Desert Sparse Vegetation Alliance
Water	Water

[1]The alliance names shown in this table do not match those found in Von Loh and others (2007) because alliance names and codes in that report were subsequently updated to USNVC Version 2.01, released March 30, 2017. The names from 2007 were cross-walked to the current names displayed here. For information on nomenclature, see FGDC (2008).

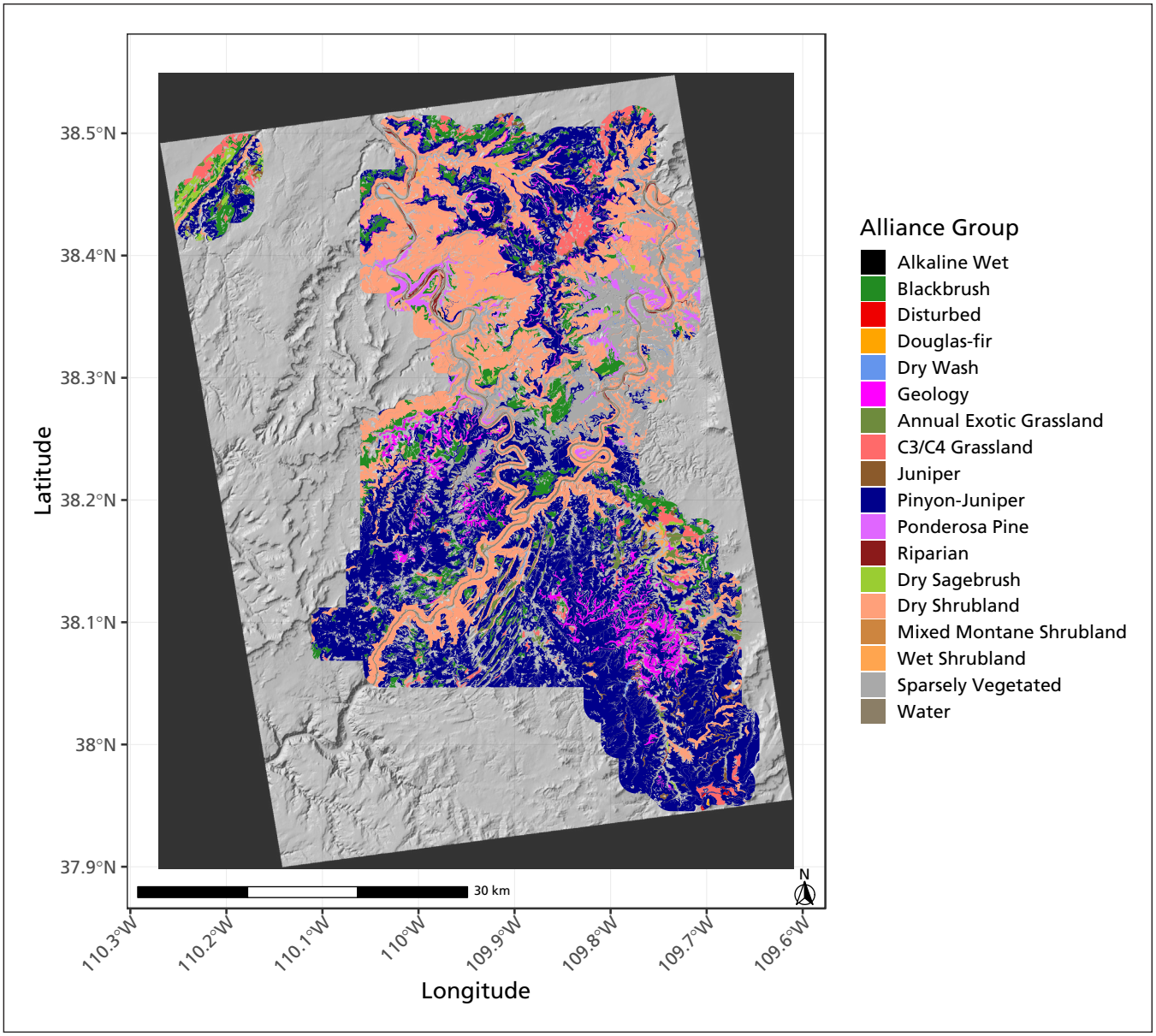

Figure 2-1. NCPN alliance groups analyzed for trends in production, phenology, and climate relations at Canyonlands National Park. Areas not colored within the study boundary are alliance polygons smaller than the minimum target area of 8.3 hectares.

in this report. Observation completeness was calculated on an annual and seasonal basis (March–November) for the 20-year study period as the percentage of pixels in each polygon that were observed under high-quality viewing conditions. In semi-arid environments, there are typically many high-quality observations during the growing season, but fewer in winter due to clouds and snow cover.

2.4 Soil Adjusted Vegetation Index

The Soil Adjusted Vegetation Index (SAVI) is a measure of primary production (Bunting et al. 2019; Qi et al. 1994) obtained from reflectance in red and near-infrared wavelengths, adjusted for soil backgrounds in semi-arid environments (Huete 1988). It is calculated as

$$SAVI = \frac{(1 + L)(NIR - Red)}{(NIR + Red + L)}$$

where L is the soil background adjustment factor (L=0.5), NIR is reflectance in the near infrared wavelengths, and Red is reflectance in red wavelengths.

These wavelengths were selected specifically because they are sensitive to the abundance of green vegetation and optimized for detecting spatial and temporal changes in vegetation. We use SAVI in this report, rather than the normalized difference vegetation index (NDVI), because of the thin vegetation cover and soil background reflectance in most NCPN parks. This combination of factors results in unfavorable signal-to noise ratios that can make remote sensing of spatial and temporal change difficult in semi-arid environments. However, in addition to working with a vegetation index specifically designed to reduce the background noise caused by soil variability (SAVI), there are many steps in the processing workflow that help further alleviate these issues.

2.5 Pixel timeseries extraction and smoothing

Despite precautions taken by the imagery providers to minimize noise and provide an analysis-ready product from the MODIS sensor, there were lingering issues that required attention prior to analysis (Thoma et al. 2017). Each polygon larger than 8.3 hectares (the area of a MODIS pixel at NCPN latitude) was analyzed independently for trends in production and phenology and its relationship with multiple climate variables. Pixels extracted from target polygons above the 90th percentile or below the 10th percentile of average greenness were removed from analysis. This step served several purposes. First, it removed pixels that fell on alliance-group boundaries if the reflectance was very different across the boundary, such as riparian ribbons adjacent to dry uplands. Second, it eliminated areas that may have been classified incorrectly in the vegetation maps if the result of misclassification included an area of substantially different reflectance. It also eliminated inclusions of contrasting reflectance (if any occurred).

After outliers were removed, each pixel was weighted according to its proportional area that fell within the target (see Section 2.2). This step further minimized the effect of any remaining pixels that overlapped target boundaries. After computing an area-averaged value at each timestep for the pixels within a polygon target, missing polygon-average values were interpolated.

Missing daily values were a consequence of the 16-day periodicity of observations and quality screening in earlier steps. Finally, a smoothing filter was used to remove high-frequency noise from the timeseries of each polygon. After smoothing across large gaps in winter, prominent dips in timeseries (artificially low values that were an artifact of the smoothing) were truncated to a minimum winter value based on pixel values that were likely reflectance from bare soil or senesced vegetation (Wang et al. 2018). This process resulted in a smoothed and complete daily timeseries for each polygon.

2.6 Water-balance model

Vegetation responds to seasonal and inter-annual variations in temperature and water availability, depending on adaptations and site conditions (Munson et al. 2015; Thoma et al. 2019). To understand climate drivers of vegetation condition and potential impacts

across large environmental gradients (hot/dry to cold/wet), we used a water-balance model to determine how different aspects of climate and site characteristics affected vegetation production and phenology. The water-balance model quantitatively accounts for temperature, precipitation, and their interactions with local site conditions (such as soil water-holding capacity, slope, and aspect) that affect soil moisture, evapotranspiration, and drought stress (Thoma et al. 2020). To calculate the water-balance variables in the model, we used 1-kilometer, gridded, Daymet temperature and precipitation data (Thornton et al. 2018).

The model partitions precipitation (P, mm) into rain (RAIN, mm) or snow (SNOW, mm of water), which accumulates until warming temperature (T, °C) causes it to melt. Soil moisture (SOIL, mm) is stored in the top meter of soil, which was treated in the model as a single layer with a maximum storage defined by its water-holding capacity. Water-holding capacity was obtained from soil surveys where data were available (NRCS 2015) but was fixed at 100 millimeters otherwise. This fixed value accommodated analyses where soil surveys have not yet been conducted and accounted for some water storage in geologic structures (cracks or porous, rocky material) that may be mapped as having no water-holding capacity, but support sparse vegetation detected by the satellite sensor. Water input that exceeds the storage capacity becomes runoff.

Potential evapotranspiration (PET, mm), calculated via the Oudin method, is the amount of water that could be evapotranspired from a short grass with available energy if water was unlimited. The Oudin method calculates PET using daily mean temperature, daylength, and solar radiation (Oudin et al. 2005). Actual evapotranspiration (AET, mm) is the loss of water from soil via evapotranspiration, limited by soil-water availability. Climatic water deficit (D, mm) is the unmet water need of vegetation, and is a measure of drought stress calculated as the difference between PET and AET (Stephenson 1998).

Water-availability variables include P, RAIN, SNOW, and SOIL. Variables that estimate water use include AET and PET; however, AET is limited by dry soil. Two aspects of heat that influence vegetation growth are average annual temperature (T) and growing-degree days (GDD) (McMaster and Wilhem 1997).

This study also evaluated two variables that could influence vegetation production and phenology: vapor-pressure deficit (VPD, Pa) and solar radiation (SRAD, W m^{-2}), available from Daymet. Vapor-pressure deficit is the difference between the amount of water vapor air can hold and the amount of vapor in the air. Solar radiation is the energy plants receive from the sun that can be used for photosynthesis (Grossiord et al. 2020; Seager et al. 2015; Stephenson 1990).

In the following sections, state variables, representing condition at a point in time (e.g., SOIL, T, VPD), are averaged (Table 2-2). Variables representing fluxes of water (water passing through the environment) are summed annually or seasonally—except for SOIL, which is presented as an average value because soil water-holding capacity has an upper limit that summation could exceed, which is physically impossible.

The effects of summing or averaging have important implications for interpreting results. Whereas additional precipitation can substantially change the cumulative magnitude of annual precipitation, it takes a large amount of water input to change an annual average soil-moisture value even a small amount. For example, 10 millimeters of additional precipitation falling on dry soil on one day in one year would increase annual precipitation by 10 millimeters, but increase average annual soil moisture by just 0.027 millimeters (10/365). Temperature and pressure variables are also summarized as means in this analysis. Units of measure are millimeters for water terms, degrees Celsius for temperature, and pascals for pressure.

Snowmelt date (Meltd) used in the phenology analysis was determined from the variable, PACK, the daily snow water equivalent (mm) stored in the snowpack that accumulated over winter. In spring, PACK declines rapidly with warming temperatures. Determining the day of complete melt is somewhat subjective, due to flashy spring

Table 2-2. Climate and water-balance variables used to identify correlations with vegetation production and phenology.

Variable	Abbreviation	Units	Type	Temporal summary
Precipitation	P	mm	flux	sum
Rain	RAIN	mm	flux	sum
Snow	SNOW	mm	flux	sum
Snowpack Water Equivalent	PACK	mm	flux	sum
Water as Rain plus Snowmelt	W	mm	flux	sum
Date of Complete Snowmelt	Meltd	day-of-year	state	day
Actual Evapotranspiration	AET	mm	flux	sum
Potential Evapotranspiration	PET	mm	flux	sum
Climatic Water Deficit	D	mm	flux	sum
Solar Radiation	SRAD	$W\ m^{-2}$	state	mean
Temperature (Annual Average)	T	°C	state	mean
Temperature (Maximum)	Tmax	°C	state	maximum
Temperature (Minimum)	Tmin	°C	state	minimum
Soil Moisture	SOIL	mm	state	mean
Vapor Pressure	VP	Pa	state	mean
Vapor-pressure Deficit	VPD	Pa	state	mean
Growing Degree Days	GDD	°C	state	sum

snow events that may linger for one to a few days, even in late spring after the initiation of vegetation growth. The algorithm used to identify day of melt begins by searching backward from May 1 (user-specified date) for PACK values greater than four millimeters (user-specified depth) for a span of three days (also user-specified). In the water-balance model, the combination of depth and span are the minimum degree days necessary to yield the user-specified depth of snowmelt water. Visual inspection of snowmelt date plotted on timeseries of daily PACK values confirmed this was a reasonable approach to differentiating between periods that were predominantly snow-covered or snow-free.

2.7 Measures of vegetation production

Because net primary production is generated through photosynthesis, and spectral indices are responsive to abundance of photosynthetically active vegetation, vegetation indices are good proxies for primary production (Paruelo et al. 2000). Characteristics of the annual repeating cycle of SAVI curves were used as proxies for production and phenology (Figure 2-2). We determined trends in three variables derived from the SAVI timeseries for each polygon: mean annual SAVI, maximum annual SAVI (maximum value regardless of month in which it occurred), and iSAVI (or sum of daily interpolated SAVI), the area under the curve during the growing season (February through October). Daily interpolation was made via linear regression with a maximum gap size of 16 days. Mean annual SAVI (sum of 16-day observations/23 periods per year) is a measure of average productivity across the calendar year. Maximum annual SAVI is an indication of peak instantaneous rate of vegetation production, or rate of maximum biomass accumulation. It is strongly correlated with both green cover and leaf-area index. Sum of SAVI (iSAVI) is a proxy for vegetation production during the growing season. It is most strongly correlated with biomass production and cumulative productivity (Garroutte et al. 2016; Johnson et al. 2018; Thoma et al. 2002).

2.8 Calculating the measures

Trends in production were assessed by tracking changes in maximum and mean

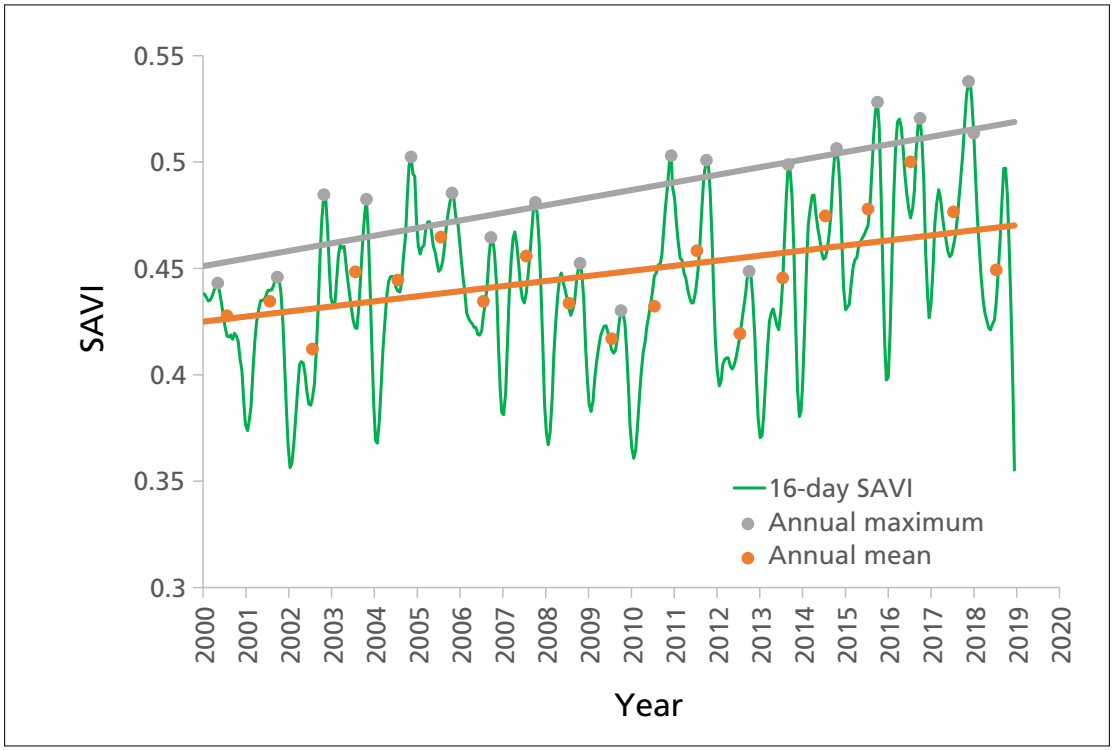

Figure 2-2. Measures of annual production from a timeseries of 16-day soil adjusted vegetation index (SAVI) derived from MODIS imagery. Linear trends against time for annual maximum and annual mean values are shown as straight lines.

annual SAVI for 2000–2019 using the annual aggregated timeseries (AAT) method and Mann-Kendall trend test (Forkel et al. 2013) (see Figure 2-2). The rate of change (regression slope) was estimated via linear regression. Significance of change was estimated by the Mann-Kendall trend test (Forkel et al. 2013). Trends in annual maximum values were more reliable than changes in mean annual values due to use of the full annual curves that include screened and gap-filled winter values. Trends in growing-season greenness were considered in the annual pivot-points analyses below.

Representing the sum of daily interpolated SAVI values during the growing season, iSAVI is an holistic measure of the cumulative production of actively photosynthesizing vegetation (Mendez-Barroso et al. 2009; Reed et al. 1994). This proxy for aboveground net primary production results from the intentional construction of spectral indices, such as SAVI, that are strongly responsive to absorbed, photosynthetically active radiation used by plant canopies to capture and store carbon and energy during growth.

Trends in iSAVI timeseries were noted in some polygons, which confounds relationships with climate unless the trend in iSAVI is removed before analysis. For this reason, we used the first difference in iSAVI, which represents the change in growing-season production from one year to the next, as an indicator of response to weather on an annual basis. This helps guard against overfitting when a trend exists in a timeseries. The annual change in iSAVI was calculated as

$$\Delta iSAVI = \frac{iSAVIt_2 - iSAVIt_1}{t_2 - t_1}$$

where $iSAVIt_1$ is sum of growing-season SAVI for year t_1, and $iSAVIt_2$ is sum of growing-season SAVI for year t_2. Positive values indicate increasing growth from one year to the next. Negative values indicate decreasing growth. This framing of the response variable makes increase or decrease in growth contingent on conditions in the previous year, allowing change to be linked to variation in weather from one year to the next. This is essentially equivalent ($r^2 \sim 0.99$) to the specific-growth concept used in plot-based

studies of vegetation response to climate over long periods of time (Munson 2013).

2.9 Climate correlates with annual production

Two types of analysis were used to explore climate relations with annual production (iSAVI).

2.9.1 Single-variable analysis

First, simple linear-regression models compared a single climate variable to the annual increase or decrease in production relative to the prior year. The adjusted r^2 measured the strength of relationships between the climate variable and vegetation production in a range between 0 and 1, with stronger relationships closer to one. This revealed the proportion of variation in ∆iSAVI explained by variation in climate.

Simple linear regression was used to determine pivot points (see Section 1.4) and production responses (Figure 2-3; see Section 1.4). Every polygon was tested against every climate and water-balance variable. After screening out relationships that were not significant (p-value >0.05), the adjusted r^2 terms were averaged across polygons from the same alliance group to see if any one climate variable outperformed the others as a predictor of vegetation production.

2.9.2 Multiple-variable analysis

Second, multiple-regression models compared multiple climate variables simultaneously with production. These included lagged climate effects characterizing climate condition 1–2 years prior to an observation. This modeling framework helps account for legacy effects, or conditions in prior years that set limits on production in a current year (Sala et al. 2012). By accounting for legacy effects, the longer-term cumulative effects of drought or good growing conditions in prior years can be considered.

Additionally, this approach can help determine if climate variables interact in important ways to influence production. Whereas the linear-regression framework used to determine pivot points only considers the influence of a single variable, such as AET, on production, multiple regression can determine interactions of AET and D, or other interactions and lags that include effects from prior years.

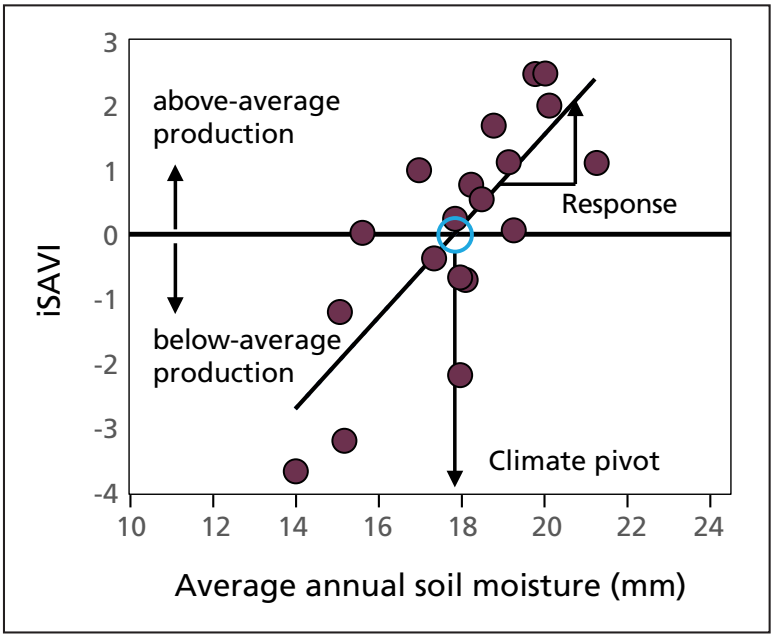

Figure 2-3. Conceptual diagram of soil-moisture pivot point and response of a single vegetation-alliance map unit to variation in annual average soil moisture. Vegetation production transitions from below- to above-average condition at the soil-moisture pivot point (blue circle). The response is the rate of change in iSAVI per millimeter of change in average soil moisture. Pivot-point figures like this can be constructed for other climate variables.

To account for multiple interacting factors that collectively influence vegetation production on an annual basis, we established a suite of a priori candidate models (Table 2-3) based on expected vegetation responses to climate variables and lags from our earlier experience working in semi-arid landscapes. In those studies (Thoma et al. 2019; Witwicki et al. 2016), we found water-balance variables to be better predictors of vegetation response than temperature and precipitation. In addition, lag effects were apparent as much as two years prior to a given satellite observation.

We then competed the models against each other using multiple regression models and identified competitive models based on delta AICc values <4 to determine the combination of climate variables acting over one or more years that have the most influence on growing-season production. Models that did not compete well (AICc >4) were excluded.

Table 2-3. A priori models of climate influence on vegetation production competed via generalized linear mixed-effects modeling to identify best correlates with production.

Model[1]	Climate variables[2]											
	AET	AET (lag1)	AET (lag2)	D	D (lag1)	D (lag2)	SOIL	SOIL (lag1)	SOIL (lag2)	P	P (lag1)	P (lag2)
AET1	X	–	–	–	–	–	–	–	–	–	–	–
AET12	X	X	–	–	–	–	–	–	–	–	–	–
AET123	X	X	X	–	–	–	–	–	–	–	–	–
AET123_D1	X	X	X	X	–	–	–	–	–	–	–	–
AET123_D12	X	X	X	X	X	–	–	–	–	–	–	–
AET123_D123	X	X	X	X	X	X	–	–	–	–	–	–
SOIL1	–	–	–	–	–	–	X	–	–	–	–	–
SOIL12	–	–	–	–	–	–	X	X	–	–	–	–
SOIL123	–	–	–	–	–	–	X	X	X	–	–	–
AET1_D1	X	–	–	X	–	–	–	–	–	–	–	–
AET12_D12	X	X	–	X	X	–	–	–	–	–	–	–
D1_SOIL1	–	–	–	X	–	–	X	–	–	–	–	–
D1_SOIL2	–	–	–	X	–	–	–	X	–	–	–	–
D1_SOIL12	–	–	–	X	–	–	X	X	–	–	–	–
P1	–	–	–	–	–	–	–	–	–	X	–	–
P12	–	–	–	–	–	–	–	–	–	X	X	–
P123	–	–	–	–	–	–	–	–	–	X	X	X

[1]See Table 2-2 for acronyms.
[2]X = variable used in model, – = variable not used in model. Lags refer to models that include the water balance term for the preceding one (lag1) or two (lag2) years.

Several models could be competitive in any given polygon because every a priori model was evaluated for every polygon. We first looked for a global best model of primary production at the park level by aggregating results from all polygons in the park. Then, we tabulated how frequently the top model occurred by NCPN alliance group to determine the best climate correlates and lags or cumulative duration of effect on production at the alliance-group level.

2.10 Conceptual basis of climate pivot points and responses

Using the pivot-point framework, annual change (ΔiSAVI) was regressed (linear regression) with climate data to determine the degree to which annual variation in weather affected production (Munson 2013). In this analysis, a pivot point is the critical magnitude of a climate or water balance variable where vegetation "teeters" between above- or below-average condition. Generally, water pivot points are important in water-limited environments. Temperature pivot points are important at higher elevations, where cold temperature limits growth (Thoma et al. 2020).

Vegetation response, or sensitivity to climate or water balance, is the rate of change in condition per unit change in water or temperature. In this analysis, vegetation response is the slope of the regression line when interannual change in iSAVI is related to the corresponding change in climate or water balance for the same period (see Figure 2-3).

Pivot points and responses are depicted graphically (see Figure 2-3) as the x-axis value where each linear-regression line crosses the horizontal line, indicating no change from one year to the next. Production values plotting above the x-axis indicate that vegetation increased in production

from the previous year. Points below the line indicate that vegetation production decreased from the previous year. If a deficit pivot point was exceeded during the growing season, then vegetation production was likely below average (because vegetation has an inverse or negative relationship with water deficit, a measure of drought stress). If an AET pivot point was exceeded during the growing season, then vegetation production was likely above average (because production is positively related to AET). Thus, the interpretation of exceeding a pivot point depends on the influence the climate variable has on vegetation (negative for water deficit, positive for water-availability variables).

Polygons that cross the horizontal line further to the left, where the x-axis variable is a water-availability metric, are considered more dry-tolerant. That is, their performance is above average at lower water availability than a polygon that crosses the horizontal line further to the right. For example, a vegetation assemblage with a precipitation pivot point of 250 millimeters is more dry-tolerant than a vegetation assemblage with a pivot point of 300 millimeters. The opposite is true if the x-axis is deficit. In that case, polygons that cross the horizontal line further to the left are less dry-tolerant; that is, their production declines to below-average condition when drought stress is relatively low.

The slope of the regression line quantifies the expected change in iSAVI per millimeter of water or degree of temperature. Polygons with steeper regression slopes are more sensitive to a change in water availability. For each unit change in a climate or water-balance variable, a more-sensitive vegetation type will have a larger change in growing-season iSAVI.

Together, pivot points and responses determined from historical observations of vegetation condition and weather are important ecological indicators of critical water amounts (in arid environments) or heat (in alpine environments) needed for growth, and how growth changes per unit change in the climate variable. For this reason, pivot points and responses are indicators of expected change in vegetation production as the climate changes in the future (Munson et al. 2011). When linked with projections of future climate, these two ecological variables can be used in quantitative vulnerability assessments as part of the Climate Smart planning framework (Stein et al. 2014), which helps managers set long-range goals achieved by near-term tactical actions (see Section 3.8).

2.10.1 Operational use of pivot points for "now-casts"

This report provides information for estimating vegetation condition using climate data. By tracking the climate variable with the strongest relationship to production in real time relative to its corresponding pivot point, we can determine if weather conditions are below, near, or above predetermined pivot points, and by what amount. In this way, we can use climate data to provide real-time "now-casts" indicating when weather conditions suggest production is likely to be above or below that of the previous year.

The interpretation of climate conditions against a pivot-point value requires consideration of pivot-point precision determined by the standard error around the regression line where it crosses the horizontal axis. The range is larger in polygons where the relationship between climate and vegetation growth is more variable. At the alliance-group level, pivot-point range is caused by variability in plant assemblages in different polygons of the same alliance, as well as variations in soil and site properties. Additional variation is caused by noise in the MODIS sensor near its sensitivity limits in sparsely vegetated environments, errors in the gridded climate data, and vegetation legacy effects that cause plants to respond differently to the same weather, depending on what happened in the recent past. All these factors contribute to the observed standard error of a pivot point that brackets weather conditions determining if vegetation is likely performing above or below average.[2]

2 Although not shown graphically, the standard error of pivot points is available for every polygon (Table S-2 in Thoma 2023a).

Vegetation performance when weather conditions are within the standard error of the pivot point is best described as "near average." When weather conditions exceed the standard error of the pivot point (above or below the pivot point), there is higher confidence that vegetation production is above or below average.

2.10.2 Lapse-rate adjustment of station data for operational use with pivot points

Operationally, vegetation condition can be reported in real time using weather-station data to calculate daily water balance (see ClimateAnalyzer.org). These data can be compared to a pivot point. The relationships between climate and vegetation in this report used Daymet (a gridded climate dataset). For this reason, before operational reporting commences using weather-station data, a relationship needs to be established between the Daymet climate dataset at a location of interest and the weather station, typically located at park headquarters. Specifically, station temperature and precipitation data should be lapse-rate adjusted for the location of interest if there is more than 500 meters' difference in elevation between the weather station and the site of interest. This is because temperature and precipitation change with elevation.

2.11 Phenology metrics and climate drivers

Phenology metrics were determined using the derivative method in the greenbrown R package (Forkel 2015) after smoothing and interpolation to daily values. The derivative method identifies growing-season phenology by recognizing inflections in the annual curves where growth rate accelerates (start), peaks (maximum) and decelerates (end) (Figure 2-4). Length of season (LOS) is the span of time between start-of-season (SOS) and end-of-season (EOS). Timing of peak growth rate (POP) occurs at the maximum annual SAVI amplitude. These values were determined for every polygon/year combination, where possible. In some cases, phenology metrics could not be determined because the amplitude of annual variation was too small to find inflection points. The LOS metric was dropped if either SOS or

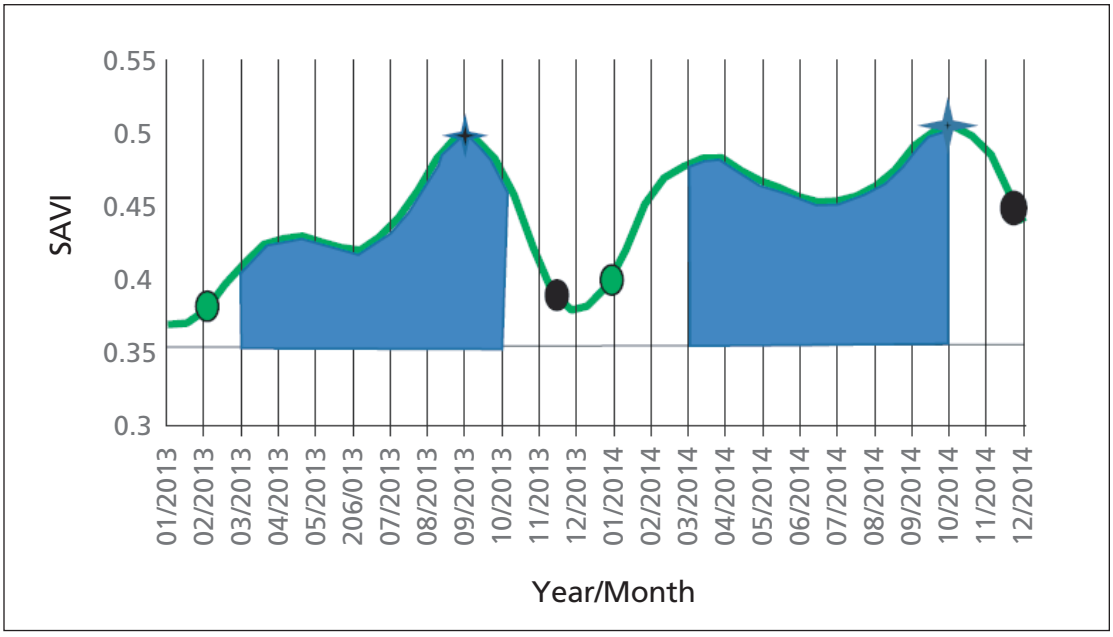

Figure 2-4. Integrated area under the growing-season curve (shaded area) for one polygon over two calendar years. The months used to calculate growing-season production are fixed and include March through October. Phenology metrics are derived using a process that determines inflection points on the annual curves using the derivative (rate of change in growth rate) method. In some years, phenology cannot be determined in semi-arid environments due to weak or noisy signals. The fixed growing-season duration used for calculating iSAVI and the start and end of growing season determined from phenology analysis may not always agree. Start of growing season (green point), peak (star), and end of growing season (black point) indicate important annual milestones in vegetation growth over two consecutive years.

EOS could not be determined. SOS, EOS, and LOS metrics were also dropped if SOS occurred in winter (November 1–April 1), due to vegetation shadows that confound satellite-based phenology assessments (Norris and Walker 2020).[3]

Polygon-level phenology metrics were summarized across alliance groups. The summary involved averaging linear-regression slopes (days of change per year) across polygons within an alliance type, then multiplying the slope by the number of years (20) in the study to determine the average days of change in each phenology metric over the course of the study. Due to variation in the regression relationships and using regression slope to convert to days of change in each metric, the change in LOS in summary tables is similar to, but not equal to the length of time between SOS and EOS.

Climate drivers of phenology were identified by focusing on SOS because plant growth in spring is most sensitive to climate (Fu et al. 2014). A suite of climate variables was reduced by dropping variables highly correlated with day-of-year (r^2 >0.7) and determining pairwise correlations between remaining explanatory variables. In the case of correlated variable pairs, the more-integrative variable was retained.

The timing of SOS, peak greenness and its magnitude, senescence, and LOS were derived from the full annual curves for each polygon, with winter-period minimums truncated to 60% of the winter maximum during the period of record. The cutoff value of 60% was determined via trial and error that both minimized lengths of winter gaps and included growing-season SAVI in every year. This prevented long periods of snow or winter cloud cover from having undue influence on the timing of phenology. The truncation of winter minimum values described above was a simplified version of published methods (Wang et al. 2018).

Two statistical methods were used to identify climate drivers of SOS, or green-up. This helped identify multiple lines of evidence for drivers if both methods yielded similar results. The first method relied on preconceived notions of phenology drivers. The second method, a machine-learning approach, let the data tell the story. In the first method, a priori models thought to be important in western rangelands were identified (Table 2-4) (St. Peter 2015). These models were competed against one another to determine top models of SOS.

Second, the random-forest machine-learning technique was used to determine important drivers of phenology and provide predictive models of SOS (Breiman 2001). Random forest is a learning method for regression that constructs a multitude of decision trees until the optimum combination of factors describing a result is obtained. In this case, a priori candidate models were not specified beforehand. Rather, the random-forest algorithm used climate and water-balance variables to identify a top model using a subset consisting of 70% of the data, which was randomly selected. The random-forest algorithm generated 2,000 decision trees with a maximum of four variables randomly chosen per split, which is the recommended number for a model testing the utility of 12 predictors. Sampling was done with replacement, which is the default setting.

The top model was validated against a hold-out dataset consisting of the remaining 30%

3 Some vegetation types (primarily conifer and shrublands) in the western US exhibit a peak satellite-observed greenness (measured using the normalized difference vegetation index, or NDVI) in winter months that is an artifact of shadows when the angle between reflected sunlight and the satellite is large (Norris and Walker 2020). It is unknown how this issue affects SAVI. The bands used to calculate SAVI are the same as those used to calculate NDVI, but a soil-correction factor is applied in SAVI to account for variable background reflectance. There is currently no known solution for resolving this shadowing effect. Thus, polygon/year combinations that exhibit winter peaks cannot be used in phenology analysis. These polygon/years were removed by determining if their annual peak of greenness occurred during winter months, defined as the period between November 1 and April 1. If any winter peaks in SAVI occurred during any year of the study period, then the polygon/year was removed from analysis for that year. This allowed retention of polygon/year combinations that did not result in spurious satellite observations, rather than removing a polygon from analysis if only a few years failed the screening rules.

Table 2-4. A priori models of climate influence on timing of green-up (start of the growing season).

Model[1]	Climate variable											
	AET	GDD	P	RAIN	D	VPD	SRAD	Tmax	Tmin	VP	SOIL	Meltd
AET	X	–	–	–	–	–	–	–	–	–	–	–
GDD	–	X	–	–	–	–	–	–	–	–	–	–
P	–	–	X	–	–	–	–	–	–	–	–	–
RAIN	–	–	–	X	–	–	–	–	–	–	–	–
D	–	–	–	–	X	–	–	–	–	–	–	–
VPD	–	–	–	–	–	X	–	–	–	–	–	–
SRAD	–	–	–	–	–	–	X	–	–	–	–	–
Tmax	–	–	–	–	–	–	–	X	–	–	–	–
Tmin	–	–	–	–	–	–	–	–	X	–	–	–
VP	–	–	–	–	–	–	–	–	–	X	–	–
GDD_P	–	X	X	–	–	–	–	–	–	–	–	–
GDD_RAIN	–	X	–	X	–	–	–	–	–	–	–	–
GDD_SOIL	–	X	–	–	–	–	–	–	–	–	X	–
GDD_AET	X	X	–	–	–	–	–	–	–	–	–	–
SRAD_AET	X	–	–	–	–	–	X	–	–	–	–	–
SRAD_P	–	–	X	–	–	–	X	–	–	–	–	–
Meltd	–	–	–	–	–	–	–	–	–	–	–	X
Meltd_SRAD	–	–	–	–	–	–	X	–	–	–	–	X
Meltd_P	–	–	X	–	–	–	–	–	–	–	–	X

[1]Models were competed via generalized linear mixed-effects modeling to identify best correlates with green-up. All climate variables were summed or averaged from January 1 to the day of year when green-up began. See Table 2-2 for acronyms.
[2]X = variable used in model, – = variable not used in model.

of observations. Variable-importance plots were used to identify which variables had the most predictive power. They consisted of percent increase in mean square error (%IncMSE), which is a measure of model improvement when adding each variable to the model, and increase in node purity (IncNodePurity), which is the difference in residual sum-of-squares in regression with or without each variable.

After model-fitting with the training data, predictions for the start of the growing season were made using the validation dataset, where SOS predictions could be compared against observations in the validation dataset. The accuracy of predictions for SOS were characterized by the mean absolute error (MAE), which is the mean value of differences between predictions and observations with units of days. The MAE is the average magnitude of error in days without specifying direction of error, thus specifying the average plus-or-minus error rate of predictions.

3 Results and Discussion

3.1 Completeness of satellite observations

Completeness of growing-season observations was 99.9% across all targets for the 20-year period of analysis. Clouds, aerosols, and snow cover reduced the average completeness of high-quality observations to 95.9% of potential observations on an annual basis across all polygon targets. The minimum completeness for any single polygon on an annual or seasonal basis was 78.5% and 80.0%, respectively.

Before analyzing satellite observations with climate and water balance, gaps were linearly interpolated to a daily timestep prior to smoothing. This removed high-frequency noise in the timeseries that could not be removed via quality screening. There were no missing climate or water-balance data.

3.2 Timeseries

At Canyonlands NP, SAVI observations reflected differences in vegetation response to climate that were apparent when observations were organized by NCPN alliance group (Figure 3-1). Some polygons were generally greener than others (indicating higher productivity and biomass accumulation), but within alliance groups there was considerable variation. That variation can be due to species assemblages within the alliance and site properties that modify the local effects of climate. Some outlier polygons within alliance groups might need to be considered separately in future analyses if interest is in the central tendency of an alliance group.

Gap-filled and smoothed timeseries illustrated a broadly similar slightly upward trend in all alliance groups during the study period (Figure 3-1). However, the alliance groups showed a high degree of variability in amplitude and timing of peak values. It was typical for some polygons in an alliance group to exhibit "outlying character," indicating they were not a good fit with other polygons in the group. This issue was most notable in the Disturbed, Dry Wash, Dry Sagebrush, and Pinyon-Juniper alliance groups, despite filtering outlying polygons that had an annual average value greater than 90th or less than 10th percentile. This could happen for several reasons. First, grouping vegetation types into alliance groups forces some dissimilarity among group members. There may have been misclassification during the vegetation-mapping process. Less commonly, post-mapping disturbance may have occurred that resulted in a different vegetation-response signal than what is characteristic of other polygons in the alliance group.

It is important to evaluate "outlier" polygons with consideration to potential effects of land use or disturbance. For instance, timeseries in the Geology alliance group were surprising because based on the alliance-group name, little if any vegetation should have been present. Strong seasonality and relatively high-amplitude SAVI suggested that (1) there was some vegetation growing in areas mapped as Dry Wash and Geology, or (2) there was some pixel overlap of polygon boundaries picking up vegetation signals that could not be removed despite the rigorous screening criteria. Without further investigation, it is not possible to know which of these issues, or a combination, were in play.

3.3 Trends in indicators of annual production

Significant upward trends ($p < 0.05$) in maximum and mean annual SAVI occurred across 58% of the study area. The greatest area of mean annual and maximum annual SAVI increase occurred in the Pinyon-Juniper, Sparsely Vegetated, and Blackbrush alliance groups, representing 56.2% of the area analyzed in and near Canyonlands NP (Table 3-1, Appendix A, Figure A-1). Only 1.9% and 2.2% of the study area decreased in maximum or mean annual SAVI, respectively. In those small areas, decreases were noted in Pinyon-Juniper, Dry Wash, Dry Shrubland, Blackbrush, and Sparsely Vegetated alliance groups. The downward trend in production may be due to natural disturbance, management actions, disease, fire, or drought, any of which could be verified by site visits. Results by polygon for significant

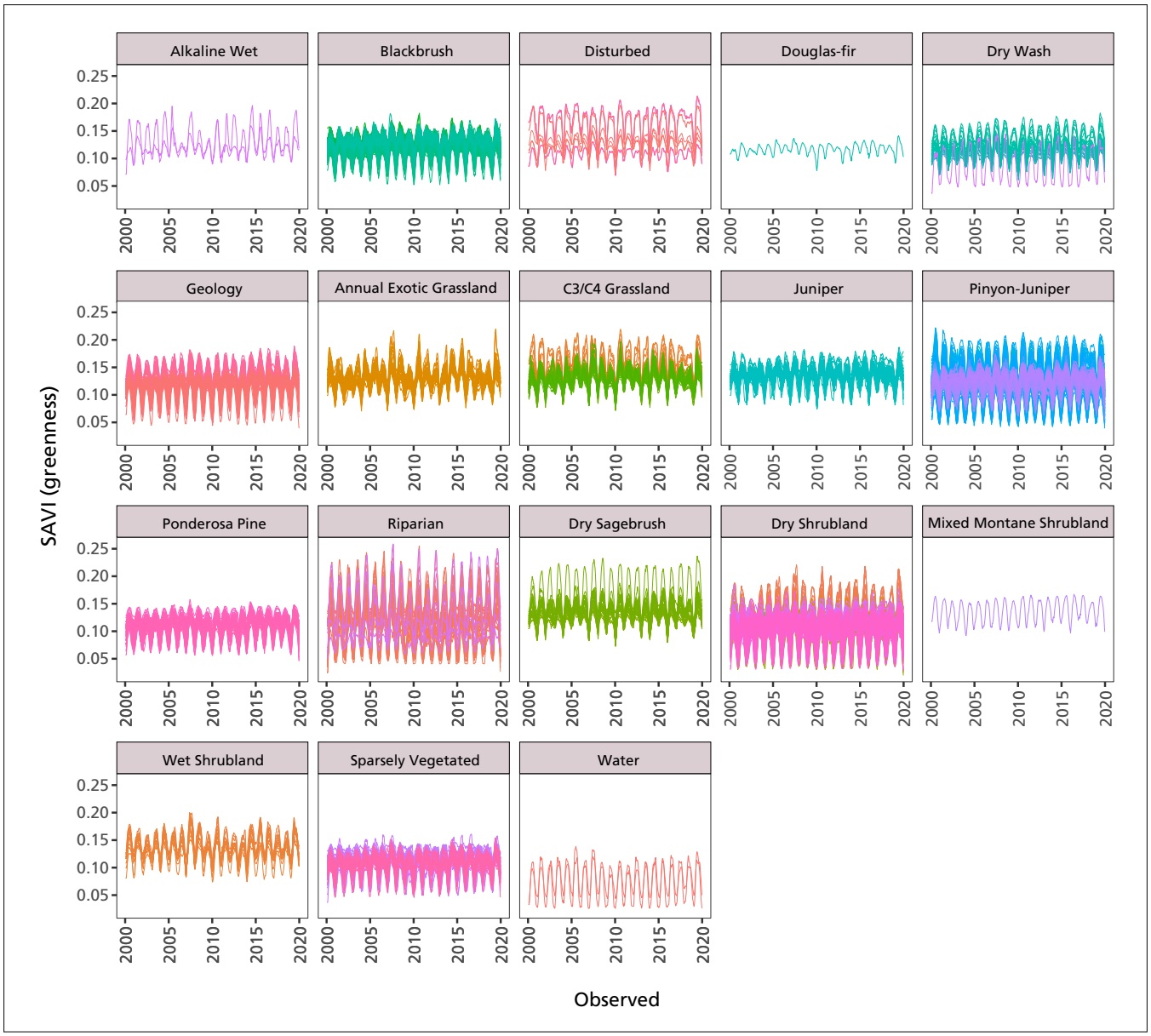

Figure 3-1. Soil-adjusted vegetation index timeseries by alliance group for 2,168 polygons analyzed for 2000–2019. Colors help differentiate individual polygon timeseries traces. Each polygon timeseries was filtered to include only high-quality pixel values, with minimum values truncated to winter minimum, gap-filled, and then smoothed with a Savitsky-Golay moving-window filter to remove high-frequency noise. Analysis was limited to polygons of >8.3 hectares. A single-line trace indicates either all polygon units have similar seasonality and interannual variation, or only one polygon of the alliance group was sampled.

Table 3-1. Amount of park area with increasing (pos) or decreasing (neg) trends in mean annual or maximum annual SAVI by alliance group.

Alliance group	Annual trend[1]		Hectares	# of polygons	% of analysis area[2]
	Maximum	Mean			
Pinyon-Juniper	pos	pos	61,779.1	477	43.75
Sparsely Vegetated	pos	pos	10,675.6	82	7.56
Blackbrush	pos	pos	6,931.4	225	4.91
Blackbrush	neg	neg	1,120.3	12	0.79
Juniper	pos	pos	883.5	57	0.63
Pinyon-Juniper	neg	neg	801.7	16	0.57
Blackbrush	pos	neg	649.9	12	0.46
Dry Wash	pos	pos	577.4	31	0.41
Dry Shrubland	pos	pos	361.1	18	0.26
Blackbrush	neg	pos	294.2	1	0.21
Pinyon-Juniper	pos	neg	234.1	11	0.17
Pinyon-Juniper	neg	pos	158.3	4	0.11
Juniper	neg	neg	76.4	6	0.05
Juniper	pos	neg	75.2	4	0.05
Juniper	neg	pos	74.6	3	0.05
Riparian	pos	pos	54.4	4	0.04
Sparsely Vegetated	pos	neg	52.1	3	0.04
Sparsely Vegetated	neg	neg	47.7	2	0.03
Dry Shrubland	neg	neg	36.1	2	0.03
Dry Wash	neg	neg	11.9	1	0.01
Mixed Montane Shrubland	pos	pos	10	1	0.01
Douglas-fir	pos	pos	9	1	0.01
Dry Wash	neg	pos	8.6	1	0.01

[1]Because there are two variables that can trend in the same or opposite directions, there can be more than one row of information for each alliance group.

trends in maximum and mean annual SAVI are in Table S-3 of Thoma (2023a).

3.4 Trends in indicators of growing-season production

Upward trends (positive-slope coefficient) in growing-season iSAVI (March through October), determined via simple linear regression, were found at the alliance-group level for all alliance groups except Riparian (Figure 3-2), which showed an abrupt drop between 2007 and 2010 followed by slow recovery. This is a classic disturbance signal. Although the regression slope for Water was positive for the entire study period, the abrupt drop in SAVI between 2007 and 2010, followed by slow recovery, is even more apparent in this alliance group. The disturbance may be related to tamarisk-beetle defoliation and recovery following beetle release in 2005 and 2006 (see Section 3.5.1).

As a subset of the annual period, the growing-season iSAVI (March–October) revealed climate-driven temporal patterns in all alliance groups. The study began in 2000, which was a low-production year. Other low production years included 2002–2003, 2006, 2012, and 2018—all corresponding with dry periods. Most dry periods were followed by recovery, which peaked in 2005 and 2019. A pronounced downward trend occurred in 2015–2018. By the end of the study, above-average levels of production were observed in most alliance groups, demonstrating the resilience of Canyonlands NP vegetation production to short-term drought stress during the study.[1]

1 This finding does not imply vegetation composition was not affected or did not change. Composition change cannot be determined from this analysis.

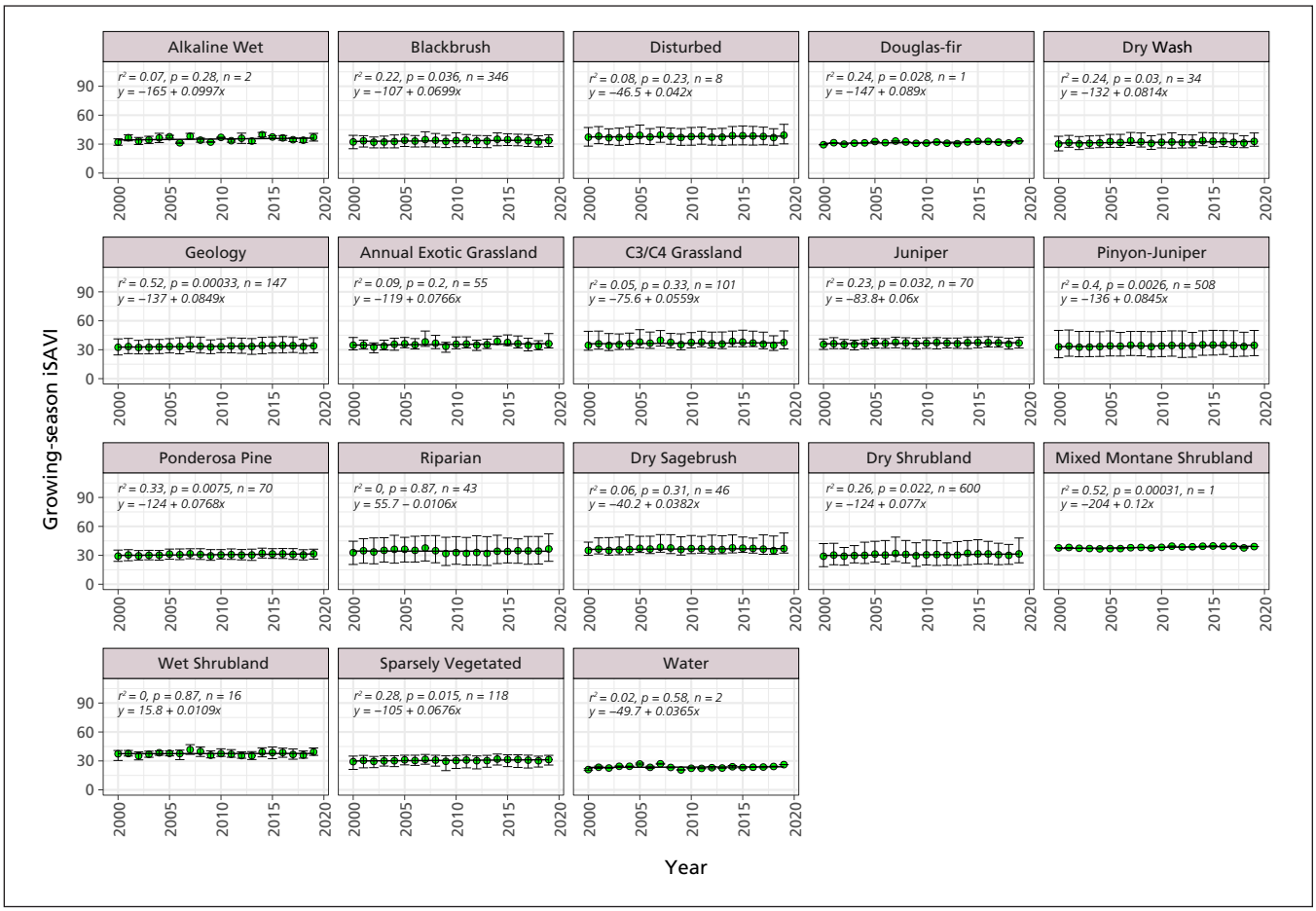

Figure 3-2. Trends in mean growing-season iSAVI by alliance group, determined via simple linear regression. Bars are standard error among polygons within each alliance group. n = number of polygons analyzed in each alliance group, r^2= coefficient of determination, p = p-value, y = growing season iSAVI, x = year.

Evaluation of simple linear-regression slopes show that Mixed Montane Shrubland increased in greenness at a faster rate than other alliance groups during the 20-year period of observations. Aside from these two alliance groups, which increased the most, there was no discernible spatial pattern of upward trends in growing-season production, because alliance groups exhibiting increases in production occurred in all areas of the park (Figure 3-3; see Figure 3-2 for slopes).

The mostly upward production trends for woody-plant alliance groups (alliance groups with shrub or tree overstory, except the Riparian group) in Canyonlands NP were consistent with other research findings on the Colorado Plateau, which showed shrubs as dominant where winter soil moisture was high and seasonal temperature variable, and grasses as dominant where summer moisture was available (Gremer et al. 2018). That study pointed out that rising temperatures and increasing temperature variability associated with climate change will result in conditions more favorable to shrubs because the change in temperature is expected to overwhelm the role of available soil moisture by late century. It also noted that shrubs are better-adapted to large temperature fluctuations than grasses. A review of woody-plant proliferation (Barger et al. 2011) found that seasonality of precipitation, land use, and atmospheric CO_2 concentrations were all important drivers of woody-plant expansion in semi-arid regions where annual PET was greater than annual P, as is the case at Canyonlands NP.

3.5 Climate relations

3.5.1 Qualitative patterns in annual precipitation and production

Between 2000 and 2019, precipitation increased in most alliance groups, as did many measures of production in this semi-arid, water-limited environment. Improved water-use efficiency due to the fertilization effect of rising atmospheric CO_2 concentrations may explain some of the increase in production, but precipitation increase was likely the largest contributor (Sorokin et al. 2017). Plotting the iSAVI difference from long-term average iSAVI with precipitation shows the temporal correspondence of interannual variation in annual precipitation and production (Figure 3-4), whereas CO_2 concentrations increased monotonically on an annual basis during the study period (https://gml.noaa.gov/ccgg/trends/). The link (i.e., covariation) between precipitation and production is most obvious in the Alkaline Wet and Dry Shrubland alliance groups (see Figure 3-4). This provides qualitative evidence that variation in production is more strongly related to precipitation than CO_2.

Trends in the Riparian and Water alliance groups were uniquely different from upland alliance groups. A large drop in iSAVI in 2007 was followed by gradual recovery in these two groups that is consistent with disturbance and recovery ecology (see Figure 3-4).

However, a deeper look into the components that are lumped into the Riparian alliance group (Fremont Cottonwood; Narrowleaf Willow - Dewystem Willow Shrubland; and Tamarisk Riparian Scrub vegetation types) indicate different responses (Figure 3-5). A 19% decline in growing-season iSAVI in Narrowleaf Willow - Dewystem Willow Shrubland and a decline of 26% in Tamarisk Riparian Scrub occurred in 2007 following the release of tamarisk beetles (*Diorhabda*) in 2005 and 2006.

Although tamarisk eradication, drought, and other factors, such as fire and flooding, can't be entirely ruled out, the change is consistent with tamarisk defoliation by beetles. For example, although the change in iSAVI may be primarily driven by defoliation, growing-season precipitation of less than 35 millimeters in 2009–2012 may have also contributed to suppressing iSAVI. Depression of the iSAVI signal in Narrowleaf Willow - Dewystem Willow Shrubland areas may have resulted from tamarisk defoliation intermixed in those map units. There is a lesser amount of iSAVI suppression in the Fremont Cottonwood type that may be due to drought or defoliation of minor amounts of tamarisk intermixed in the pixel footprints that contain the Fremont Cottonwood stands.

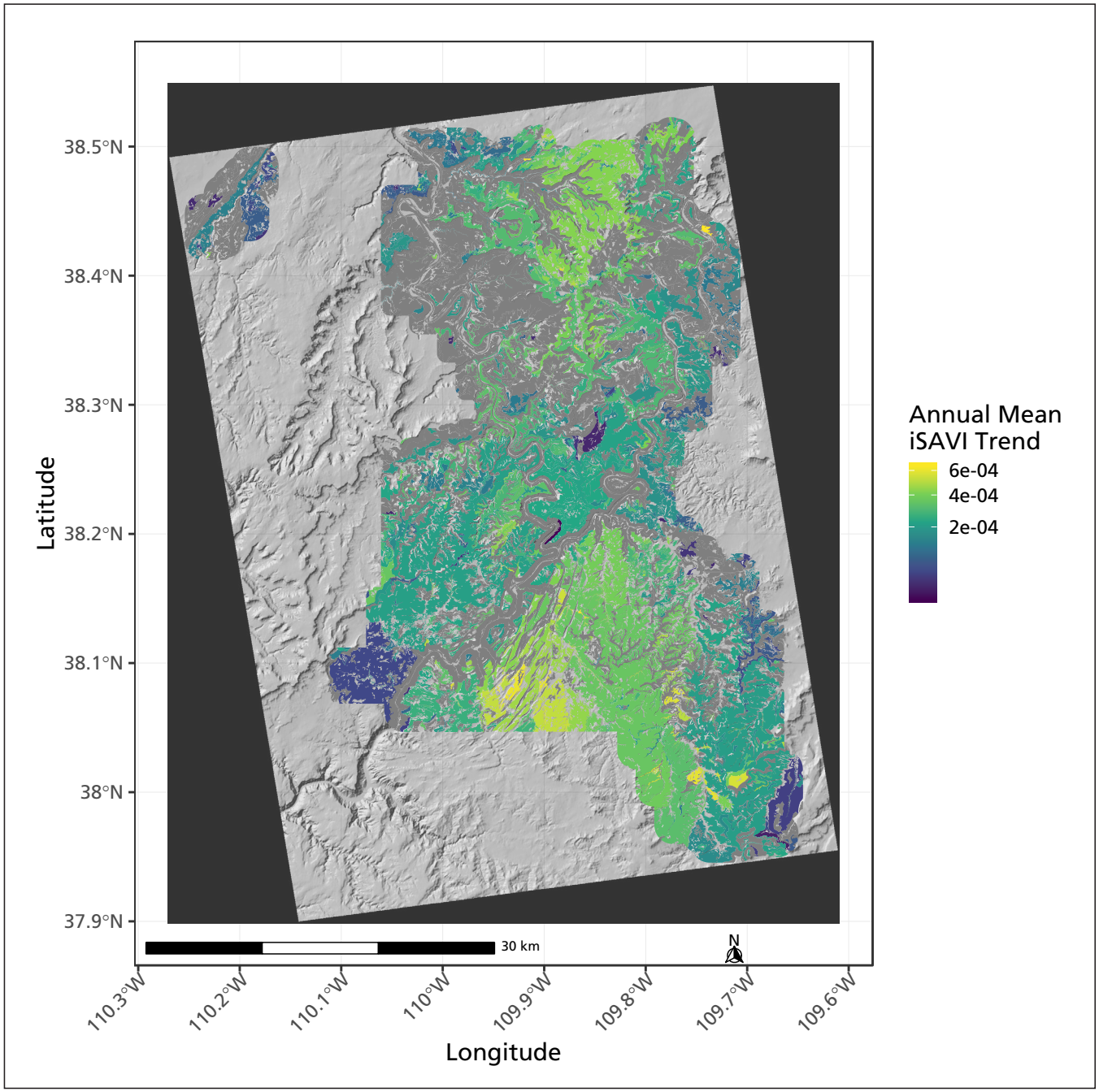

Figure 3-3. Spatial pattern of trends in mean annual iSAVI. Trend is average change in iSAVI per year for 2000–2019. Yellows are more positive and blues are less positive trends. Gray indicate areas of no detectable trend.

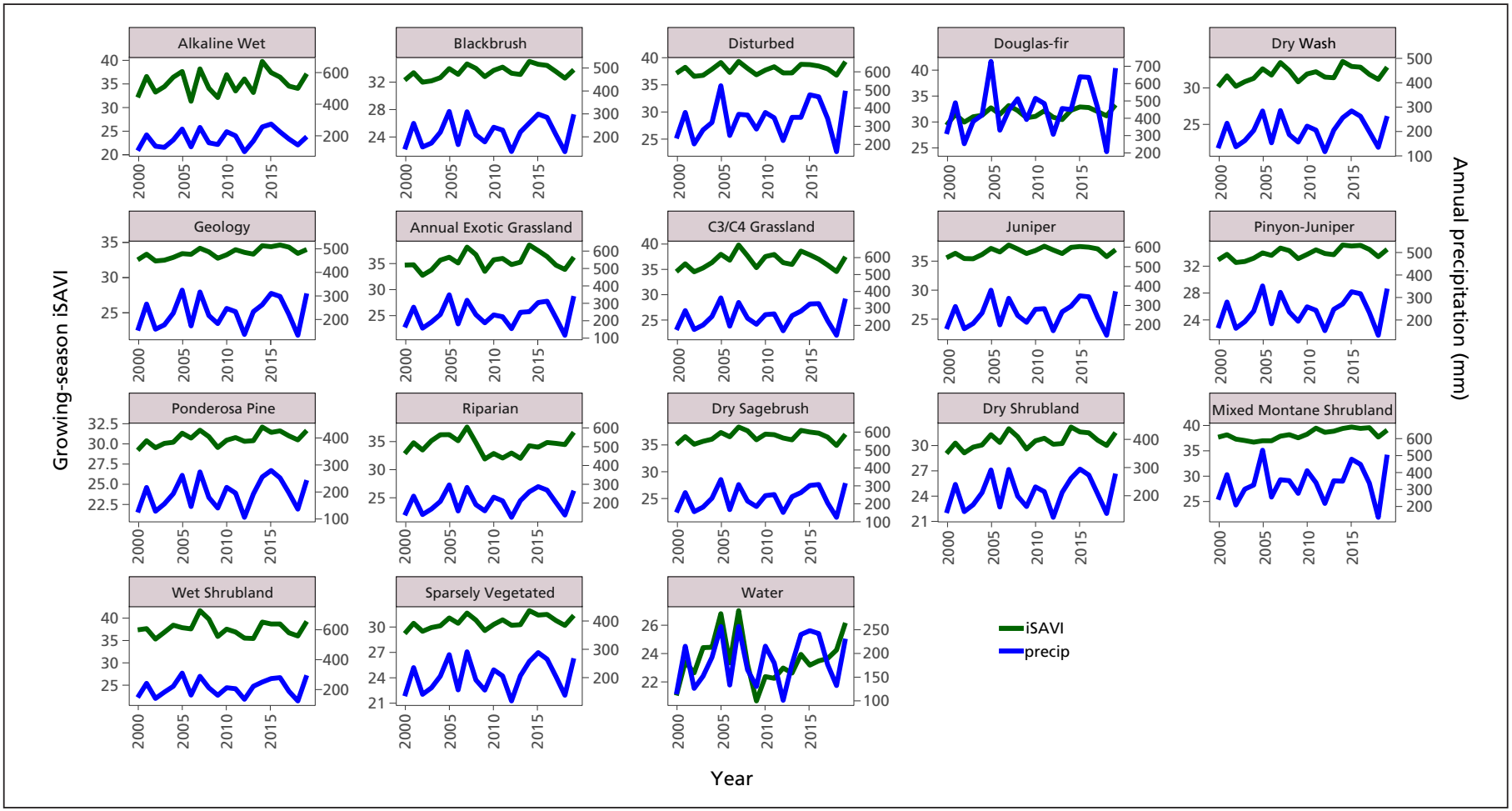

Figure 3-4. Covariation in growing-season production, estimated as the iSAVI between March and October and water-year cumulative precipitation averaged within alliance groups, demonstrating the link between climate and vegetation production in the park at the annual scale. The timeseries shown here is intended to illustrate precipitation as a primary climate driver of production in semi-arid environments. Statistical analyses of the relation of production to precipitation and all other climate variables is the subject of following sections.

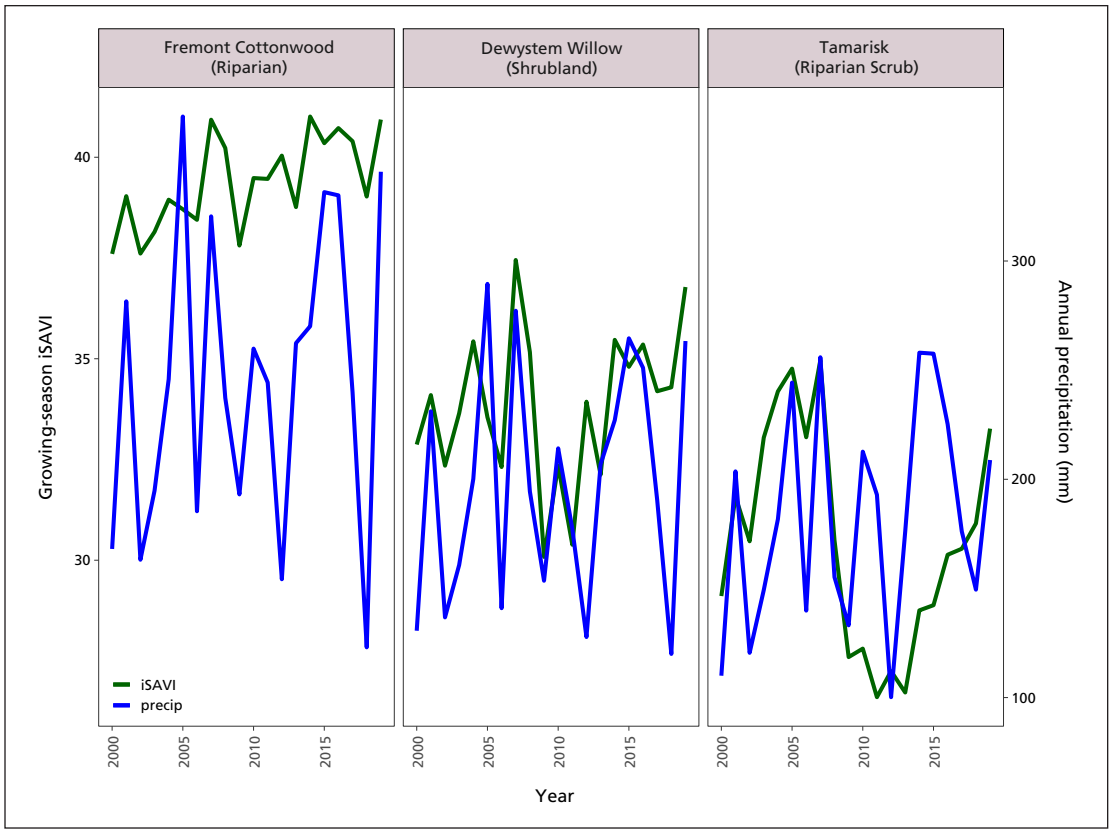

Figure 3-5. Three components of the Riparian alliance group in Figure 3-4 show differential impacts of tamarisk beetle. Some tamarisk may be present in the middle panel.

Other studies have shown that multiple biophysical stressors can substantially alter tamarisk cover. These changes can be detected with remote sensing. For instance, flooding and defoliation by *Diorhabda* reduced tamarisk cover 75% along the lower Virgin River in Nevada (González et al. 2020). Another study on the Colorado Plateau (Nagler et al. 2018) used a satellite-derived vegetation index as an indicator of both tamarisk defoliation and changes in evapotranspiration. After beetle introduction, defoliation led to a mosaic of tamarisk cover which resulted in an 11% reduction in the index used to indicate cover.

While peaks and valleys in iSAVI roughly coincided ith those of precipitation, there were differences in the magnitude of vegetation response to precipitation, and evidence of a response delay that varied by alliance group. iSAVI peaks in annual production corresponded with interannual precipitation peaks in most alliance groups, but a lag in vegetation response can be caused by legacy effects of vegetation condition in prior years that carry over to subsequent years.

Such legacy effects have been noted in semi-arid vegetation response to precipitation where prior conditions set the stage for current-year production. For example, a wet year following a drought may not be as productive as a wet year following an average precipitation year due to legacies in tillers, stems, root density, and seed production, which are limited in a drought (Noy-Meir 1973; Thoma et al. 2016). Because of prior conditions, the largest peaks in annual production do not always coincide with the largest peaks in annual precipitation.

In addition, the timing and magnitude of response to precipitation are affected by the structural and physiological traits of plants, including rooting depths, stomatal control of gas exchange, leaf morphology, annual or perennial life cycle, and the site conditions where they grow (Munson et al. 2015). Plant physiology may explain why peaks and valleys in annual production are more pronounced in C3/C4 Grasslands than in

Pinyon-Juniper or Ponderosa Pine alliance groups. Additionally, evergreens that retain leaves for multiple years have lower-amplitude seasonal cycles (Yang et al. 2019). Grasslands are generally more responsive to interannual weather variation, while woodlands with deeper rooting systems can be buffered from short-term droughts. Additionally, variation in the magnitude of vegetation response to variation in precipitation could be due to higher runoff in high precipitation years if a large proportion of precipitation fell in a few storm events.

Collectively, the response of vegetation to interannual variation in weather is complex. The study of these interactions across space and time is greatly aided by the high frequency of satellite observations coupled with continuous daily climate observations over the same period. Organizing the remotely sensed observations by management-relevant vegetation types provides insights that may be useful in climate adaptation planning.

3.5.2 Single-variable drivers of production

At the park level, relationships between growth and climate variables were generally weak due to the highly variable response relationships with climate across vegetation types. However, when examined by alliance groups, better relationships emerged (Figure 3-6).

Vegetation production in all alliance groups was correlated with multiple aspects of climate. Across alliance groups, the water-abundance variables (P, RAIN, SNOW, AET, SOIL) were positively correlated with annual production. Variables representing heat, unmet water need, or atmospheric dryness (T, GDD, D, VPD) were negatively correlated with production. Within alliance groups with multiple polygons, there was variation in relationship strength among polygons, indicated by error bars in Figure 3-6 (also see Table S-2 in Thoma 2023a). This can be caused by variation in species assemblages and abundances that differ among map units of the same alliance.

Generally, P, RAIN, and SOIL had the strongest positive relationships with production in most alliance groups. Deficit generally had the strongest negative relationship with production (see Figure 3-6). However, on an annual basis, most of the water-balance variables were no better correlated with production than with P. Every polygon that had a significant relationship with a temperature variable (PET, T, GDD) exhibited a decrease in production with warmer temperature (Table S-2 in Thoma 2023a). This is typical in water-limited environments, where warmer temperature increases evaporative demand that is often not met by available water.

Some vegetation types respond more strongly to seasonal weather than annual conditions. For these plants, warming temperatures in the spring initiate growth. Then, as soil moisture decreases throughout the growing season, other variables, such as water deficit, typically take on greater importance. Depending on the species, most growth may occur in spring or late summer. Thus, the timing of seasonal water and energy availability may be more important to annual vegetation production than annual water and energy availability (Barnes et al. 2016). These kinds of seasonal responses to weather are difficult to characterize on an annual basis with a single variable because the important climate drivers switch seasonally and there may be long-term memory effects from earlier growing seasons that affect current-year production (Thoma et al. 2016).

In other words, multiple aspects of climate and water balance act over both short and long periods to affect annual production. Thus, a simple linear-regression approach that considers single-variable influences on production over the course of an entire year is an oversimplification of important vegetation/climate relations. This may explain coefficients of determination of <0.5 (see Figure 3-6), which may seem unimpressive but are similar to results of species responses to single variables in plot studies (Munson et al. 2011).

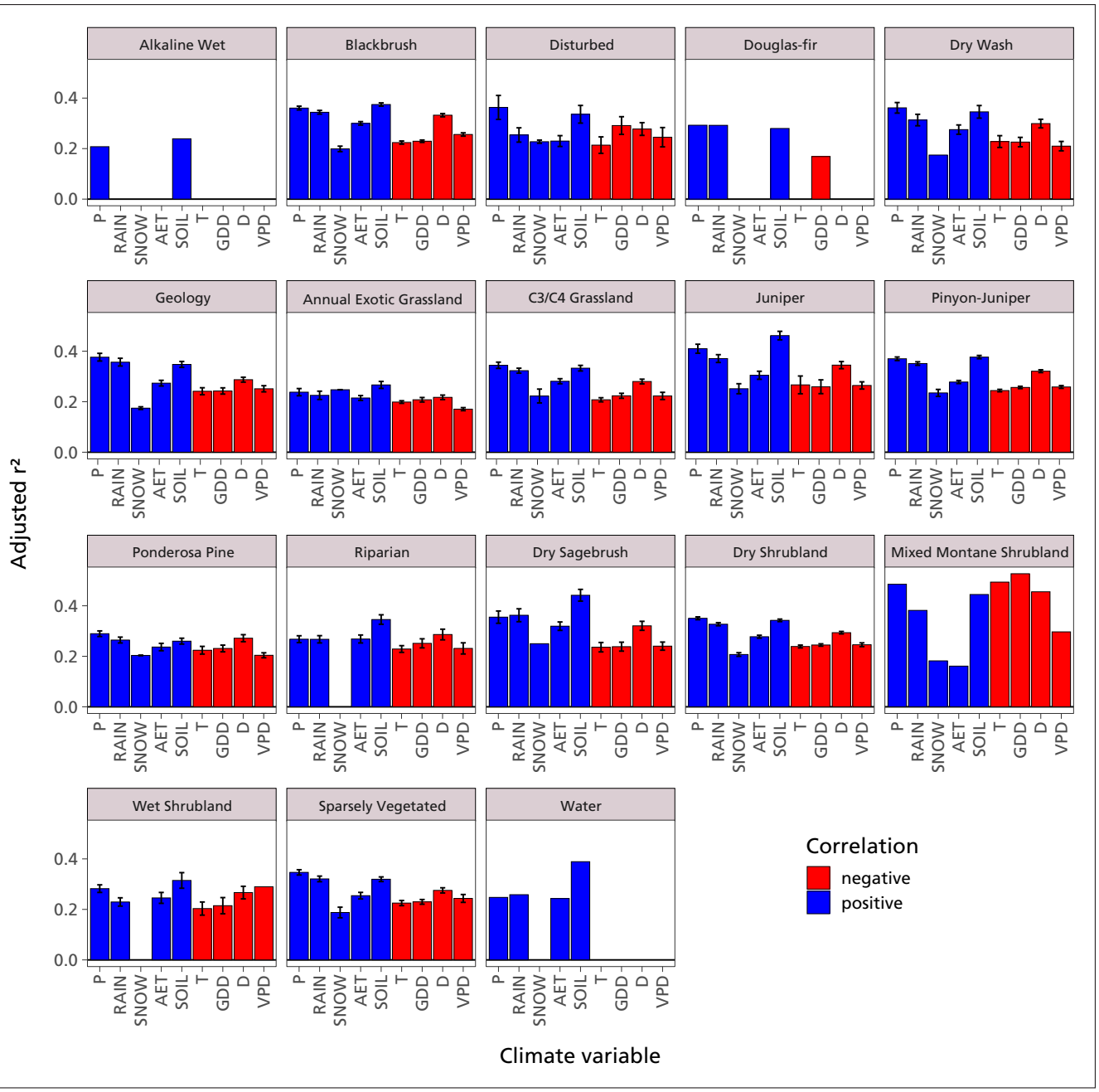

Figure 3-6. Significant (p-value <0.05) relationships between water-year climate variables and first difference of growing season iSAVI, 2000–2019. Bar height is the mean variation in iSAVI explained by variation in climate or water-balance variable on the x-axis. Bars are standard error. Blue bar color indicates positive correlation. Red bar color indicates negative correlation. P = precipitation (mm), RAIN = precipitation as rain (mm), SNOW = precipitation as snow (mm of water), AET = actual evapotranspiration (mm), SOIL = average soil moisture (mm), T = average temperature (°C), GDD = growing degree days (°C), D = water deficit (mm), VPD = vapor-pressure deficit (Pa).

Nevertheless, there is value in determining single-predictor regressions because they can identify important drivers that result in increases or decreases in annual production and represent a practical way to derive critical water needs and drought-stress indicators (Munson et al. 2016; Thoma et al. 2019) that can be tracked using data from weather stations. The best single-variable indicator of annual vegetation production can be determined by alliance group from visual inspection of Figure 3-6 (tallest bar = best relationship), or by polygon from Table S-2 in Thoma (2023a).

Annual precipitation at Canyonlands NP was generally among the climate or water-balance variables most strongly correlated with annual production, so it is used in the following sections that further explore climate/vegetation relationships. Multiple predictors and time lags of annual production response are considered in a later section.

3.6 Pivot points

3.6.1 Pivot points indicate drought tolerance

Plant species with smaller pivot points for water-abundance variables (e.g., P, RAIN, SNOW, AET, SOIL) demonstrated a higher degree of drought tolerance, because less water was needed to achieve above-average production (Thoma 2023a, Tables S-2 and S-4).[2] Conversely, larger pivot points for variables representing heat, unmet water need, or atmospheric dryness also indicated a higher degree of drought tolerance, because more drought was tolerated before production dropped below average.

At Canyonlands NP, the most drought-tolerant alliance group (i.e., the one with the lowest precipitation pivot point) other than Water was Alkaline Wet, followed by the Ponderosa Pine, Dry Wash, and Sparsely Vegetated alliance groups (Figure 3-7). Drought tolerance in wet or low-lying vegetation types is due to accumulation of water from upslope positions, which makes these alliance groups less drought-prone in low-precipitation years. Because the water-balance model used in this report does not account for flow accumulation from upslope positions, it cannot account for the likely cause of drought tolerance in this alliance group.

Ponderosa pine is among the most drought-tolerant alliance groups, likely because it occurs in shaded, north-facing areas, areas of flow accumulation, lower positions of bedrock slopes that capture and channel water below ground, or areas where water is supplied by groundwater from sandstone aquifers. The distribution of this alliance group by aspect is even (47% of polygons north-facing; 53% south-facing); thus, mechanisms other than shading may be important. Nevertheless, the physical processes that collect or store water in these locations will continue to collect water in the future, which will likely make this alliance group less susceptible to drought than other upland alliance groups, as indicated in Figure 3-7.

The Douglas-fir, Mixed Montane Shrubland, and Disturbed alliance groups were least drought-tolerant. This is unsurprising, as Douglas-fir and Mixed Montane Shrubland occur at elevations that receive more precipitation than lower areas of the park. The higher precipitation pivot point of Disturbed areas may be due to species establishment that occurred in these areas during years of above-normal precipitation. Grasslands and other shrublands are more drought-tolerant than the Juniper or Pinyon-Juniper woodland groups, likely due to seasonal growth traits and dormancy during the driest times of year.

With the exception of the Water and Alkaline Wet alliance groups, pivot points for a specific geographic area were related (but not always equal) to the mean annual climate value where a pivot point was deter-

2 The pivot points differed among water-abundance variables because they represent different pools, periods, and magnitudes of water availability. For example, soil moisture is a fraction of total precipitation (P), because some P runs off and is not available to plants. Similarly, rain and snow represent fractions of total P that supply water for vegetation at different times of the year. Thus, each variable represents a different "pool" and phase of water (solid, liquid, or gas) that may be seasonally active or present during different seasons.

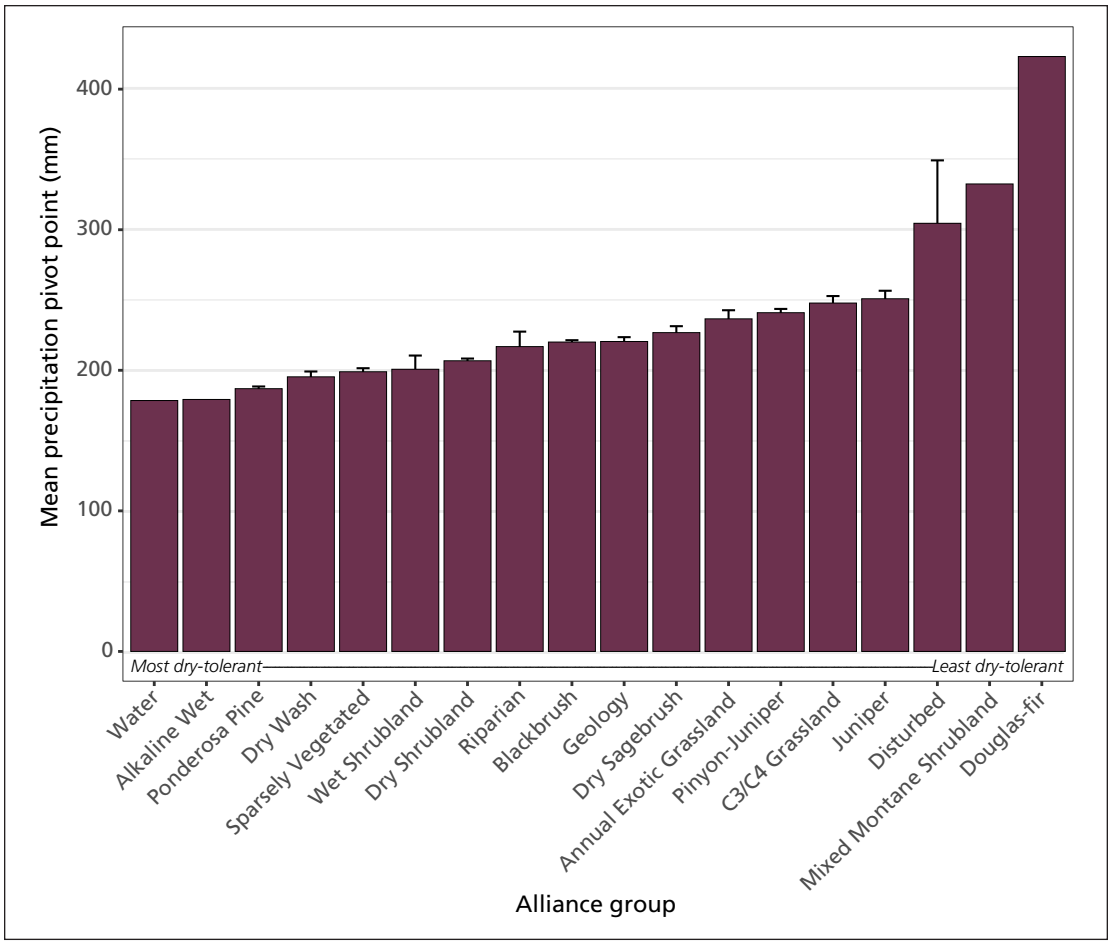

Figure 3-7. The mean precipitation pivot-point values shown here represent critical water needs for the different alliance groups. Standard error bars indicate range in variability of pivot points among polygons of an alliance group if more than one polygon had a statistically significant relationship ($p < 0.05$) with precipitation. Pivot points identify the critical water need that achieves average production for each alliance group.

mined. For this reason, spatial patterns in pivot points often follow precipitation and temperature gradients with elevation. This can be seen in the order of alliance-group pivot points at Canyonlands NP. Lower-elevation alliance groups generally have lower precipitation pivot points, consistent with these species being considered more drought-tolerant (see Figures 3-7 and 3-8). Salt Creek, Horse Creek, and Davis Canyon have higher precipitation pivot points than Lavender Canyon (to the east) and Butler Wash (to the west), yet vegetation communities and soils are similar across all these areas (Matt Van Scoyoc personal comm.). Similar vegetation in areas that receive different precipitation levels may reflect the adaptive capacity of vegetation in these canyons to tolerate a range of annual precipitation.

Near the end of this study, in winter 2018–2019, widespread mortality of juniper trees was noted in the Four Corners region (Figure 3-9). This mortality event coincided with precipitation shortfalls that resulted in the worst two-year drought during the study period. US Forest Service entomologists and plant pathologists who examined affected trees south of Canyonlands NP concluded the damage was due to drought stress, rather than pathogens (Davis et al. 2022). Examination of the climate record revealed that those two years represented the driest period in 125 years. They also noted that patterns of mortality were associated with higher canopy density (likely because there is increased competition for water in denser stands), as well as topography and slope, which also control water distribution

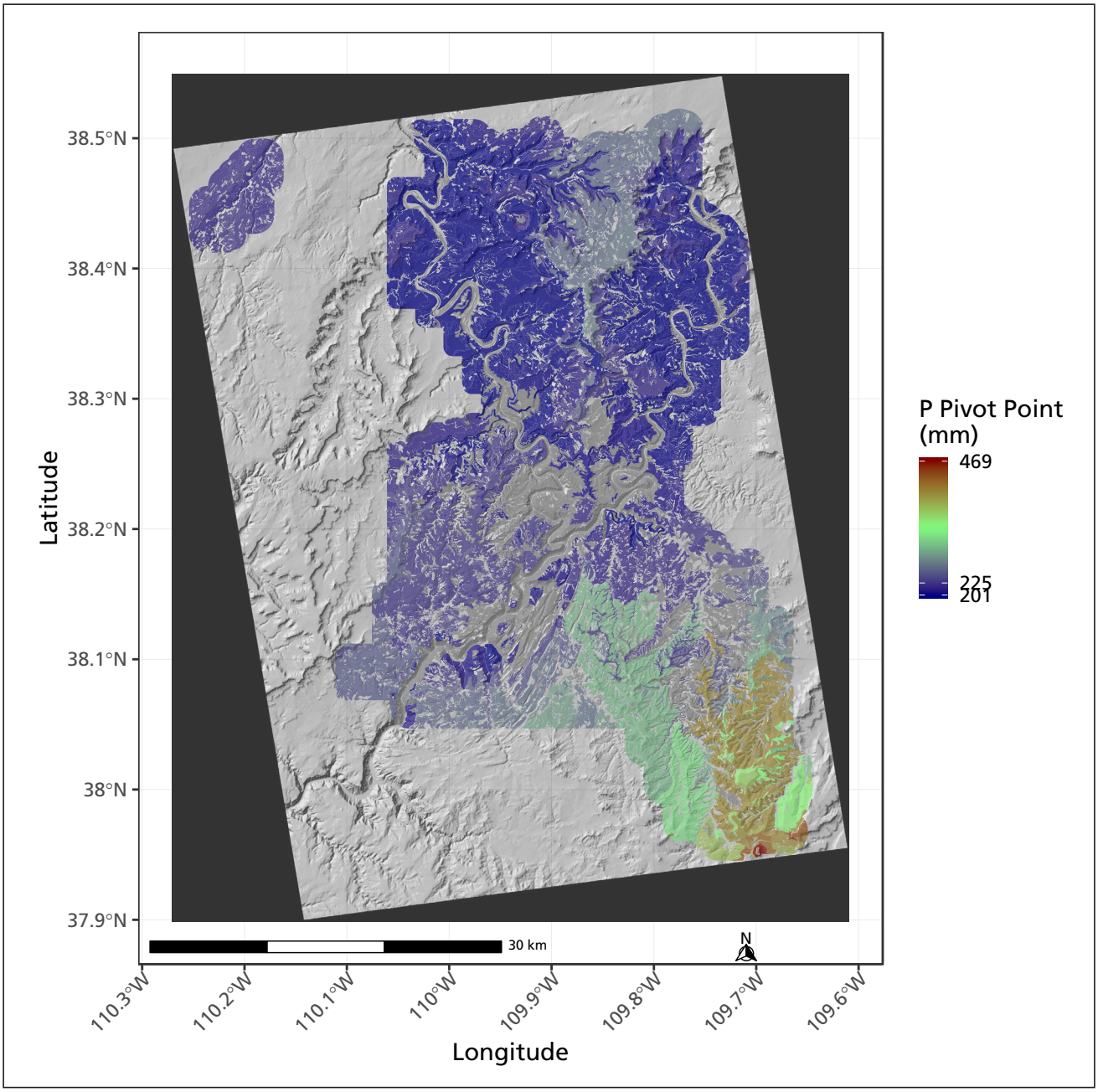

Figure 3-8. Precipitation pivot points for polygons with a significant relationship (p-value <0.05) between water-year annual precipitation and change in annual vegetation production, assessed as the interannual difference in iSAVI. The mean precipitation pivot-point values shown here represent spatial patterns in the critical water needs of vegetation.

and retention. This drought was sufficiently long and deep to kill trees that have multiple drought-resistance mechanisms via osmotic regulation and stomatal closure (Dickman et al. 2015).

A study by Peterman and others (2012) found that soil properties explained more than 70% of the spatial pattern of pinyon mortality caused by the 2003–2004 drought in the southwestern US (a mortality event also noted by park managers in Southeast Utah Group parks in 2003; Dana Witwicki pers. comm.). Interactions between vegetation and precipitation that are modified by site conditions affecting water storage (such as soil properties and aspect) are accounted for in this study by using water-balance variables as climate indicators. For this reason, pivot points for soil moisture and other water-balance variables are included in Appendix A and Tables S2 and S4 of Thoma (2023a).

NPS/DANA WITWICKI



Figure 3-9. A patch of dying junipers with the Abajo Mountains in the background, Cedar Mesa, Utah, 2019. In the two years before this photo was taken, water deficit was higher than at any time since 1980.

An ad hoc study of remotely sensed vegetation condition and corresponding drought stress for the periods preceding the 2003 and 2018 juniper mortality events suggests that a two-year cumulative water deficit of 164–195 millimeters may cause juniper mortality near Natural Bridges NM, approximately 30 miles southwest of The Needles (Thoma 2023b). Climate data for the location of juniper mortality in this area showed that the cumulative two-year water deficit in 2002 and 2003 was 164 millimeters, while the cumulative two-year deficit in 2017 and 2018 was 195 millimeters. This suggests that a two-year cumulative deficit of 164–195 millimeters can kill juniper trees near Natural Bridges NM.

Further, between 1980 and 2019, water deficit increased by 2.9 millimeters per year, equating to, on average, 110 millimeters (4.3 inches) more deficit in 2018 than 1980. What this tells us is that to bring deficit (drought stress) back to the level experienced by juniper trees in 1980, an additional 4.3 inches of precipitation would have been needed in 2018. By comparing that "need" for water to the average annual precipitation from 1980 to 2018—7.8 inches—we find that collectively, precipitation would need to increase by about 50% of the long-term average to bring drought stress back to what trees experienced at the location Natural Bridges NM in 1980. Overall, we know water deficit is a meaningful indicator of drought stress experienced by plants, and the two-year cumulative deficit may provide an early warning of drought conditions sufficient to kill juniper trees. Whether the actual values provided above—for a site near Natural Bridges NM—may be indicative of extreme drought stress in other locations would need to be evaluated before drawing any broader conclusions.

3.6.2 Spatial patterns of drought tolerance

The map of precipitation pivot points shows that the amount of moisture required to increase production above that of the previous year generally increased with elevation toward the south, approaching the Abajo Mountains (see Figure 3-8). This pattern stemmed from the distribution of vegetation groups that generally followed changes in mean climate values. More specifically, it reflected the tendency of water availability (soil moisture) to increase with elevation, and unmet water need (deficit) to decrease with elevation (Stephenson 1998).

3.6.3 Pivot points for other climate variables

Pivot points for other climate and water-balance variables generally reflected the average climate conditions where alliance groups were found (Figure 3-10, Appendix A, Figure A-2). However, the range in pivot points within alliance groups, and the variation in species assemblages within and between polygons of each alliance group, reflected some variation beyond a pattern purely determined by elevation gradient. In semi-arid environments like Canyonlands NP, pivot points for variables AET, P, SOIL, RAIN, and SNOW are generally lower than the pivot point for D, an indicator of drought. This is because vegetation in these environments is adapted to handle relatively low water availability and high drought stress.

All results shown here are statistically significant. For this reason, any of these alliance group-level pivot points can be compared against historic, present, or future projected growing-season climate conditions to

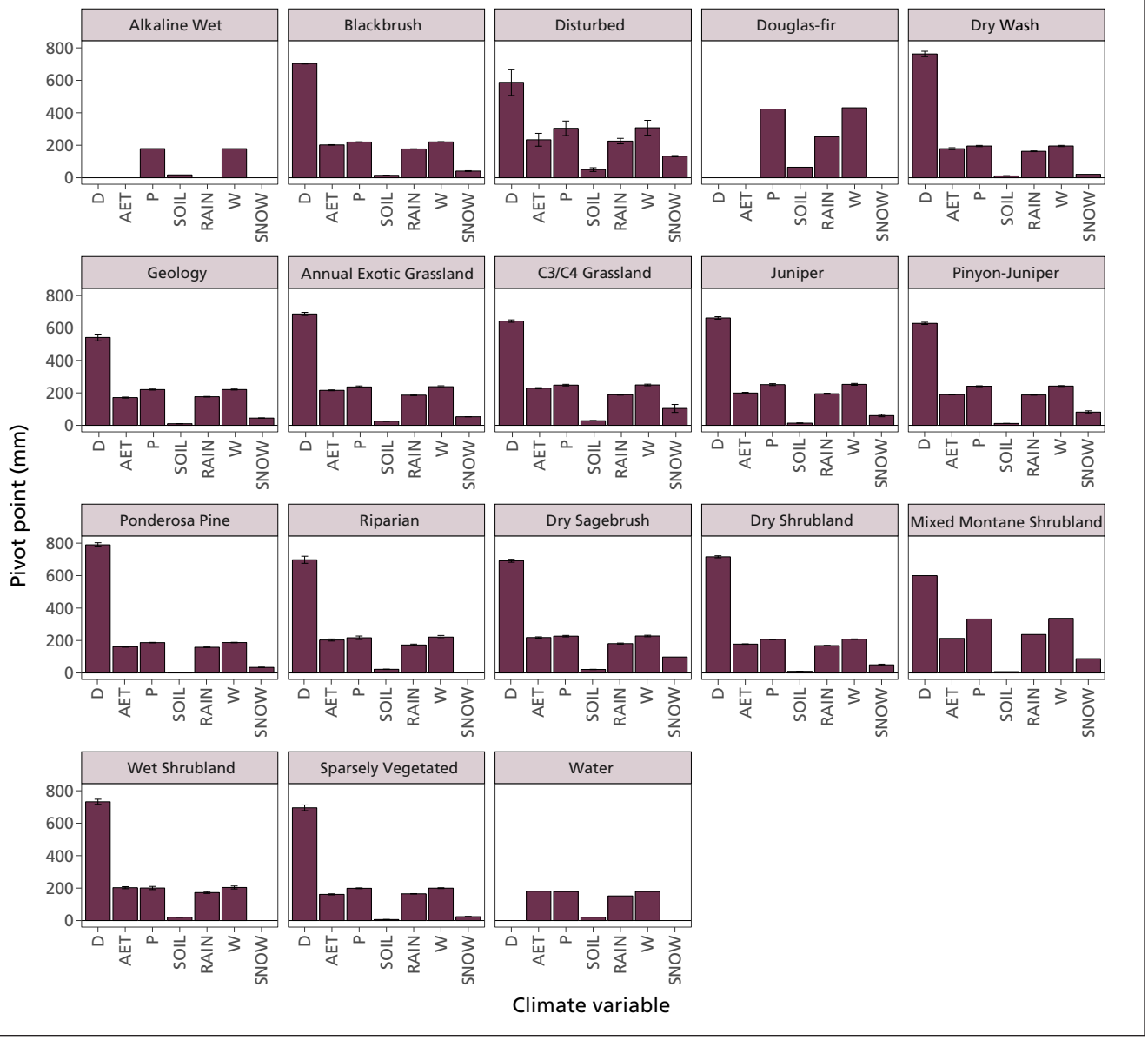

Figure 3-10. Significant (p <0.05) water-related pivot points by alliance group. See Tables A-2 and A-4 of Thoma (2023a) for the pivot-point values. The magnitude of each pivot point reflects generally average conditions for polygons in each alliance group. The mean pivot-point values are the critical values where annual production switches from below to above average (relative to previous year) for the different alliance groups. P = precipitation (mm), RAIN = precipitation as rain (mm), SNOW = precipitation as snow (mm), PACK = maximum water content of snowpack whenever it occurs (mm); W = snowmelt plus rain (mm) AET = actual evapotranspiration (mm), SOIL = average soil moisture (mm), D = water deficit (mm).

determine if those conditions are likely to result in below- or above-average vegetation production.

Pivot points for each climate variable by polygon are provided in Table S-2 of Thoma (2023a), and by alliance group in Table S-4. These can be used with data on climate exposure to identify conditions conducive to above- or below-average growth—useful information for vulnerability assessments associated with Climate Smart Conservation planning (Stein et al. 2014) (see Chapter 4).

3.7 Vegetation response

3.7.1 Vegetation response and climate sensitivity

When they interact with climate, plant traits

determine which species grow under different conditions of water availability. The result is a spatial organization of alliance groups that reflects local climate and the sensitivity of vegetation to climate (Figure 3-11). The higher climate sensitivity of some polygons in the Island in the Sky district is associated with grasslands like Gray's Pasture that have higher sensitivity than shrubby or Pinyon-Juniper alliance groups in surrounding areas. The interactions between plant traits, site characteristics, and climate-determined patterns of vegetation distribution in the past will determine how vegetation in Canyonlands NP will be shaped by climate in the future.

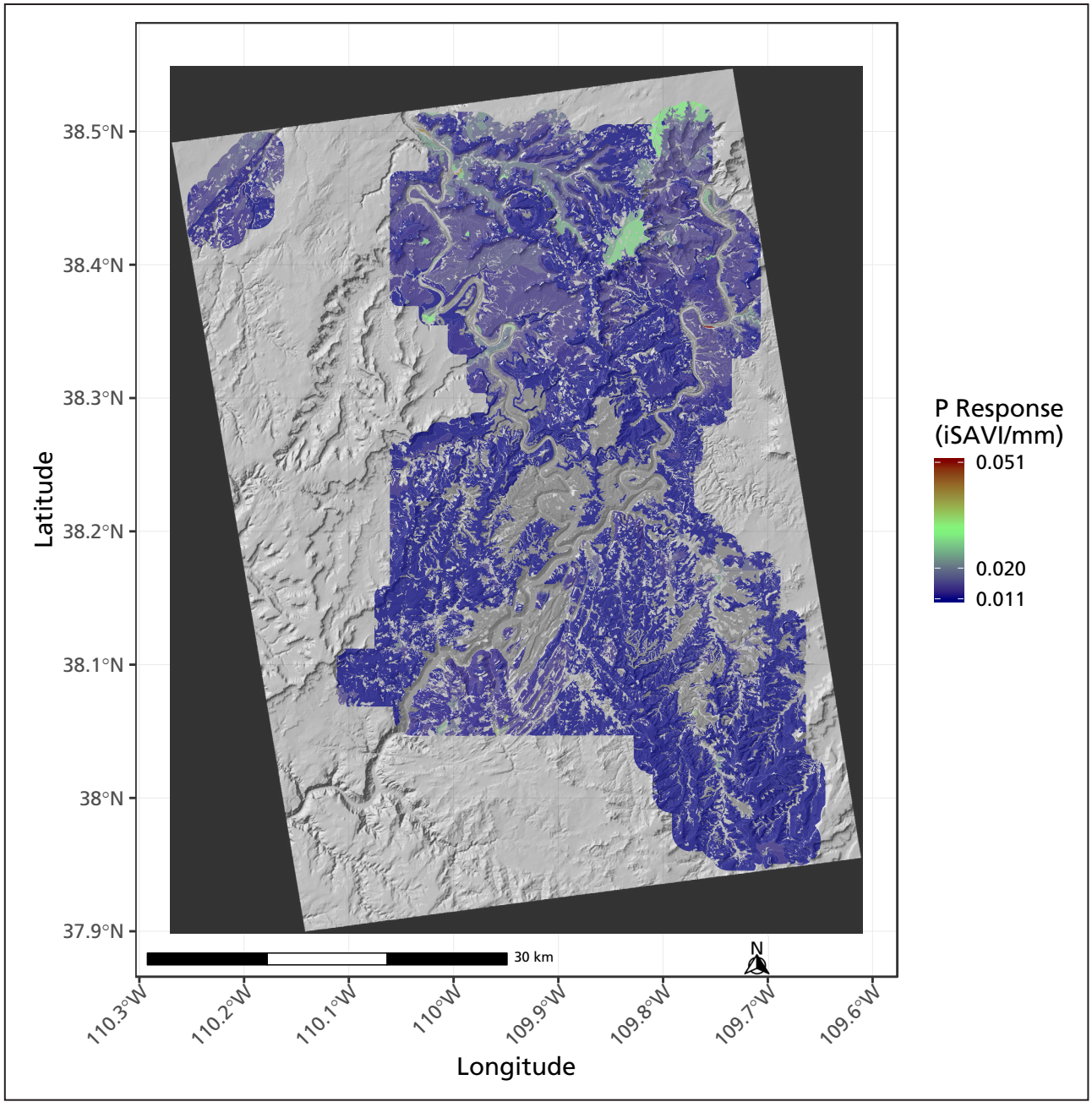

Figure 3-11. Sensitivity of growing-season vegetation production to annual water-year precipitation. This figure shows which vegetation types will experience change first. Groups with highest response rates are most likely to see change happen first and fastest as the climate shifts. Response is the slope of the linear-regression relationship between annual precipitation and iSAVI change from the previous year (i.e., the change in iSAVI expected per millimeter of change in annual precipitation). Areas without color were either smaller than the minimum area required for mapping (<8.3 ha) or did not have a significant relationship with annual precipitation. Areas that were not significantly related to annual precipitation may be related to other climate metrics. Statistics for sensitivity of each polygon to each climate metric, including quality of relationships and regression coefficients, can be found in Table S-2 of Thoma (2023a).

Vegetation response is a formal component of vegetation vulnerability assessments used in Climate Smart Conservation (Stein et al. 2014). The importance of response is related to the need to understand which vegetation groups may respond sooner or more strongly to a given amount of climate-change exposure. While a unit change in iSAVI is not quantitatively linked to vegetation cover or biomass in this analysis, it is representative of change in both of those attributes. In this way, the iSAVI response indicates where change is likely to happen first and fastest as the climate shifts.

At Canyonlands NP, the Alkaline Wet, Wet Shrubland, and C3/C4 Grassland alliance groups were the most responsive upland vegetation types. The strong response in the single polygon of the Water alliance group was likely due to upland areas near water that have responsive grass species included in the analysis footprint. Interestingly, alliance groups affiliated with water (Riparian, Wet Shrubland, Water, and Alkaline Wet) were among the most sensitive to annual precipitation. The site characteristics and vegetation composition of each polygon can be evaluated to determine why. For instance, the relatively high response rate of Alkaline Wet and Wet Shrubland groups may be influenced by water accumulation in low-lying areas consisting of non-shrub components, such as annual grasses or sedges that are more responsive to precipitation than shrubs (Figure 3-12). Finer soil textures in these alliance groups may also retain more moisture, allowing shrubs to maintain production longer than in coarser-textured soils. The high response rate in these areas may also result from non-linear water accumulation due to local topography. For instance, an inch of precipitation may result in many inches of water accumulation in depressions. Finer

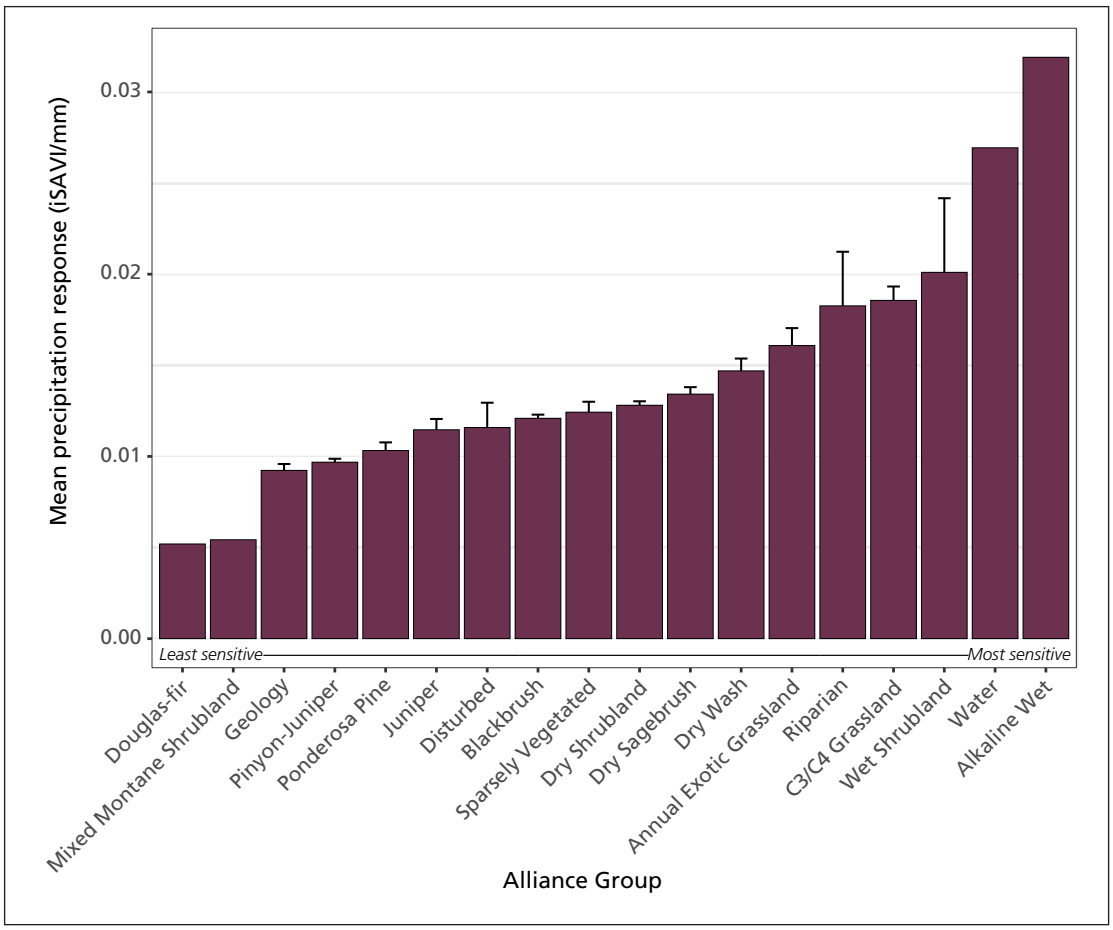

Figure 3-12. Responses of different vegetation alliance groups to precipitation. Standard error bars indicate range in variability of responses among polygons of an alliance group if more than one polygon had a statistically significant relationship ($p < 0.05$) with precipitation.

soil textures in these locations may also retain water longer. The high response of C3/C4 grasses is expected from plants that have seasonal growth physiology and the ability to increase biomass quickly when water is available. The Douglas-fir, Mixed Montane Shrubland, and Geology alliance groups were least sensitive to changes in precipitation, likely because these species are deeply rooted and slow-growing. Alliance-group sensitivities to other water-balance variables can be found in Appendix A, Figure A-3.

Generally, there was a pattern across the park in which sensitivity increased at lower elevations, where precipitation was least. This was partly due to vegetation structure: the slow-growing forest and montane shrubland species occur at higher elevations. If disturbance, such as fire or forest disease, replaced the woodland alliance groups with grassland or shrubland, then the response would shift to reflect the dominant vegetation structure.

Areas dominated by slow-growing and slow-responding juniper and pinyon-juniper woodlands were less sensitive to variation in annual precipitation. This partly explains the pattern of response, also related to duration of greenness, in which species with longer seasons of green leaves were less responsive to weather or water balance.

Responsiveness was modified by soil properties; for example, where grasslands occurred in deeper soils and shrublands and forests in soils that are shallow or have low water-holding capacity (Duniway et al. 2022). Sensitivity to soil moisture integrates these complex factors into a single metric (see Figure A-2). Annual Exotic Grasslands had a similar precipitation response rate to C3/C4 Grasslands, meaning they may be competitive against C3/C4 Grasslands when precipitation is abundant. In years when precipitation is higher than normal, vegetation in the Annual Exotic Grassland alliance group could become a management concern in or near the park because its rate of response to precipitation input is similar to that of native vegetation. However, C3/C4 Grasslands were slightly more responsive to soil moisture than Annual Exotic Grasslands, which may imply a competitive advantage for native species.

3.7.2 Spatial patterns of response

The alliance groups most sensitive to precipitation were wet areas and C3/C4 Grasslands. The least-sensitive alliance groups were single polygons of Douglas-fir and Mixed Montane Shrubland. Additional response maps, found in Appendix A, Figure A-3, illustrate spatial patterns in the sensitivity of alliance groups to deficit and soil moisture.[3]

3.7.3 Influence of site characteristics

Spatial patterns in soil and site properties, including percent sand and clay, depth to root-restrictive layers, water-holding capacity, slope, and aspect, influenced drought tolerance and sensitivity to climate variables. This was apparent from similar patterns seen in the soil-properties maps (Figure 3-13) and the response maps (e.g., Figure 3-11). For instance, the average water-holding capacity in the top meter of soil was 41 millimeters parkwide, but 76 millimeters in the Alkaline Wet and Wet Shrubland alliance groups (see Table S-2 in Thoma 2023a). This correspondence was further evidence of the interactions between climate, site properties, and vegetation traits (deep- or shallow-rooted, perennial or annual) that influence vegetation condition, trends, and climate sensitivity.

By relating pivot points and responses with site properties (see Table S-2 in Thoma 2023a), we can quantify the strength of influence that site properties have in modifying climate effects. Steeper regression slopes in relationships between vegetation responses or pivot points and site properties (such as those in Appendix A, Figure A-4) indicate a stronger effect of a given site property on either the pivot point or climate response.

3 Response to soil moisture is greater than sensitivity to precipitation or deficit because incremental changes in soil moisture in this analysis are expressed as a water-year mean, whereas precipitation and deficit are sums (see Table 1-1). However, the pattern in response to soil moisture is tied to spatial variation in soil properties that play important roles in storing precipitation between events.

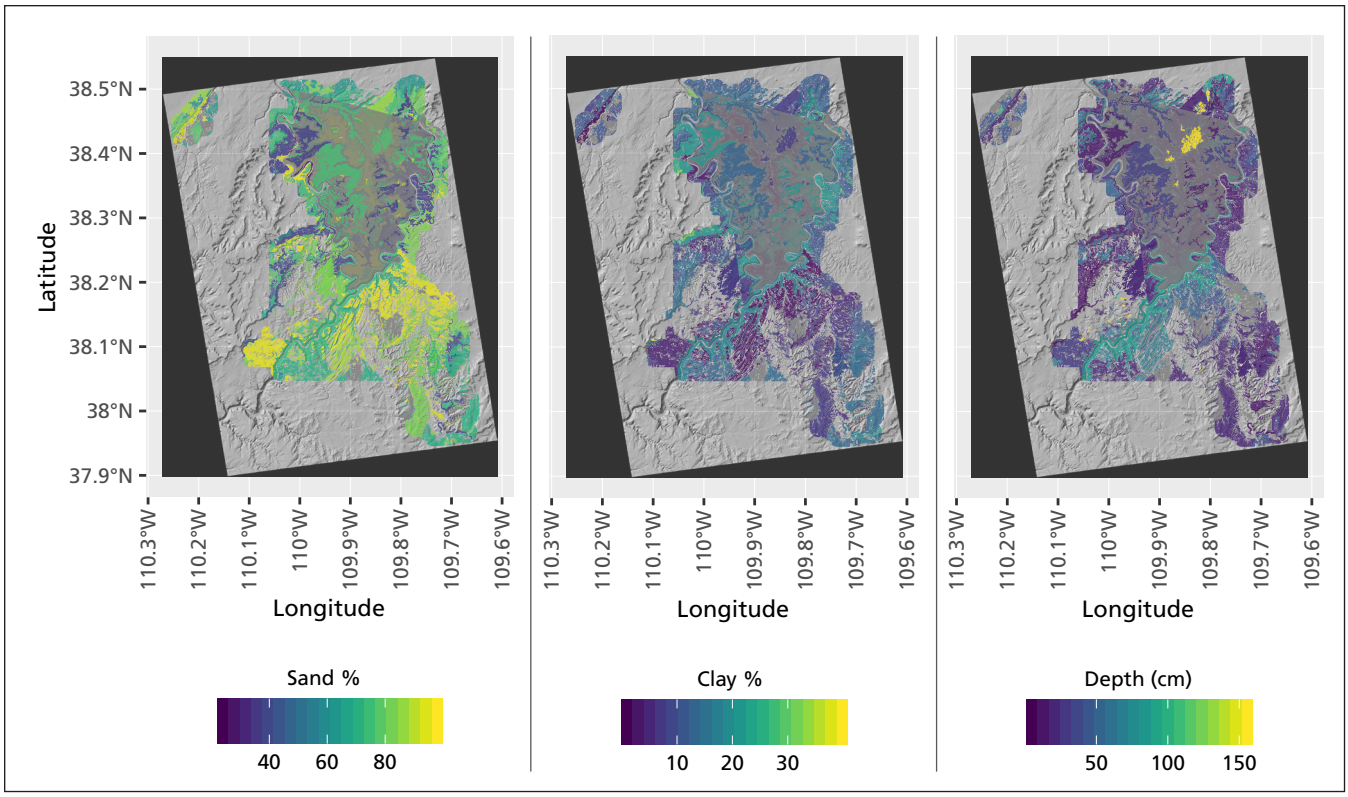

Figure 3-13. Maps of percentage sand and clay content in top meter of soil, and depth to restrictive layer in alliance groups. Spatial patterns of soil properties correspond with patterns in vegetation response to climate. Areas of no color fill indicate missing soil-properties data or depth greater than 100 centimeters.

For example, there is weak evidence that Blackbrush is more sensitive to precipitation as soil water-holding capacity increases (see Table S-6 of Thoma 2023a; response = 3E-05 * water holding capacity (mm) + 0.01; r^2 = 0.075) and less drought-tolerant as clay content increases (Table S-6; pivot = 1.4 * clay% + 234, r^2 = 0.063).

These relationships suggest soil texture may play a role in determining which of the Blackbrush alliance groups are likely to be affected by climate change first. For instance, Blackbrush growing on soil with the lowest clay content (1%) needs 35.7 millimeters more annual precipitation to sustain production than Blackbrush growing on soil with the highest clay content (27%), indicating that precipitation is more effective at promoting Blackbrush-alliance production on soils that store more precipitation for plants. Site properties affected drought tolerance and climate sensitivity by influencing water retention and distribution in the soil profile, and possibly heat-loading due to the slope and aspect of the site relative to the sun.

These site-specific properties locally modified the influence of climate and were important determinants of vegetation condition and patterns on the landscape. They can be quantitatively introduced into vulnerability assessments at the polygon scale by use of a water-balance model that accounts for these complex interactions using the data in Table S-4 of Thoma (2023a).

3.7.4 Patterns within alliance groups

While pivot points and responses provide different information, they are linked by plant traits: as precipitation pivot points decrease (i.e., cross the horizontal "no change" line further to the left), response rate increases (Figure 3-14). Alliance groups with steeper slopes (e.g., Wet Shrubland, C3/C4 Grassland) are considered more responsive to changes in water availability. These groups increase production with less precipitation, demonstrating that responsiveness to precipitation is greatest where vegetation is most drought-tolerant. This is consistent with the earlier generalization that response rate increases as elevation decreases.

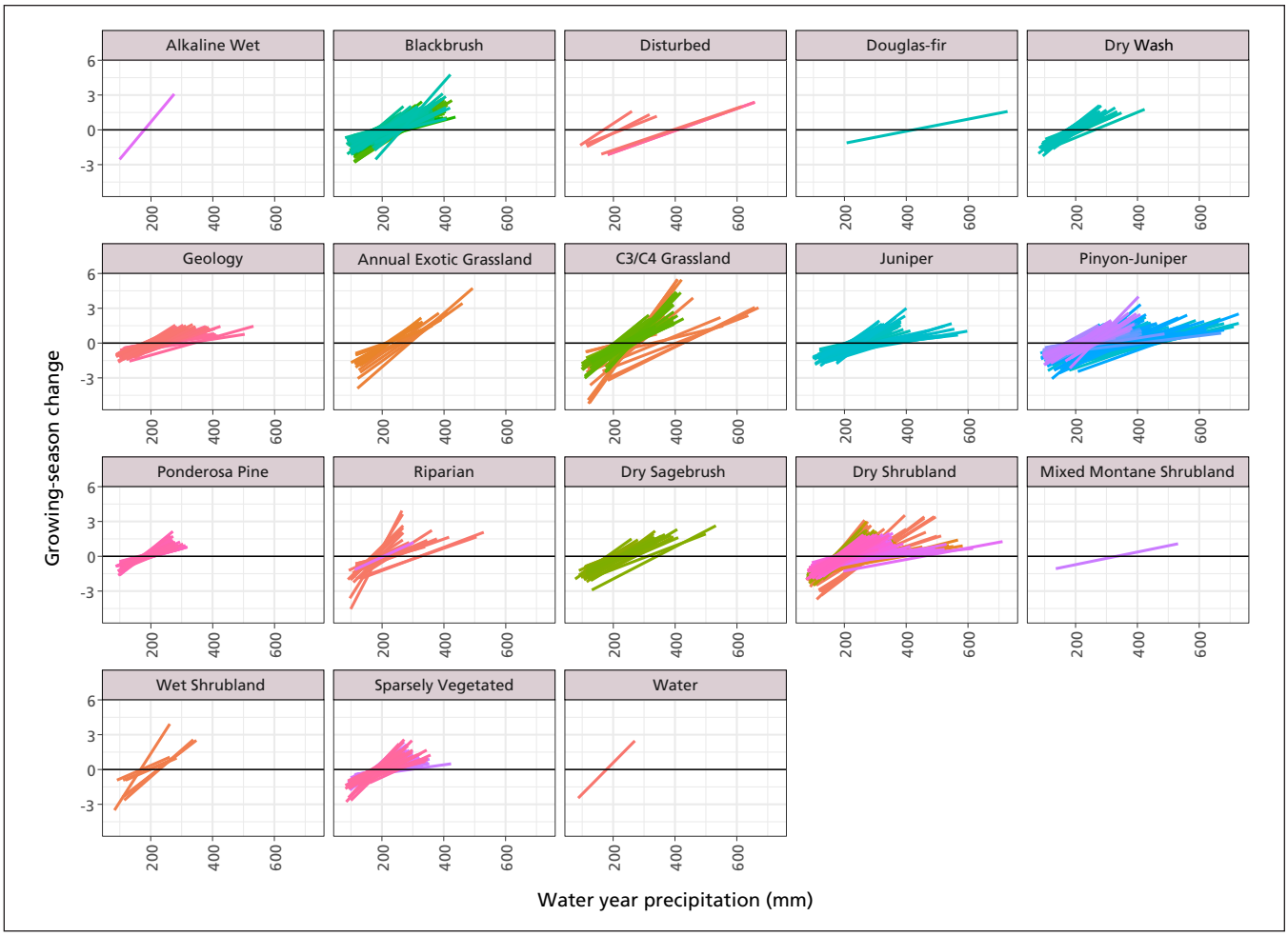

Figure 3-14. Graphical depiction of the relationship between pivot points and responses in polygons that showed a significant relationship (p-value <0.05) between iSAVI and water-year precipitation (e.g., critical water need vs. rate of growing-season iSAVI change per mm precipitation). Polygon-level pivot points and responses are provided in Table S-2 of Thoma (2023a). Alliance groups with steeper slopes are considered more responsive to changes in water availability. Alliance groups and alliance polygons within alliance groups that cross the horizontal axis further left are more drought-resistant. This is because they shift to above-average condition with less precipitation. Only significant relationships are shown. Panels without lines represent alliance groups with no significant relationships between iSAVI and climate variables. Colors help differentiate individual polygons within alliance groups.

There was a large range in pivot points and responses, reflecting a wide range of plant traits responding differently to climate variability across the park. The patterns of pivot points and responses quantify unique climatic habitats occupied by the different alliance groups, and can serve as a guide to anticipate what, where, when, and why vegetation change may occur. For example, this analysis suggests that positive growth response to high precipitation will be greater in areas already considered wet, moreso than in Dry Sagebrush or Blackbrush alliance groups.

Information in this report can be used in conjunction with data on weather conditions during the growing season to indicate vegetation condition at the polygon or alliance-group scale, depending on management interest (Tables S-2, S-4, Thoma 2023a). Generally, within alliance groups, vegetation response increased as precipitation decreased. The degree of responsiveness was determined by traits that allowed plants to either resist drought or rapidly respond to water availability. The result was that vegetation response to climate could be considered coarsely at the alliance-group level, but at higher spatial resolution and often, with higher accuracy, at the polygon level. For example, in the C3/C4 Grassland alliance group, precipitation explained 34% of interannual variation in production. But by polygon (n = 76), precipitation explained between 16% and 75% of interannual varia-

tion in production.

Multiple factors can introduce additional variability in pivot points and responses within alliance groups. These include differences in species assemblages, plant spacing, and soil properties that affect the retention and distribution of water in the soil profile that is accessible to different growth forms (e.g., plants with shallow or deep roots) (Lauenroth and Bradford 2012; Schlaepfer et al. 2011; Schlaepfer et al. 2014).

3.7.5 Production response to water and non-water variables

Assemblages with higher responses (steeper regression slopes) were more sensitive to climate. Depending on the climate variable, the slope could be positive (as with semi-arid environments and water variables, such as precipitation and actual evapotranspiration), or negative (in response to water deficit or potential evapotranspiration, which are related to temperature) (Figure 3-15; also see Tables S-2 and S-4, Thoma 2023a).

Direct comparison of water variables to non-water variables, such as GDD and VPD, is difficult due to their different units of measure. Similarly, it is important to note that response to change in an average annual value, such as soil moisture, is strong partly because this variable is averaged (because soil has an upper limit of water-holding capacity), which weights its effect on vegetation more per unit change than other climate variables that are summed (see Table 2-2). Therefore, small changes in average soil moisture have a larger effect than small changes in annual precipitation. Responses to temperature variables GDD and T should also be considered similarly, because GDD is a summed variable, while T is averaged. Variable importance is considered in the following sections.

3.8 Multi-variable indicators of annual vegetation production

Pivot points and responses are ecological measures of annual production, but production is affected by multiple aspects of weather before and during a growing season, as well as conditions in prior growing seasons that set the stage for production potential in the current year (Sala et al. 2012).[4]

In the multi-model comparison of climate correlates with interannual differences in growing-season iSAVI across all alliance groups, climate indicators of annual production showed that regardless of alliance group, most (70%) polygons were influenced by three years of soil moisture. The next most-common indicator of production was two years of soil moisture (Figure 3-16). These patterns generally held within alliance groups (Figure 3-17). A list of top-performing models (AICc <4) by polygon can be found in Table S-5 of Thoma (2023a).

Most alliance groups responded to multiple years of soil moisture, highlighting the importance of legacy effects across years in a semi-arid environment where water is the growth-limiting factor in most years (Bisigato et al. 2013). Soil properties that help sustain higher average soil moisture, perhaps through finer soil textures, reduced runoff, or deep infiltration, provide additional benefit.

3.9 Land-surface phenology trends at Canyonlands National Park

Changes in land-surface phenology result from interactions between temperature, moisture, plant traits that control growth rates, and CO_2 concentrations that affect water-use efficiency. Generally, warming reduces growth rates in semi-arid environments, while elevated CO_2 increases water-use efficiency of production for the same amount of water. Thus, warming may initiate an earlier start to the growing season, and elevated CO_2 may increase water-use efficiency, resulting in more production for a given amount of water use. But efficiency is ultimately limited if conditions become sufficiently dry and growth ceases. For this reason, and given projected drying on the Colorado Plateau, increases in efficiency may be small and short-lived in the face of disturbance caused by drought or wildfire (Allen et al. 2015). Tracking changes in phe-

4 This is one reason why the annual relationships described above are not as strong as monthly relationships described in earlier work (Thoma et al. 2016).



Figure 3-15. Vegetation response to summed water-flux variables (regression slopes from iSAVI versus annual climate-variable sum). Statistics for these relationships and all other variables can be found in Tables S-2 and S-4 of Thoma (2023a). D = deficit (mm), AET = actual evapotranspiration (mm), P = precipitation (mm), RAIN = precipitation as rain (mm), W = combination of rain and snowmelt (mm), SNOW = precipitation as snow (mm of water).

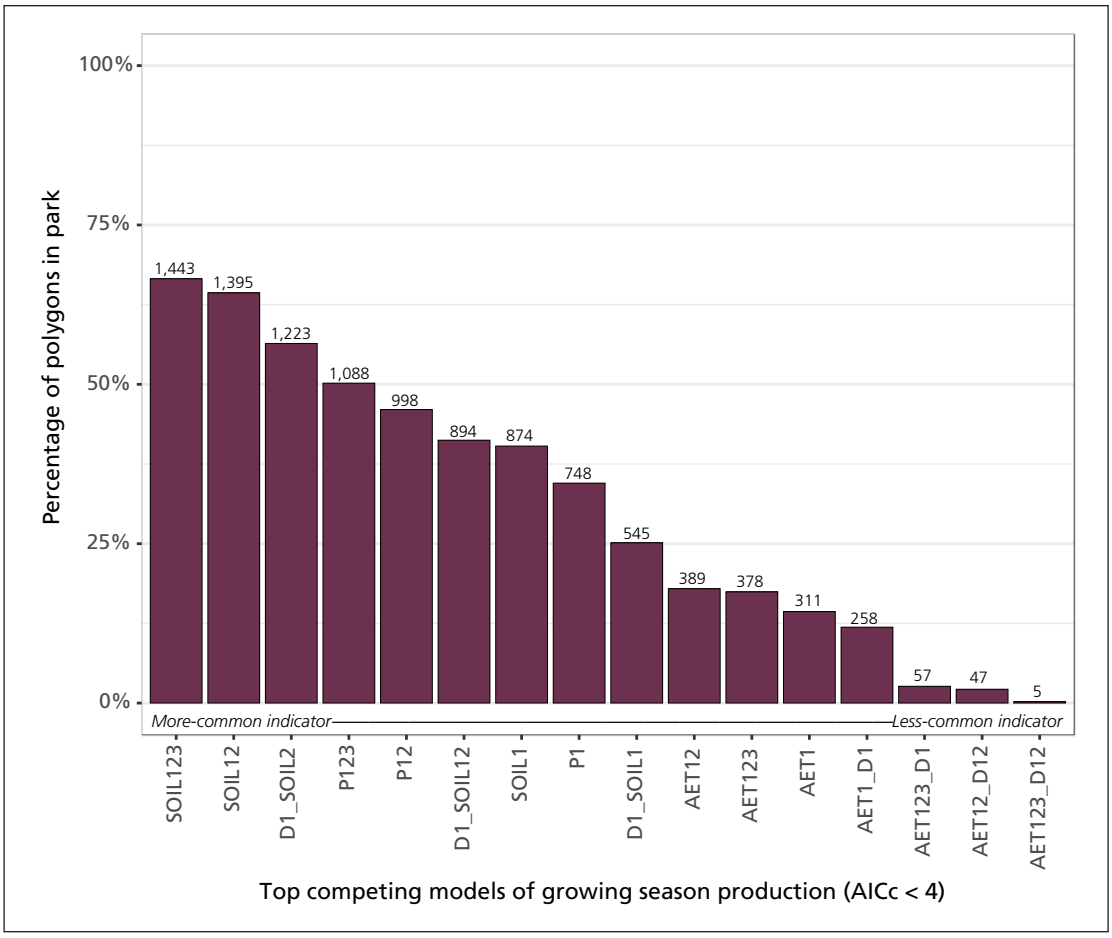

Figure 3-16. Top models in multi-model comparison of climate correlates with interannual differences in growing-season iSAVI across all alliance groups. Percentages indicate proportion of polygons where each model was competitive. Numbers above bars indicate polygon count. Each polygon may have more than one competitive model; thus, the sum of percentages exceeds 100 across all models. The x-axis labels refer to the a priori climate models in Table 2-3. SOIL = annual average soil moisture; D = annual deficit; AET = annual evapotranspiration; P = annual precipitation. Numbers indicate current and prior years included in each model. 1 = current year; 12 = current and previous year; 123 = current and previous two years.



Figure 3-17. Top models of growing-season production by alliance group in multi-model comparisons of climate correlates with interannual differences in growing-season iSAVI. The x-axis labels refer to the a priori climate models in Table 2-3. The y-axis represents the proportion of polygons in each alliance group where each model was competitive. Numbers above bars indicate polygon count. Each polygon may have more than one competitive model; thus, the sum of percentages can exceed 100 across models. SOIL = annual average soil moisture, D = annual deficit, AET = annual evapotranspiration, P = annual precipitation. Numbers are 1 = current year, 12 = current plus previous year, 123 = current plus previous two years.

nology in NCPN parks, and linking those changes to seasonal changes in temperature and CO_2 concentrations, could help further clarify the vulnerability of semi-arid vegetation to multiple aspects of climate change (Sorokin et al. 2017).

Over the duration of the study at the park scale, on average, the start of growth advanced 12.6 days earlier and the end of growth occurred 11.2 days later. Collectively, these changes resulted in a growing season that was on average 23.8 days longer by the end of the study. At the end of the study, timing of peak growth occurred 1.7 days later than at the start (see Table S-7 of Thoma 2023a).

A trend in earlier SOS occurred in all alliance groups except for Alkaline Wet, for which SOS occurred 31.2 days later (Table 3-2; Appendix A, Figure A-5). It is unclear why the start of season was delayed by a month in this alliance group, but the sample size was only two polygons and the rate of change was much greater in one polygon (CANY_19435) than in the other (CANY_19444) (see Tables S-2 and S-6 of Thoma 2023a). In recent years, the EOS was occurring later for most alliance groups, but earlier (by 0.6–4.7 days) for the Alkaline Wet, C3/C4 Grassland, and Annual Exotic Grassland alliance groups. Collectively, these changes resulted in a longer growing season for every alliance group except Annual Exotic Grasslands, which was one half-day shorter, and Alkaline Wet, which was 40.9 days shorter, on average, by the end of the study.

These changes were consistent with rising temperatures and increasing annual growing degree days that can extend the growing season when moisture is available. They were also consistent with increasing CO_2 concentrations that boost vegetation production through a process known as CO_2 fertilization (Sorokin et al. 2017), which enhances water-use efficiency. However, the strength of the relationship between production and annual precipitation over the study period (see Figure 3-5), along with findings from Section 3.7 showing a positive relationship between vegetation production and water

Table 3-2. Changes in land-surface phenology in days averaged by alliance group during the 20-year study.

Alliance group	Hectares	Polygon count	% area	Δ SOS	Δ EOS	Δ LOS	Δ POP
Pinyon-Juniper	62,973.1	508	44.6	–13.7	10.3	22.6	4.4
Dry Shrubland	36,548.8	600	25.9	–12.3	15.1	26.4	0.1
Sparsely Vegetated	11,398	118	8.1	–11.5	18.7	29.9	–0.7
Blackbrush	10,977.8	346	7.8	–16.0	10.2	28.0	1.0
Geology	5,444.4	147	3.9	–13.2	11.6	23.1	1.5
C3/C4 Grassland	3,847	101	2.7	–6.8	–4.7	7.8	7.7
Ponderosa Pine	2,985.9	70	2.1	–11.7	18.5	30.1	–4.9
Water	1,731.8	2	1.2	–5.1	10.0	13.5	–3.2
Annual Exotic Grassland	1,297.5	55	0.9	–3.0	–4.7	–0.5	10.6
Juniper	1,109.7	70	0.8	–16.7	6.6	26.2	0.0
Dry Sagebrush	1,021.1	46	0.7	–12.7	7.8	23.4	–2.2
Riparian	701.6	43	0.5	–4.7	10.7	12.9	0.8
Dry Wash	607.8	34	0.4	–13.9	14.8	29.8	–0.2
Disturbed	273.7	8	0.2	–5.3	8.6	16.9	12.2
Wet Shrubland	261.1	16	0.2	–3.0	6.3	9.9	–5.3
Alkaline Wet	19.4	2	0	31.2	–0.6	–40.9	31.2
Mixed Montane Shrubland	10	1	0	–26.5	16.7	41.3	5.4
Douglas-fir	9	1	0	–10.9	13.4	24.7	10.7

ΔSOS = days change in start of season; ΔEOS = days change in end of season; ΔLOS = days change in length of season; ΔPOP = days change in period of peak growth. Trends for each polygon are in Table S-7 (Thoma 2023a). Significant trends can be found by filtering Table S-7 on p-value <0.05.

availability, suggested most of the increase in production was related to increases in water availability during the study, which may have been augmented by increases in CO_2.

3.10 Drivers of green-up

3.10.1 A priori model selection method

At the park scale, the most common a priori competitive model of green-up timing (see Table 2-4) was GDD and cumulative P between January 1 and the SOS date. Other competitive models included AET, which incorporates both the water and heat needed for growth (Figure 3-18). At the alliance-group level, GDD and P were the only variables important in every group (Figure 3-19).

Growing degree days are likely important because spring soil moisture is typically at its highest level of the year after the winter recharge period, and warming temperatures are necessary to break dormancy. The importance of P during the calendar year may indicate that the water-holding capacity of soil requires spring precipitation to fill to capacity in some years. Otherwise, insufficient precipitation may limit the initiation of growth. This can occur when dry fall and winter periods result in low spring moisture levels that could become a co-limiting factor to temperature following dry winters.

3.10.2 Random-forest method

Variable-importance plots showed the best predictors of SOS were Meltd, Tmin, P, GDD, and AET (Figure 3-20). These findings were like those in the multi-variable regression models, where T and P were important,

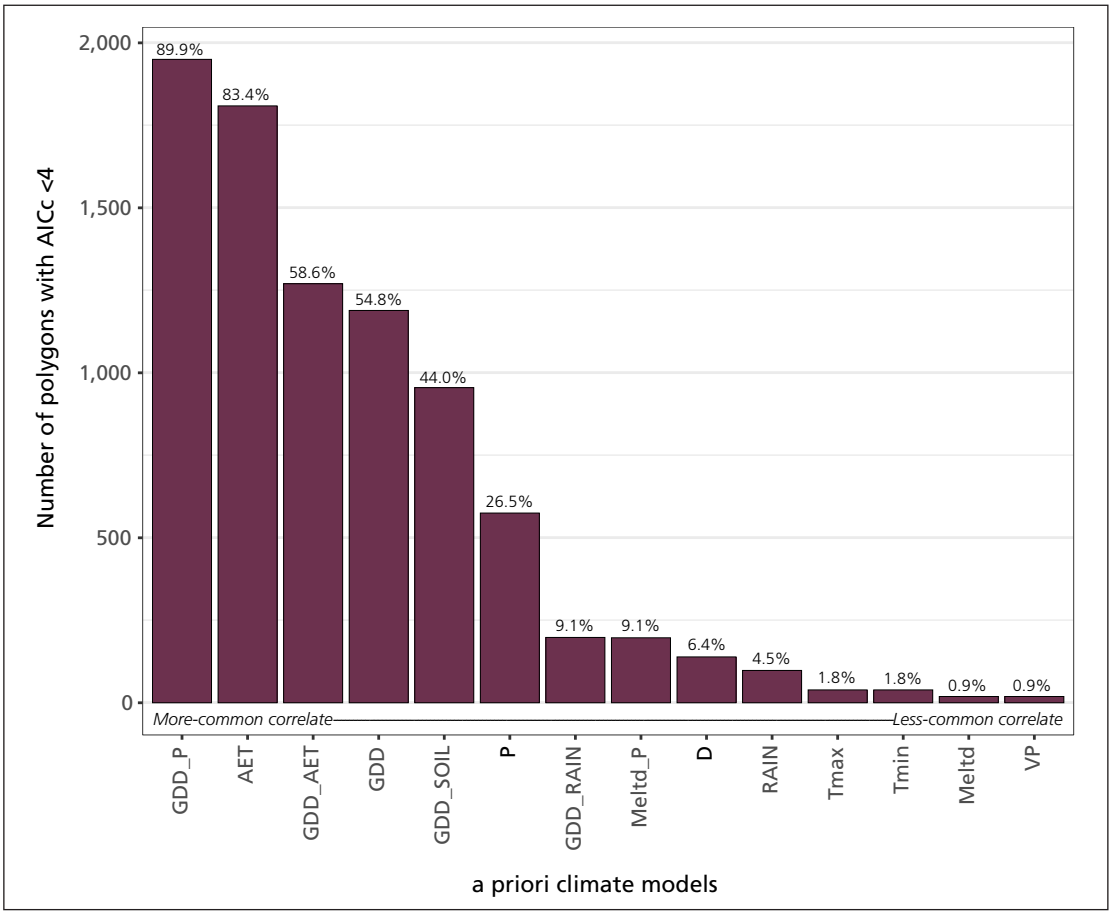

Figure 3-18. Top models in multi-model comparisons of climate correlates with start-of-season at the whole-park scale. The x-axis labels refer to a priori climate models as determinants of SOS. GDD = growing degree days, SOIL = soil moisture, RAIN = precipitation as rain, Tmax = maximum temperature, Tmin = minimum temperature, Srad = solar radiation, Meltd = day of complete snowmelt, AET = actual evapotranspiration, P = precipitation, VPD = vapor-pressure deficit.

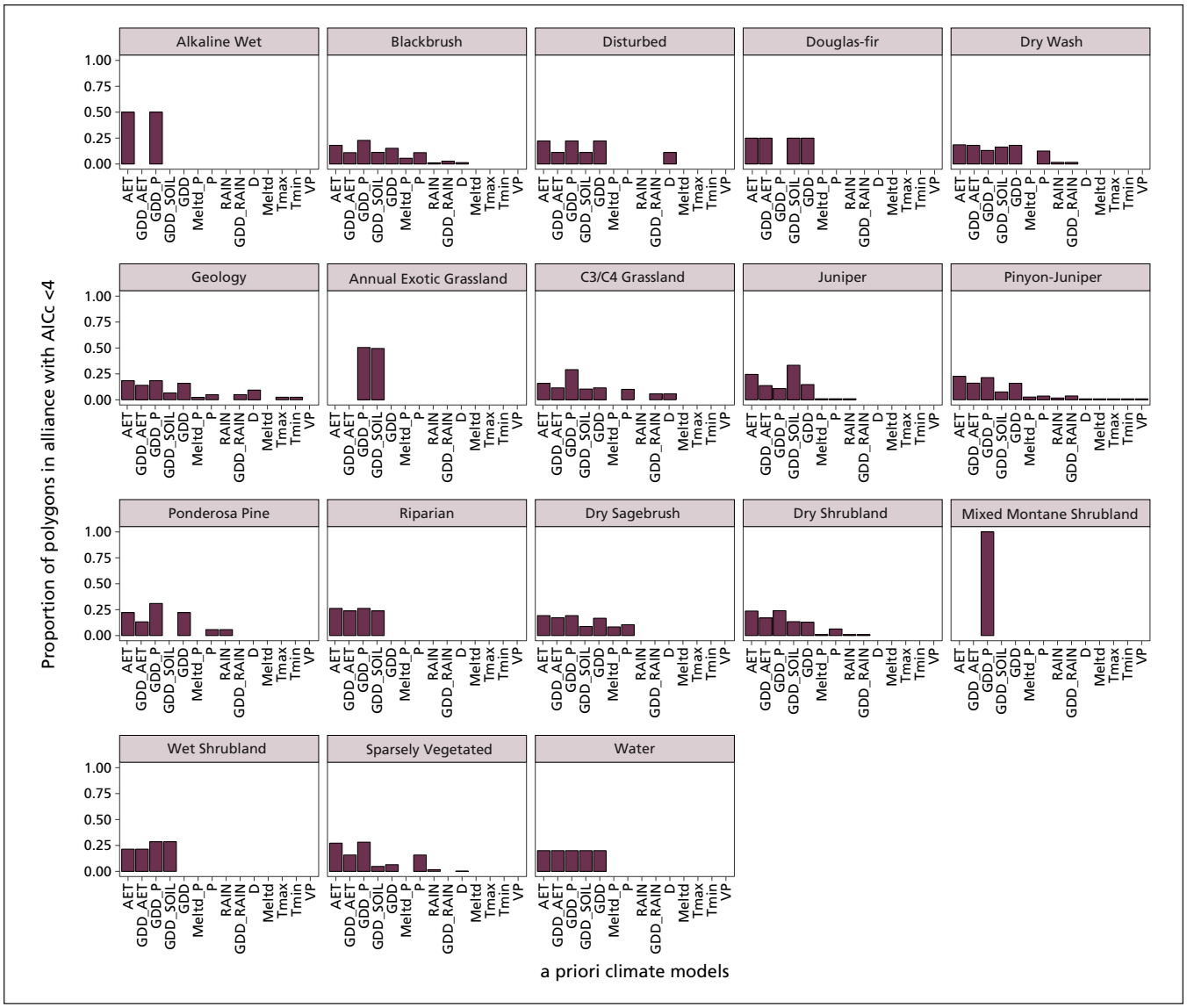

Figure 3-19. Top models in multi-model comparisons of climate correlates with start-of-season at the alliance-group scale. The x-axis labels refer to a priori climate models as determinants of SOS. GDD = growing degree days, SOIL = soil moisture, RAIN = precipitation as rain, Tmax = maximum temperature, Tmin = minimum temperature, Srad = solar radiation, Meltd = day of complete snowmelt, AET = actual evapotranspiration, P = precipitation, VPD = vapor-pressure deficit.

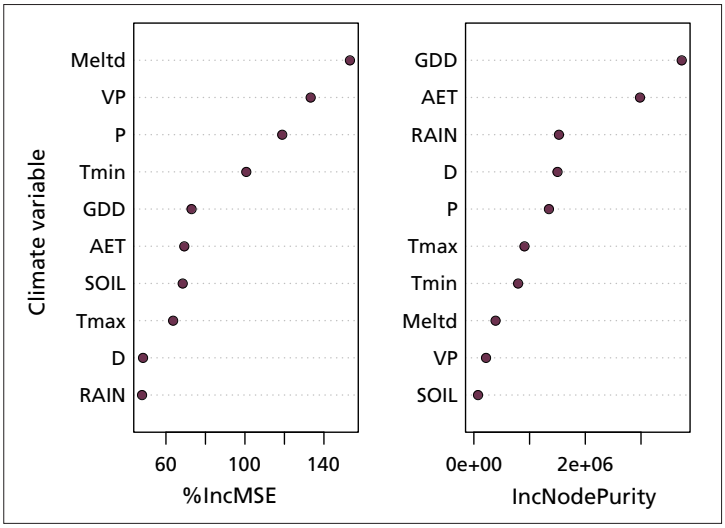

Figure 3-20. Variable importance in the random-forest model of climate drivers of SOS. Percent increase in mean square error (%IncMSE) is a measure of model performance with each variable. Increase in node purity (IncNodePurity) is the difference in residual sum of squares in regression with or without each variable.

but with the addition of Meltd and VP as important variables.

Findings from the two modeling methods suggested a combination of temperature and moisture are important indicators of SOS, as is expected in cold, semi-arid climates. The loss of snow cover that exposes vegetation to warming and solar radiation in spring makes intuitive sense as a driver for the start of growth at higher elevations, where snow accumulates over winter. The effect of spring precipitation is less intuitive unless soil moisture was not sufficiently replenished over winter to meet plant needs.

The random-forest model obtained from the training dataset was used to model SOS in the validation dataset to determine predictive performance. It predicted SOS date at the park scale with a mean absolute error of +/1.5 days (Figure 3-21). When separated by alliance group, the model performed equally well (Figure 3-22).[5]

Inspection of SOS outliers in Figures 3-21 and 3-22 suggests they may have resulted from low-amplitude and monotonic (straight-line) increase in SAVI in some years. This combination makes it difficult

5 The analysis was conducted at the park scale, rather than by polygon (as in Section 3.7.2.1) to increase sample size for the random forest modeling process.

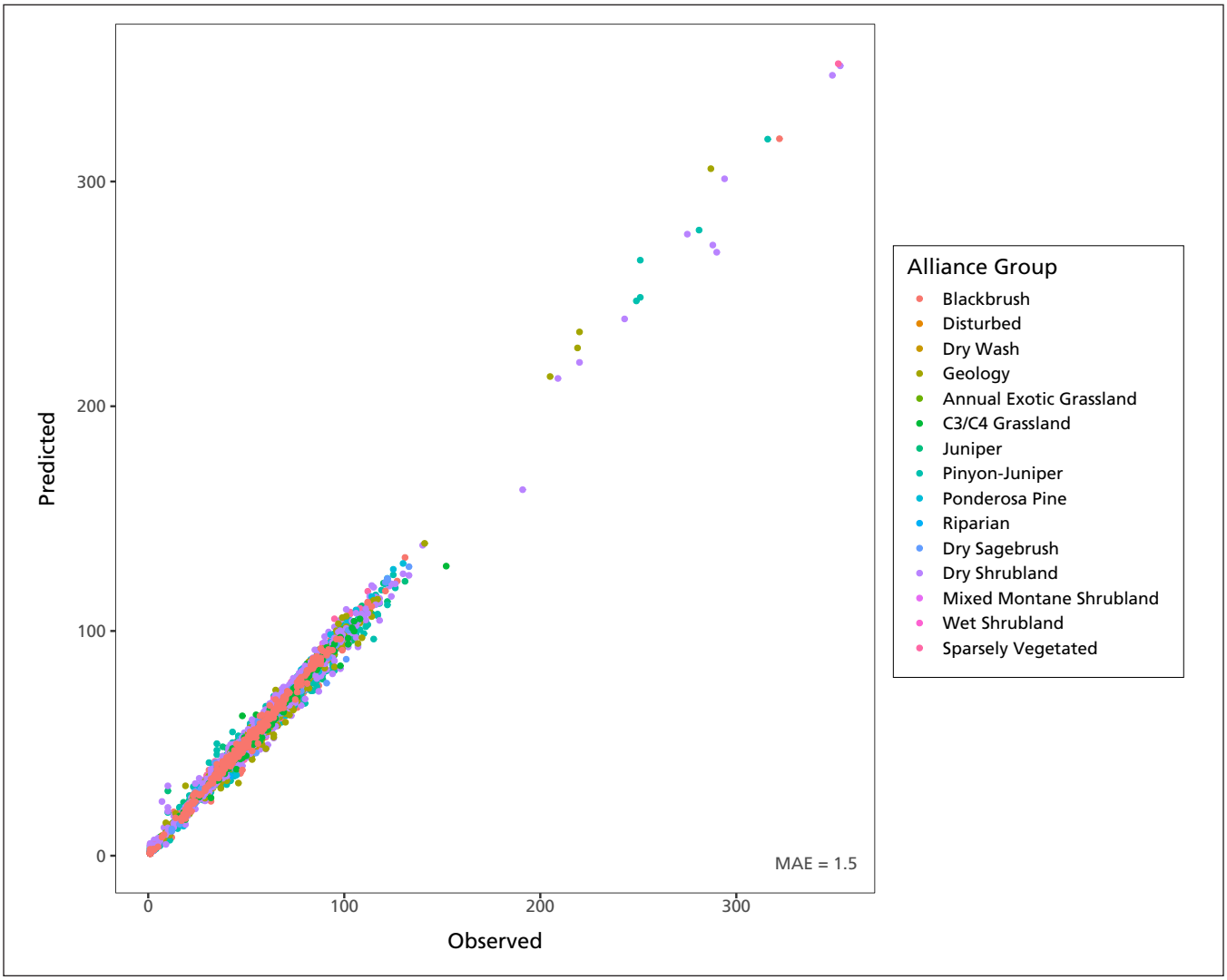

Figure 3-21. Predicted SOS date versus observed SOS date in the holdout dataset used for validation of the random-forests model for all polygons in Canyonlands NP. MAE is mean absolute error of prediction in days. Polygons with annual peaks (POP) occurring between November 1 and April 1 were removed prior to this analysis to minimize effects of vegetation shadows that confound determination of phenology (Norris and Walker 2020).

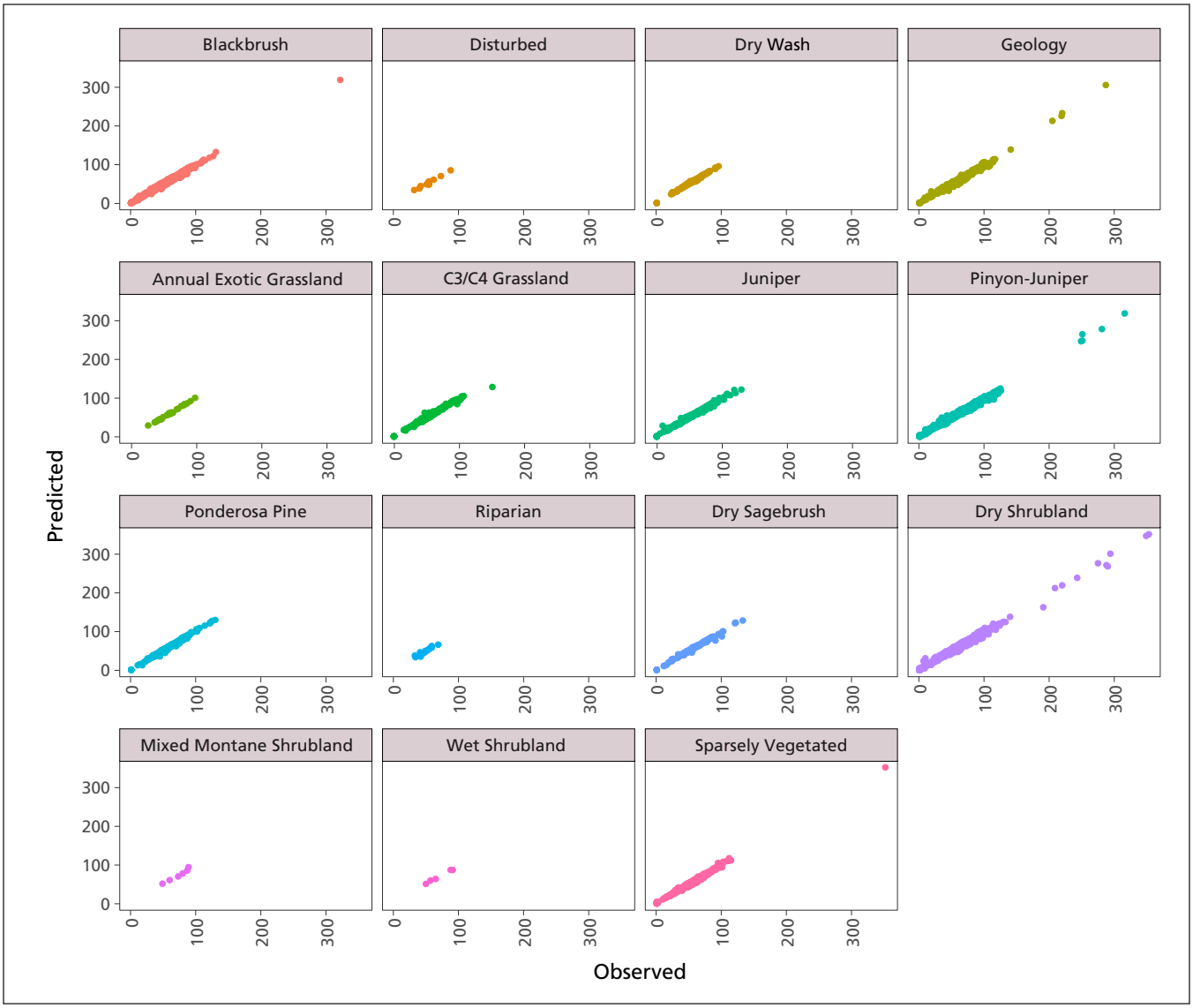

Figure 3-22. Predicted SOS date versus observed SOS date in the holdout dataset used for validation of the random-forests model for alliance groups. Polygons with annual peaks (POP) occurring between November 1 and April 1 were removed from this analysis. Outliers are likely due to difficulty in discriminating SOS when SAVI changes monotonically during a growing season in low-productivity years.

to identify meaningful SOS dates using the derivative method that relies on change in the acceleration of growth rate in spring to determine when growth starts. Even though polygon/year combinations with winter SAVI peaks were screened out of the analysis (per Norris and Walker 2020), it is not clear how SOS may be affected by the shadowing noted in pinyon-juniper and shrubland habitats by Norris and Walker. This is because the shadowing effect is partially dependent on vegetation structure and spacing, which is a continuum of conditions across landscapes. For this reason, modeled SOS dates should be considered with skepticism in the Pinyon-Juniper, Juniper, and all shrubland alliance groups, as well as in polygons that yield outliers in the model of SOS.

Despite these potential shortcomings, the validation demonstrates a strong predictive model of SOS using climate data for most of the Canyonlands NP landscape. This means climate projections could be used to model SOS dates in the future. This could be helpful in assessing potential vulnerabilities caused by phenological mismatch between pollinators and flowering species, as well as potential impacts to migrating birds and mammals, such as deer. Mule deer in some western states "surf the green wave" of vegetation as it greens up progressively across

gradients of latitude and elevation (Aikens et al. 2017; Merkle et al. 2016; van Wijk et al. 2012). Presently, it is unknown if animal species in NCPN parks time their movements with SOS or the green wave thereafter, but this information could be used to help assess whether animals are keyed into this land-surface process.

3.11 Climate patterns

Annual temperature, precipitation, and estimates of actual evapotranspiration, climatic water deficit, and soil moisture derived from the water-balance model for 1980–2019 exhibited high interannual variability (Figure 3-23 and Appendix A, Figure A-6). This variation caused large interannual changes in annual vegetation production.

During 2000–2019, there was a weak, though statistically insignificant ($p > 0.05$) increase in P of 2–4 millimeters per year (Figure 3-24). Average annual T remained stable during the study period (see Figure 3-14 and Figure A-6). The increase in P resulted in a corresponding increase in AET of 1–2 millimeters per year. The effect of these seemingly small changes was important, as illustrated by the significant upward trends in production in some of the alliance groups shown in Section 3.3.

An interesting decadal oscillation in precipitation was evident: peaks in the middle of each decade since 1980 translated to similar peaks in other water-balance variables. The same pattern was apparent in SOIL, AET, and D (Appendix A, Figure A-6), although for D the peaks (maximum drought stress) coincided with the times of least P (Appendix A, Figure A-6). If the periodicity of these cycles continues in the future, it could serve as a useful guide for timing restoration efforts that require substantial planning efforts, long-term investments, and multiple years of minimal drought stress for germination and establishment.

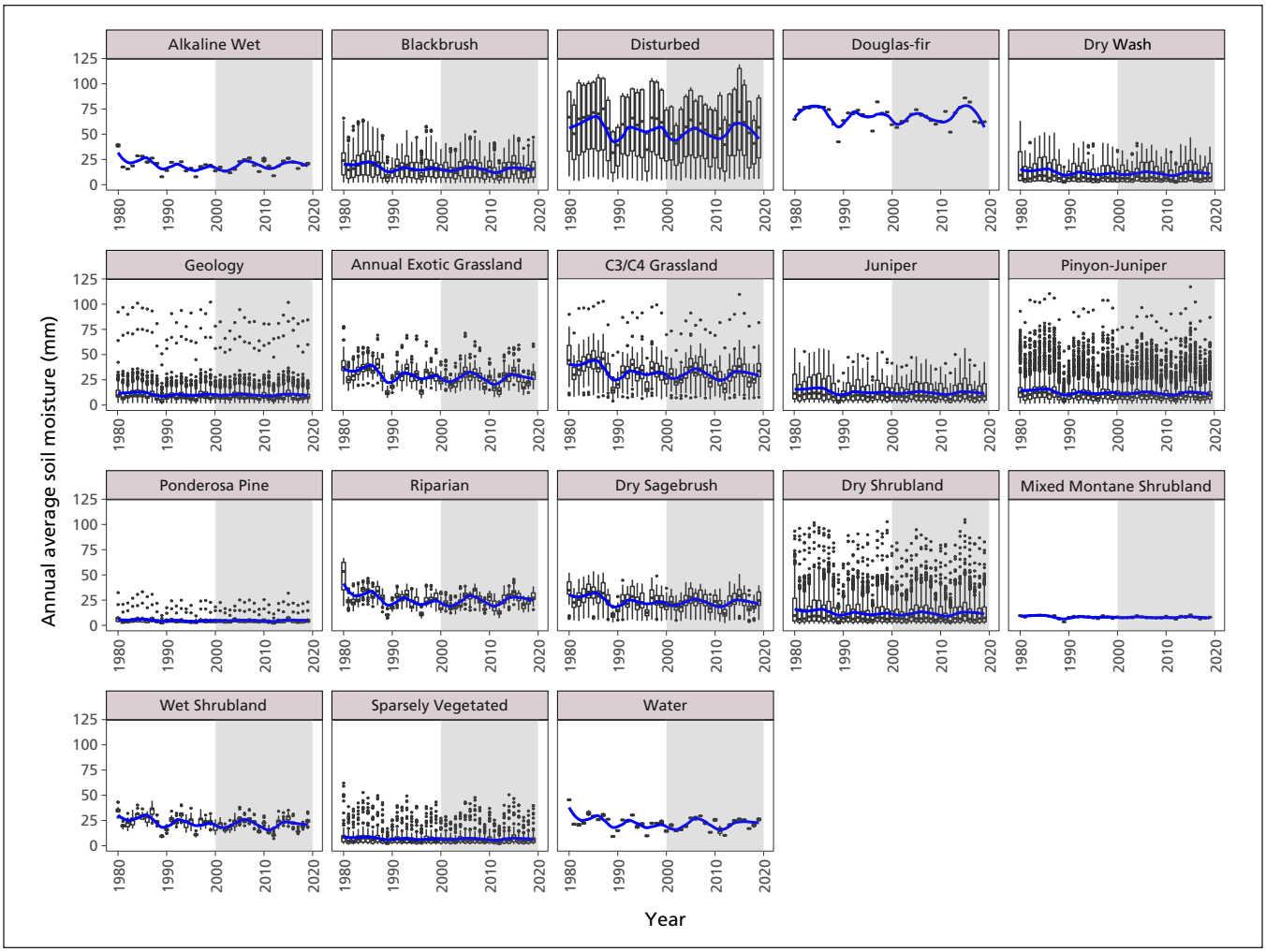

Figure 3-23. Long-term temporal patterns in precipitation in vegetation alliance groups. Box plots demonstrate the range of variation by year. The line is a loess smooth with a 25% span to illustrate multi-year patterns. Gray shaded area includes the period between 2000 and 2019, investigated for relationships between production and climate when satellite imagery and climate data were both available. Study-period trends and associated statistics for the other water-balance variables are presented in Appendix A, Figure A-6.

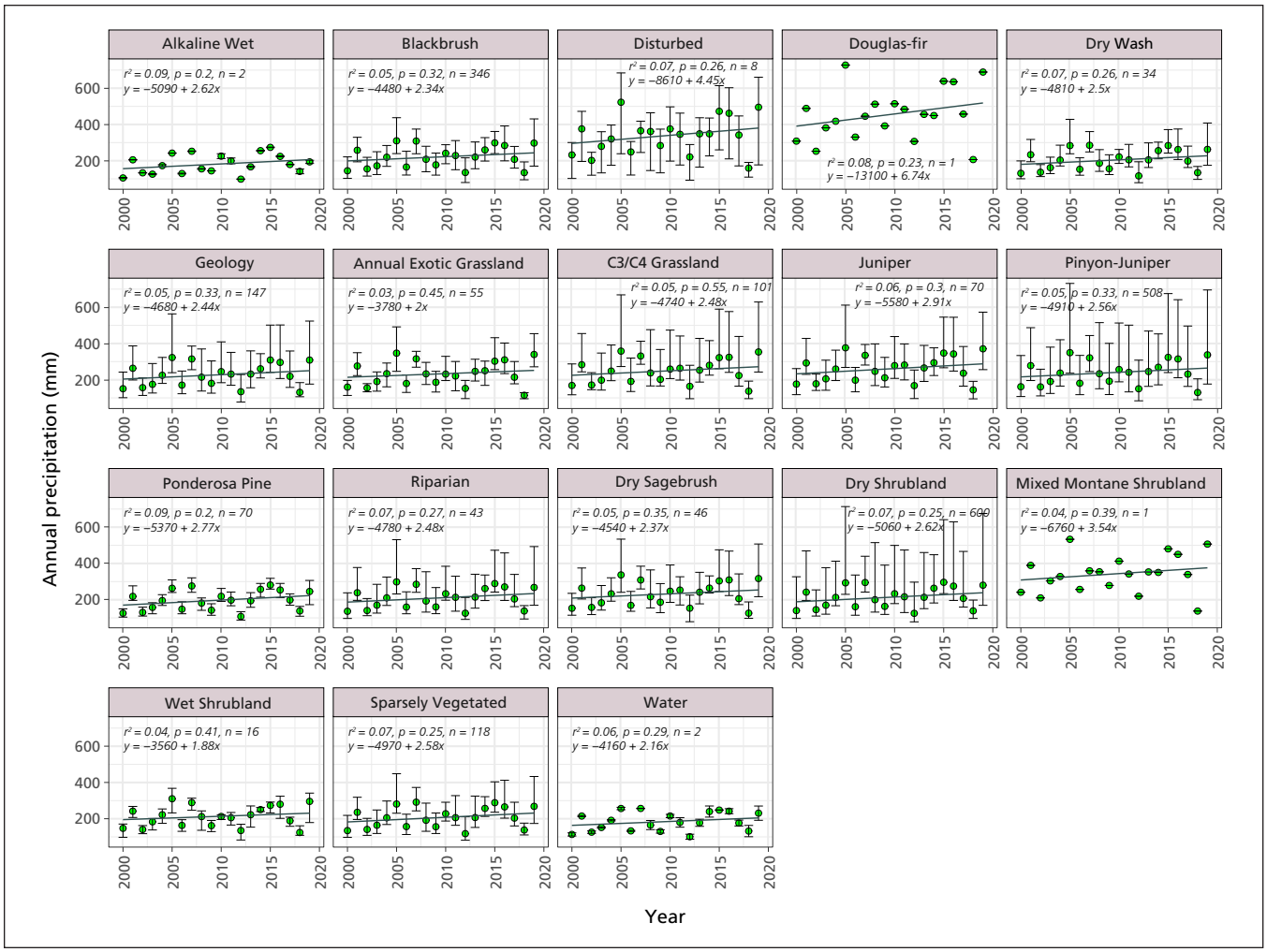

Figure 3-24. Annual precipitation trend over time, 2000–2019. Bars are standard error.

4 How to Use this Report in Climate Smart Conservation Planning

This report provides information that feeds directly into the Climate Smart Conservation framework (Figure 4-1), the process used by the NPS Climate Change Response Program (CCRP) and other federal agencies to make climate-adaptation plans based on plausible future climate and resource responses in climate-scenario planning (NPS 2021; Stein et al. 2014). Results from this report inform Step 2 (Figure 4-1), which assesses climate exposure, vegetation sensitivity, and vulnerability of vegetation to climate change considering inherent adaptive capacity and management actions that help reduce vulnerability (adapted from NPS 2021).

4.1 Identifying management goals

The first step in Climate Smart Conservation is to identify management goals that will inform the planning process. This is usually an iterative process in which initial goals are periodically re-evaluated based on values, vulnerability, and adaptive management. Goals may be determined via planning processes, current threats, or changes that have already occurred. Clearly defined goals help make the rest of the Climate Smart planning process more efficient. In addition to vulnerability and values, management goals may also consider management paradigms of resisting, accepting, or directing change (NPS 2021; Schuurman et al. 2020). The appropriate paradigm depends on the goals informed by values and vulnerability assessments. It may be necessary to implement strategies that reflect more than one paradigm to achieve goals.

4.2 Vulnerability assessment

This report advances understanding of climate as a driver of vegetation production and phenology at alliance-polygon, alliance-group, and whole-park scales at Canyonlands NP. The historical perspective in this report provides the necessary background for understanding the range in variability of climate and vegetation response while also informing how vegetation is likely to respond to weather in the near term and climate change in the long-term. Specifically, results identify how vegetation condition and sensitivity are linked to incremental changes in weather and climate. Thus, this report can be used to determine how vegetation production and phenology may change (increasing or decreasing production) if the relationships described here carry into the

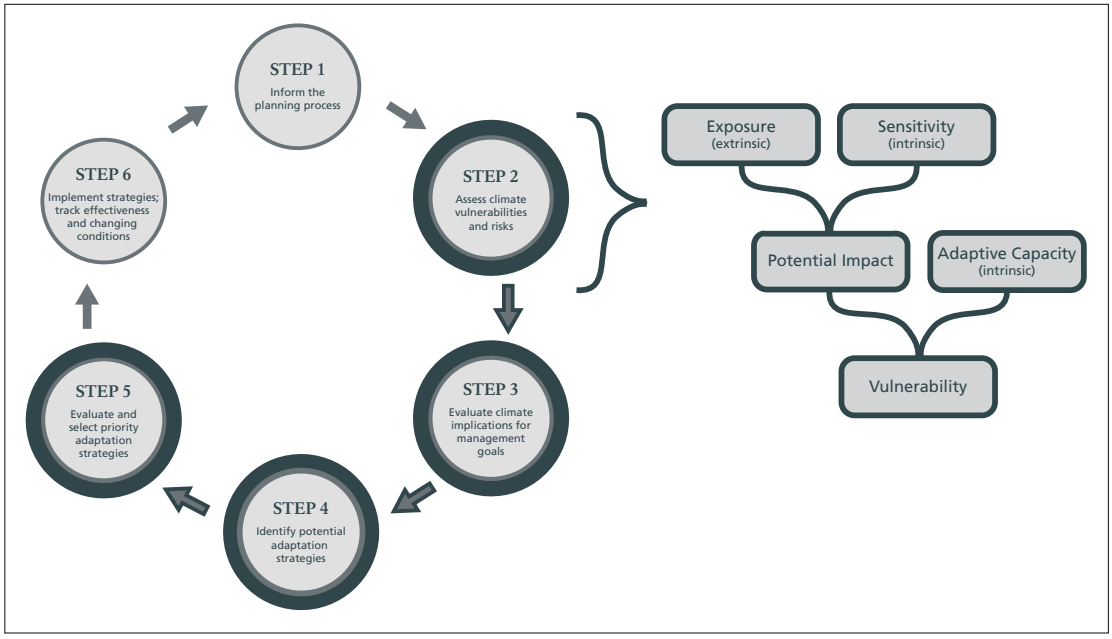

Figure 4-1. The Climate Smart Conservation framework. The concentric circles represent different scenarios that can guide the planning process.

future. Disruption of those relationships can be caused by gradual transitions of native vegetation, exotic-species invasions, disturbance, or land-use change.

Vegetation response in this report is synonymous with the concept of climate sensitivity in the Climate Smart Conservation context (see Figure 4-1), which is a critical step in determining vulnerability to climate change. Sensitivity to climate determines how much, and how rapidly, vegetation production changes with climate. Sensitivity is obtained from the slope of the regression line in the relationship between interannual variation in growing-season iSAVI (surrogate for change in annual production) and any one climate variable (see Figure 2-3 and Thoma 2023a, Tables S-2 and S-4).

This report and Thoma (2023a; Tables S-2 and S-4) are designed for use as a vegetation vulnerability assessment at the polygon and alliance-group levels for Canyonlands NP. Quantitative vulnerability assessments evaluate climate-change exposure and vegetation sensitivity, and indicate how they will likely interact in the future to affect vegetation condition. They can be used to determine what, where, when, and why change may occur. The information in this report can be used to identify what is likely to change (based on alliance-group and polygon composition and sensitivity), where change is likely (the location of each climate-sensitive polygon), when changes may occur (soon, or later this century), and why change is likely (based on strength of relationship between production and water deficit, precipitation or other variable).

Historic and future exposure to many climate variables are included in this report (Appendix A, Figure A-6; Christensen et al. 2021). Pivot points and sensitivity by polygon or alliance group are summarized in maps, charts, and tables (Appendix A, Figures A-2 and A-3; Thoma 2023a, Tables S-2 and S-4), as is the role of site characteristics, such as soil properties, that modify sensitivity (see Figure 3-13). Future vulnerability (Figure 4-2) is determined by comparing different climate projections (climate scenarios in Christensen et al. 2021) to pivot points for each polygon (Table S-2 in Thoma 2023a). This quantifies how frequently production falls below average conditions. If future production consistently falls below historic average conditions, then a vegetation assemblage is likely to transition into another better-suited to the new climate conditions. The following section demonstrates how to use data in this report for a polygon-level vulnerability assessment.

4.3 Using pivot points and responses in climate-adaptation planning

The annual pivot points and responses described here are useful for understanding how different aspects of climate (water availability, water use, water need, and temperature) affect vegetation. Additionally, pivot points and responses are integrative, useful ecological variables that complement assessments of exposure and sensitivity used for climate-adaptation planning. They combine effects of temperature, precipitation, and plant traits with site characteristics into single-variable descriptions of water use (AET) and unmet water need (D) (Tercek et al. 2021) that are place-based and uniquely identified for each alliance polygon.

Water-balance pivot points and responses are well-suited for applications that benefit from the simplicity of single-variable descriptions of climate exposure (such as T and P), but are more biophysically related to natural-resource response (Stephenson 1998; Thoma et al. 2020). The quantitative assessment of vegetation sensitivity to climate and water-balance variables on an annual basis is a good starting point for the initial phase of long-range climate-adaptation planning.

4.4 Example vulnerability assessment

Below, an example of a quantitative vulnerability assessment for Canyonlands NP is presented using a pivot point and two future scenarios. Rather than considering all possible climate futures (currently, 24 scenarios are available for consideration), which can be overwhelming, two scenarios shown in Christensen and others (2021) were intentionally selected to bracket a wide range of

plausible future conditions at Canyonlands NP. These include a best-case scenario of warming and increasing precipitation, and a worst-case scenario of warming and reduced precipitation. Climate exposure at Canyonlands NP will increase over time (Christensen et al. 2021) as declines in soil moisture and increases in water deficit play out under either a warmer and wetter or warmer and drier future. This is because the rate of warming under both scenarios will result in drying that will outstrip projected changes in precipitation, even for the wetter scenario. In both scenarios, the interaction of T and P will result in earlier and longer dry seasons (Christensen et al. 2021).

For illustrative purposes, a vulnerability analysis for a single Pinyon-Juniper polygon in Canyonlands NP identifies exposure (change in climate over time), drought tolerance (pivot point determined from remote sensing), and vulnerability (frequency of pivot-point exceedance) in the future (Figure 4-2). The vulnerability assessment for this polygon, located near the park's center, was made by comparing pivot points (critical water need) to future water-balance conditions at Canyonlands NP. In this case, the annual soil-moisture pivot point for polygon CANY_17090 was 3.5 millimeters (calculated as the mean Gridmet deficit, which is the historic climate dataset appropriate for use with climate projections).

Under the warm-and-wet (best-case) scenario, annual soil moisture will only achieve the historical soil moisture pivot point occasionally—meaning that even in the best case, soil moisture will not be sufficient to meet vegetation needs in this polygon. This will likely result in transition to a different vegetation assemblage due to drought stress.

Under the warm-and-dry (worst-case) scenario, soil moisture will be lower than the best-case scenario in most years. This will result in more intense and prolonged drought stress that will likely make transitions happen sooner. It may also result in more dry-adapted vegetation composition than in the best-case scenario.

The greatest uncertainty in this analysis is the representative concentration pathway

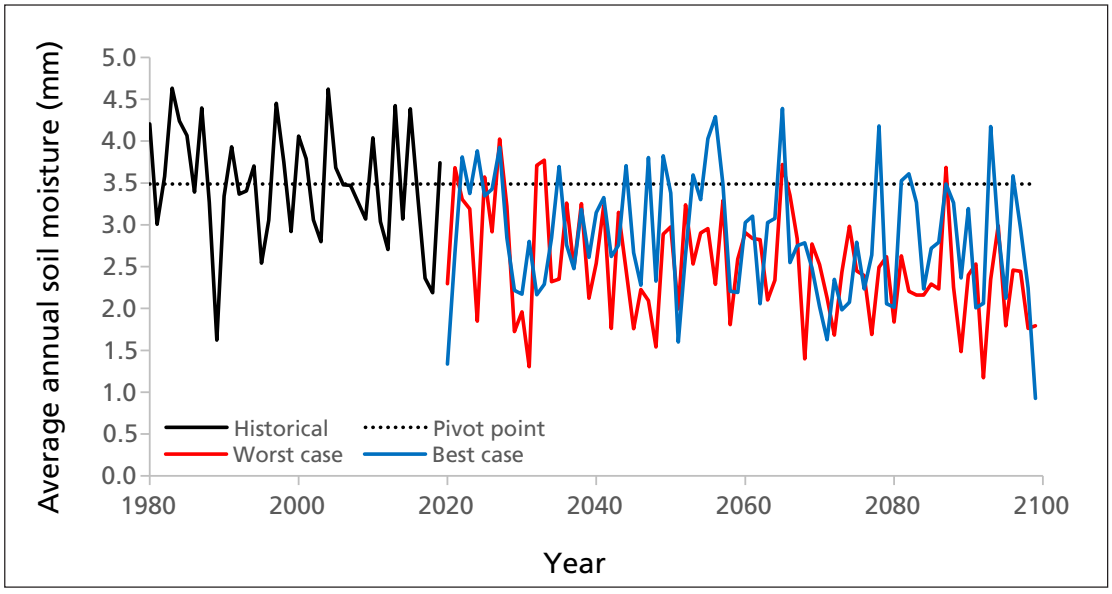

Figure 4-2. Quantitative vulnerability analysis for a single Pinyon-Juniper polygon. Here, the projected change in annual average soil moisture relative to the pivot point is shown for a location at the park centroid (polygon CANY_17190), which falls in the Pinyon-Juniper alliance group. The average annual soil-moisture pivot point for this polygon was determined as 3.5 millimeters per year from the historical Gridmet climate dataset compatible with climate projections (screenedcleanedsummaries.s3-website-us-west-2.amazonaws.com). The best- and worst-case scenarios were selected from a range of many plausible futures derived from temperature and precipitation projections from the World Climate Research Program CMIP5 experiments (CMIP5; wcrp-climate.org). The temperature and precipitation data were passed through the water-balance model to generate future projections of the water-balance variables. The wetting scenario is the "best" case in this example. The projection data used to build this figure were from the climate-exposure analysis summary used to create the report in Christensen and others (2021).

(RCP) (4.5/best-case or 8.5/worst-case) that models CO_2 emissions resulting from societal choices to reduce greenhouse emissions—far more so than the uncertainty in vegetation response to climate. For this reason, the next decade will be important to determining the trajectory of exposure.

The analysis demonstrated here can be recreated to determine site-specific vulnerability for any polygon in Canyonlands NP. Until such analyses using climate projections are quantitatively linked to pivot points in this report (as in Figure 4-2), users can gain a sense of vulnerability by sorting on pivot or slope in Tables S-3 and S-4 of Thoma (2022) to identify the most-sensitive and most drought-tolerant polygons and alliance groups.

4.5 Identify and implement management actions

In planning for the future, the importance of vulnerability assessments for understanding and managing through climate change is underscored by statements from the Intergovernmental Panel on Climate Change (IPCC). As the summary for policymakers of their recent report states, "Global surface temperature will continue to increase until at least the mid-century under all emissions scenarios considered. Global warming of 1.5°C and 2°C will be exceeded during the 21st century unless deep reductions in carbon dioxide (CO_2) and other greenhouse gas emissions occur in the coming decades." It goes on to say, "Continued global warming is projected to further intensify the global water cycle, including its variability, global monsoon precipitation and the severity of wet and dry events" (IPCC 2021).

Vulnerability assessments can help identify the timing and type of management actions needed to achieve management goals in the face of an uncertain future. Additionally, they can help determine if existing actions are likely to achieve existing goals, if new management strategies are needed to achieve goals, or if management goals are unrealistic and need to be revised. After management goals and vulnerability assessments are reconciled, management options likely to achieve management goals can be identified and implemented (Steps 3–6 in Figure 4-1).

4.6 Tools to inform near-term management

Tracking weather conditions that lead up to or surpass pivot points during the growing season is a useful climate-based tool for assessing vegetation condition—but it provides an indirect assessment. Additional tools can provide real-time assessments of vegetation condition by identifying both trends in vegetation greenness and the vegetation anomaly (a comparison of current versus past growing conditions). With these tools, users can iteratively identify both the spatial pattern and strength of trends and where disturbance or unusual events are happening in near-real time.[1] Interpreting the link between those patterns and climate requires contemporaneous climate data. Gridded climate data used in this report were created from weather-station data, typically in the year following a full year of data collected at weather stations. Weather-station data are better suited to investigations of real-time change in conditions, especially extreme events that garner interest as they happen or soon after—as was the case when park managers noted juniper mortality in 2018 and 2019 (see Section 3.6.1).

The NCPN supports ClimateAnalyzer.org, which makes accessing weather-station data intuitive and easy. Data from the park weather station and other sources can be used to determine how weather and vegetation condition vary together in near real-time. This could be the basis for real-time condition assessments used in the tactical decisions needed to achieve long-range management goals. Care must be taken when analyzing trends from weather-station data due to missing values and outliers. Nevertheless, over the period of time analyzed in this report, the upward trend in station precipitation and no-trend in average temperature were consistent with the trends found using Daymet, the gridded climate data used in analysis for this report.

1 More information on these tools can be obtained from the author of this report.

5 Conclusions

The US Southwest has been in an extended drought over the past 20–30 years. However, even during extended drought there can be periods of increased precipitation. This study, which began in 2000 and ended in 2019, needs to be considered in that context.

The years 2000–2003 were among the driest between 1980 and 2019. In this study, the initial extremely dry conditions set the stage for subsequent trends in which precipitation increased (from the near-record low in 2000), resulting in increases in vegetation growth relative to conditions at the start of the study. The variation in vegetation condition across wet and dry years was evaluated to identify which alliance groups were most drought-tolerant (Water, Alkaline Wet, and Ponderosa Pine), and which were least drought tolerant (Douglas-fir, Mixed Montane Shrubland, and Disturbed). Similarly, variation in climate over the study period was used to determine that Wet Shrubland, C3/C4 Grassland, and Annual Exotic Grassland were the most sensitive to precipitation, while Douglas-fir and Mixed Montane Shrubland were least-sensitive.

The climate variable most strongly correlated with vegetation production was three years of soil moisture. Growing degree days and calendar-year precipitation were the primary determinants of green-up timing. Over the study period, the start of growing season shifted earlier, and the length of growing season increased, likely due to warming and a slight increase in precipitation during the study.

The variation in weather conditions and corresponding vegetation response provide a window into the past that will inform understanding and management of vegetation that has always responded—and will continue to respond—to climate at Canyonlands NP. Much of the specific information in this report will soon be outdated. However, some of the findings described here, such as pivot points and sensitivity of vegetation to weather and climate, have long-term value and are unlikely to change until vegetation composition changes in the future. This is because drought tolerance and response to weather are factors inherent to the natural-history traits of vegetation and where it grows.

However, climate is changing rapidly, and extreme weather events are becoming more frequent. The tools developed for these analyses can help National Park Service managers to anticipate and plan for climate change—and to manage change as it happens. This report demonstrates how combining satellite observations of vegetation condition with climate data can help determine the right time and place for action needed in the near term to help achieve long-range management goals for stewarding park resources through continuous change.

6 Literature Cited

Aikens, EO, MJ Kauffman, JA Merkle, SPH Dwinnell, GL Fralick, and KL Monteith. 2017. The greenscape shapes surfing of resource waves in a large migratory herbivore. Ecology Letters. https://doi.org/10.1111/ele.12772.

Allen, CD, DD Breshears, and NG McDowell. 2015. On underestimation of global vulnerability to tree mortality and forest die-off from hotter drought in the Anthropocene. Ecosphere 6. https://doi.org/10.1890/ES15-00203.1.

Barger, NN, SR Archer, JL Campbell, C Huang, JA Morton, and AK Knapp. 2011. Woody plant proliferation in North American drylands: A synthesis of impacts on ecosystem carbon balance 116, 1–17. https://doi.org/10.1029/2010JG001506.

Barnes, ML, MS Moran, RL Scott, TE Kolb, GE Ponce-Campos, DLP Moore, MA Ross, B Mitra, and S Dore. 2016. Vegetation productivity responds to sub-annual climate conditions across semi-arid biomes. Ecosphere 7:1–20. https://doi.org/10.1002/ecs2.1339.

Bisigato, AJ, L Hardtke, and HF del Valle. 2013. Soil as a capacitor: Considering soil water content improves temporal models of productivity. Journal of Arid Environments 98:88–92. https://doi.org/10.1016/j.jaridenv.2013.08.004.

Breiman, L. 2001. Random forests. Machine Learning 45:5–32. https://doi.org/10.1201/9780367816377-11.

Bunting, EL, SM Munson, and JB Bradford. 2019. Assessing plant production responses to climate across water-limited regions using Google Earth Engine. Remote Sensing of Environment 233:111379. https://doi.org/10.1016/j.rse.2019.111379.

Christensen, J, D Thoma, M Tercek, and J Gross. 2021. Historical and projected water balance report for Canyonlands NP National Park. Unpublished report. https://irma.nps.gov/DataStore/Reference/Profile/2299344.

Davis, RS, M Newcomb, and D Ott. 2022. USFS Intermountain Region Forest Health Protection: Southeast Utah Juniper dieback–2021 follow-up measurements of survey plots. FHP trip report OFO-TR-21-18. USDA Forest Service, Intermountain Region, Forest Health Protection, Ogden, Utah.

de Beurs, KM, and GM Henebry. 2010. Spatio-temporal statistical methods for modelling land surface phenology. Pages 177–208 *in* IL Hudson and MR Keatley, eds., Phenological research: Methods for environmental and climate change analysis. Springer Science+Business Media BV. https://doi.org/10.1007/978-90-481-3335-2.

Dickman, LT, NG McDowell, S Sevanto, RE Pangle, and WT Pockman. 2015. Carbohydrate dynamics and mortality in a piñon-juniper woodland under three future precipitation scenarios. Plant, Cell, and Environment 38(4):729–739. https://doi.org/10.1111/pce.12441.

Didan, K, AB Munoz, R Solano, and A Huete. 2015. MODIS vegetation index user's guide (Collection 6). University of Arizona, Tucson, AZ.

Dunn, HA, and KM de Beurs. 2011. Land surface phenology of North American mountain environments using moderate resolution imaging spectroradiometer data. Remote Sensing of Environment 115(5):1220–1233. https://doi.org/10.1016/j.rse.2011.01.005.

Federal Geographic Data Committee (FGDC). 2008. National Vegetation Classification Standard, Version 2. February. U.S. Geological Survey, Reston, Virginia. http://usnvc.org/wp-content/uploads/2011/02/NVCS_V2_FINAL_2008-02.pdf.

Forkel M. 2015. greenbrown land surface phenology and trend analysis. https://greenbrown.r-forge.r-project.org/.

Forkel, M, N Carvalhais, J Verbesselt, M Mahecha, CSR Neigh, and MD Reichstein. 2013. Trend change detection in NDVI Timeseries: Effects of inter-annual variability and methodology. Remote Sensing 5(5):2113–2144. https://doi.org/10.3390/rs5052113.

Fu, Y, H Zhang, W Dong, and W Yuan. 2014. Comparison of phenology models for predicting the onset of growing season over the northern hemisphere. PLoS ONE 9(10):e109544. https://doi.org/10.1371/journal.pone.0109544.

Garroutte, E, A Hansen, and R Lawrence. 2016. Using NDVI and EVI to map spatiotemporal variation in the biomass and quality of forage for migratory elk in the Greater Yellowstone Ecosystem. Remote Sensing 8(5):404. https://doi.org/10.3390/rs8050404.

González, Eduardo, Patrick B. Shafroth, Steven R. Lee, Steven M. Ostoja, and Matthew L. Brooks. 2020. Combined effects of biological control of an invasive shrub and fluvial processes on riparian vegetation dynamics. Biological Invasions 22(7):2339–2356. https://doi.org/10.1007/s10530-020-02259-9.

Gremer, JR, C Andrews, JR Norris, LP Thomas, SM Munson, MC Duniway, and JB Bradford. 2018. Increasing temperature seasonality may overwhelm shifts in soil moisture to favor shrub over grass dominance in Colorado Plateau drylands. Oecologia 188:1195–1207. https://doi.org/10.1007/s00442-018-4282-4.

Grossiord, C, TN Buckley, LA Cernusak, KA Novick, B Poulter, RTW Siegwolf, JS Sperry, and NG McDowell. 2020. Plant responses to rising vapor-pressure deficit. New Phytologist 226:1550–1566. https://doi.org/10.1111/nph.16485.

Huete, AR. 1988. A soil-adjusted vegetation index (SAVI). Remote Sensing of Environment 25(3):295–309. https://doi.org/10.1016/0034-4257(88)90106-X.

Intergovernmental Panel on Climate Change (IPCC). 2021. Summary for policymakers, *in* Climate change 2021: The physical science basis. Contribution of Working Group I to the Sixth Assessment Report of the Intergovernmental Panel on Climate Change, V Masson-Delmotte, P Zhai, A Pirani, SL Connors, C Péan, S Berger, N Caud, Y Chen, L Goldfarb, MI Gomis, M Huang, K Leitzell, E Lonnoy, JBR Matthews, TK Maycock, T Waterfield, O Yelekçi, R Yu, and B Zhou, eds. https://www.ipcc.ch/report/ar6/wg1/downloads/report/IPCC_AR6_WGI_SPM_final.pdf.

Jennings, MD, D Faber-Langendoen, OL Loucks, RK Peet, and D Roberts. 2009. Standards for associations and alliances of the US National Vegetation Classification. Ecological Monographs 79:173–199. https://doi.org/10.1890/07-1804.1.

Johnson, HE, DD Gustine, TS Golden, LG Adams, LS Parrett, EA Lenart, and PS Barboza. 2018. NDVI exhibits mixed success in predicting spatiotemporal variation in caribou summer forage quality and quantity. Ecosphere 9. https://doi.org/10.1002/ecs2.2461.

Kariyeva, J, and WJD van Leeuwen. 2011. Environmental drivers of NDVI-based vegetation phenology in Central Asia. Remote Sensing 3(2):203–246. https://doi.org/10.3390/rs3020203.

Lauenroth, WK, and JB Bradford. 2012. Ecohydrology of dry regions of the United States: Water balance consequences of small precipitation events. Ecohydrology 5:46–53.

McMaster, GS, and WW Wilhem. 1997. Growing degree days: One equation, two interpretations. Agricultural and Forest Meteorology 87(4):291–300.

Mendez-Barroso, LA, ER Vivoni, CJ Watts, and JC Rodriguez. 2009. Seasonal and interannual relations between precipitation, surface soil moisture and vegetation dynamics in the North American monsoon region. Journal of Hydrology 377(1–2):59–70. https://doi.org/10.1016/j.jhydrol.2009.08.009.

Merkle, JA, KL Monteith, EO Aikens, MM Hayes, KR Hersey, AD Middleton, BA Oates, H Sawyer, BM Scurlock, and MJ Kauffman. 2016. Large herbivores surf waves of green-up during spring. Proceedings of the Royal Society B: Biological Sciences 283:1–8. https://doi.org/10.1098/rspb.2016.0456.

Munson, SM. 2013. Plant responses, climate pivot points, and trade-offs in water-limited ecosystems. Ecosphere 4(9):1–15. https://doi.org/10.1890/ES13-00132.1.

Munson, SM, MC Duniway, and JK Johanson. 2016. Rangeland monitoring reveals long-term plant responses to precipitation and grazing at the landscape scale. Rangeland Ecological Management 69(1):76–83.

Munson, SM, RH Webb, J Belnap, JA Hubbard, DE Swann, and S Rutman. 2011. Forecasting climate change impacts to plant community composition in the Sonoran Desert region. Global Change Biology 18(3):1083–1095. https://doi.org/10.1111/j.1365-2486.2011.02598.x.

Munson, SM, RH Webb, DC Housman, KE Veblen, KE Nussear, EA Beever, KB Hartney, MN Miriti, SL Phillips, RE Fulton, and NG Tallent. 2015. Long-term plant responses to climate are moderated by biophysical attributes in a North American desert. Journal of Ecology 103(3):657–668. https://doi.org/10.1111/1365-2745.12381.

Nagler, PL, U Nguyen, HL Bateman, CJ Jarchow, EP Glenn, WJ Waugh, and C van Riper. 2018. Northern tamarisk beetle (*Diorhabda carinulata*) and tamarisk (*Tamarix* spp.) interactions in the Colorado River basin. Restoration Ecology 26(2):348–59. https://doi.org/10.1111/rec.12575.

National Park Service (NPS). 2021. Planning for a changing climate: Climate-Smart Planning and Management in the National Park Service. NPS Climate Change Response Program, Fort Collins, Colorado. https://irma.nps.gov/DataStore/Reference/Profile/2279647.

Natural Resources Conservation Service (NRCS). 2015. Web soil survey. http://websoilsurvey.nrcs.usda.gov.

Norris, JR, and JJ Walker. 2020. Solar and sensor geometry, not vegetation response, drive satellite NDVI phenology in widespread ecosystems of the western United States. Remote Sensing of Environment 249:112013. https://doi.org/10.1016/j.rse.2020.112013.

Noy-Meir, I. 1973. Desert Ecosystems: Environment and producers. Annual Review of Ecology and Systematics 4:25–51. https://doi.org/10.1146/annurev.es.04.110173.000325.

Oudin, L, F Hervieu, C M, C Perrin, V Andréassian, F Anctil, and C Loumagne. 2005. Which potential evapotranspiration input for a lumped rainfall-runoff model? Part 2 Towards a simple and efficient potential evapotranspiration model for rainfall-runoff modelling. Journal of Hydrology 303(1–4):290–306. https://doi.org/10.1016/j.jhydrol.2004.08.026.

Paruelo, JM, M Oesterheld, CM Di Bella, M Arzadum, J. Lafontaine, M Cahuepé, and CM Rebella. 2000. Estimation of primary production of subhumid rangelands from remote sensing data. Applied Vegetation Science 3(2):189–195. https://doi.org/10.2307/1478997.

Peterman, W, RH Waring, T Seager, and WL Pollock. 2012. Soil properties affect pinyon pine juniper response to drought. Ecohydrology 6(3):455–463. https://doi.org/10.1002/eco.1284.

Qi, J, A Chehbouni, AR Huete, YH Kerr, and S Sorooshian. 1994. A modified soil adjusted vegetation index. Remote Sensing of Environment 48(2):119–126. https://doi.org/10.1016/0034-4257(94)90134-1.

Reed, BC, JF Brown, D VanderZee, TR Loveland, JW Merchant, and DO Ohlen. 1994. Measuring phenological variability from satellite imagery. Journal of Vegetation Science 5(5):703–714. https://doi.org/10.2307/3235884.

Sala, OE, LA Gherardi, L Reichmann, E Jobbagy, and D Peters. 2012. Legacies of precipitation fluctuations on primary production: theory and data synthesis. Philosophical Transactions of the Royal Society B: Biological Science 367(1606):3135–3144. https://doi.org/10.1098/rstb.2011.0347.

Schlaepfer, DR, WK Lauenroth, and JB Bradford. 2011. Ecohydrological niche of sagebrush ecosystems. Ecohydrology 5(4):453–466. https://doi.org/10.1002/eco.238.

——. 2014. Modeling regeneration responses of big sagebrush (*Artemisia tridentata*) to abiotic conditions. Ecological Modeling 286.

Schuurman, GW, CH Hoffman, DN Cole, DJ Lawrence, JM Morton, DR Magness,

AE Cravens, S Covington, R O'Malley, and NA Fisichelli. 2020. Resist-accept-direct (RAD): A framework for the 21st-century natural resource manager. Natural Resource Report NPS/NRSS/CCRP/NRR—2020/ 2213. National Park Service, Fort Collins, Colorado. https://doi.org/10.36967/nrr-2283597.

Seager, R, A Hooks, AP Williams, B Cook, J Nakamura, and N Henderson. 2015. Climatology, variability, and trends in the U.S. Vapor-pressure deficit, an important fire-related meteorological quantity. Journal of Applied Meteorology and Climatology 54(6):1121–1141. https://doi.org/10.1175/JAMC-D-14-0321.1.

Sorokin, Y, TJ Zelikova, D Blumenthal, DG Williams, and E Pendall. 2017. Seasonally contrasting responses of evapotranspiration to warming and elevated CO_2 in a semi-arid grassland. Ecohydrology 10(7):e1880. https://doi.org/10.1002/eco.1880.

St. Peter, JR. 2015. A model for determining drivers of phenology in western United States rangelands. University of Montana, Graduate Student Theses, Dissertations, & Professional Papers. 4444.

Stein, BA, P Glick, N Edelson, and A Staudg. 2014. Climate-smart conservation: Putting adaption principles into practice. National Wildlife Federation, Washington, DC.

Stephenson, NL. 1990. Climatic control of vegetation distribution: The role of the water balance. The American Naturalist 135(5):649–670. https://doi.org/10.1086/285067.

——. 1998. Actual evapotranspiration and deficit: Biologically meaningful correlates of vegetation distribution across spatial scales. Journal of Biogeography 25(5):855–870. https://doi.org/10.1046/j.1365-2699.1998.00233.x.

Tercek, M, D Thoma, JE Gross, K Sherrill, S Kagone, and GB Senay. 2021. Historical changes in plant water use and need in the continental United States. PLoS One 1–19. https://doi.org/10.1371/journal.pone.0256586.

Thoma, D. 2023a. Supplemental tables for report on landscape phenology, vegetation condition, and relations with climate at Canyonlands NP National Park, 2000–2019. https://irma.nps.gov/DataStore/Reference/Profile/2299344.

——. 2023b. Juniper mortality in southeast Utah: A consequence of drought? Unpublished document. https://irma.nps.gov/DataStore/Reference/Profile/2299344.

Thoma, D, J Norris, and P Lauck. 2017. Satellite-based vegetation phenology and condition, and snow cover extent monitoring protocol for the Northern and Southern Colorado Plateau networks. Natural Resource Report. NPS/SCPN/NRR—2017/1533. National Park Service. Fort Collins, Colorado. https://irma.nps.gov/DataStore/Reference/Profile/2246068.

Thoma, DP, DW Bailey, DS Long, GA Nielsen, MP Henry, MC Breneman, and C Montagne. 2002. Short-term monitoring of rangeland forage conditions with AVHRR imagery. Journal of Range Management 55(4):383–389. https://doi.org/10.2307/4003475.

Thoma, DP, SM Munson, KM Irvine, DL Witwicki, EL Bunting, and J Paruelo. 2016. Semi-arid vegetation response to antecedent climate and water balance windows. Applied Vegetation Science 19(3):413–429. https://doi.org/10.1111/avsc.12232.

Thoma, DP, SM Munson, and DL Witwicki. 2019. Landscape pivot points and responses to water balance in national parks of the southwest U.S. Journal of Applied Ecology 56(1):157–167. https://doi.org/10.1111/1365-2664.13250.

Thoma, DP, MT Tercek, EW Schweiger, SM Munson, JE Gross, and ST Olliff. 2020. Water balance as an indicator of natural resource condition: Case studies from Great Sand Dunes National Park and Preserve. Global Ecology and Conservation 24:e01300. https://doi.org/10.1016/j.gecco.2020.e01300.

Thornton, PE, MM Thornton, BW Mayer, Y Wei, R Devarakonda, RS Vose, and RB Cook. 2018. Daymet: Daily surface

weather data on a 1-km grid for North America; Version 3.

van Wijk, RE, A Kölzsch, H Kruckenberg, BS Ebbinge, GJDM Müskens, and BA Nolet. 2012. Individually tracked geese follow peaks of temperature acceleration during spring migration. Oikos 121(5):655–664. https://doi.org/10.1111/j.1600-0706.2011.20083.x.

Von Loh, JK, A Landgraf, T Evenden, S Owens, and MR Blauer. 2007. Vegetation classification and mapping project report, Canyonlands NP National Park. Natural Resource Technical Report NPS/NCPN/NRTR—2007/061. National Park Service, Fort Collins, Colorado.

Wang, C, J Chen, Y Tang, TA Black, and K Zhu. 2018. A novel method for removing snowmelting-induced fluctuation in GIMMS NDVI3g data for vegetation phenology monitoring: A case study in deciduous forests of North America. IEEE Journal of Selected Topics in Applied Earth Observations and Remote Sensing 11(3):800–807. https://doi.org/10.1109/JSTARS.2017.2778076.

Witwicki, DL, SM Munson, and DP Thoma. 2016. Effects of climate and water balance across grasslands of varying C3 and C4 grass cover. Ecosphere 7(11):1–19. https://doi.org/10.1002/ecs2.1577.

Workie, TG, and HJ Debella. 2018. Climate change and its effects on vegetation phenology across ecoregions of Ethiopia. Global Ecology and Conservation 13:e00366. https://doi.org/10.1016/j.gecco.2017.e00366.

Yang, Y, T Wu, S Wang, J Li, and F Muhanmmad. 2019. The NDVI-CV method for mapping evergreen trees in complex urban areas using reconstructed Landsat 8 time-series data. Forests 10(2):139. https://doi.org/10.3390/f10020139.

Appendix A. Supplemental Figures for Landscape Phenology, Vegetation Condition, and Relations with Climate at Canyonlands National Park, 2000–2019

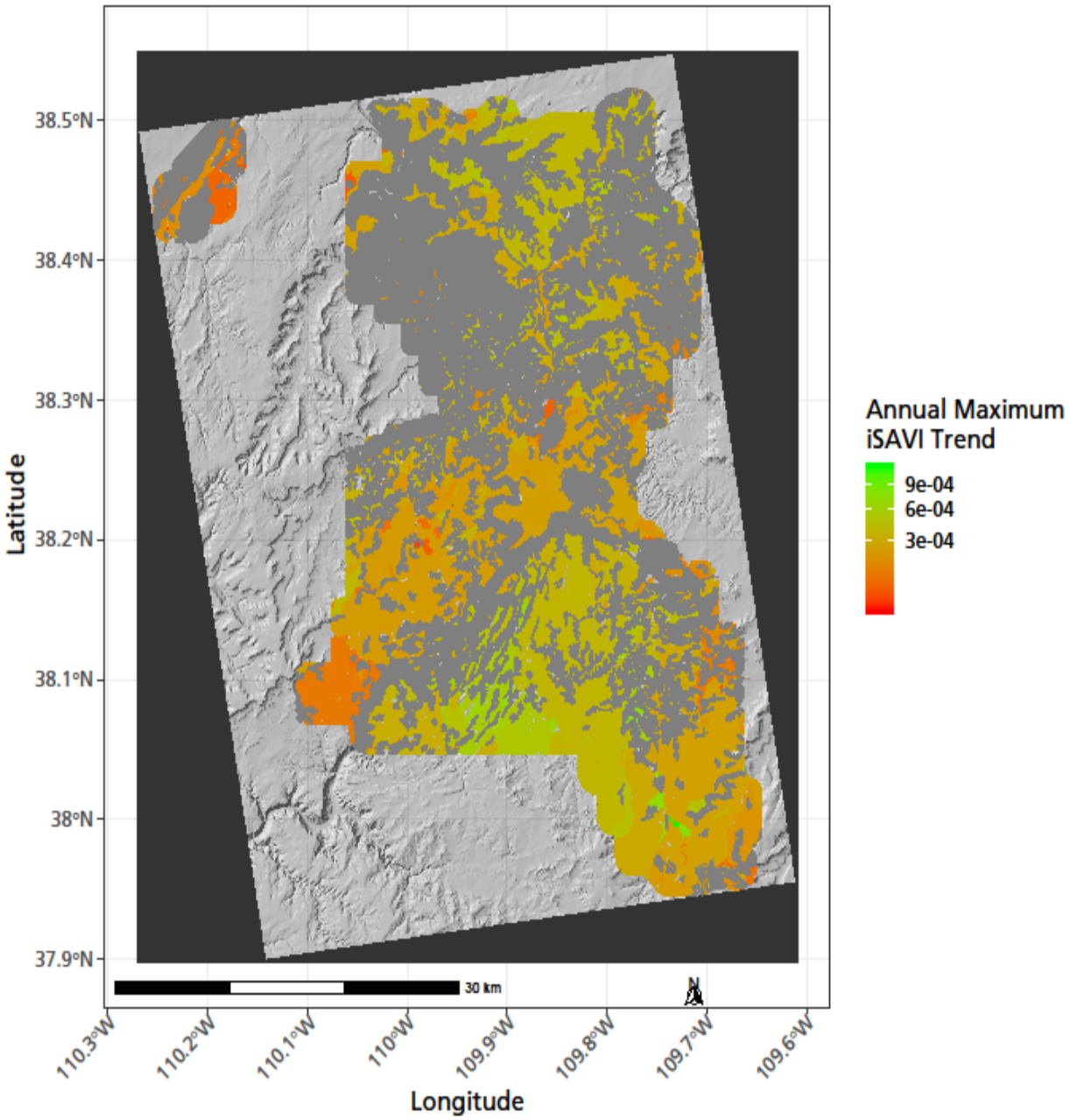

Figure A-1. Spatial pattern of trends in maximum annual iSAVI. Trend is average change in iSAVI per year for the period 2000–2019.

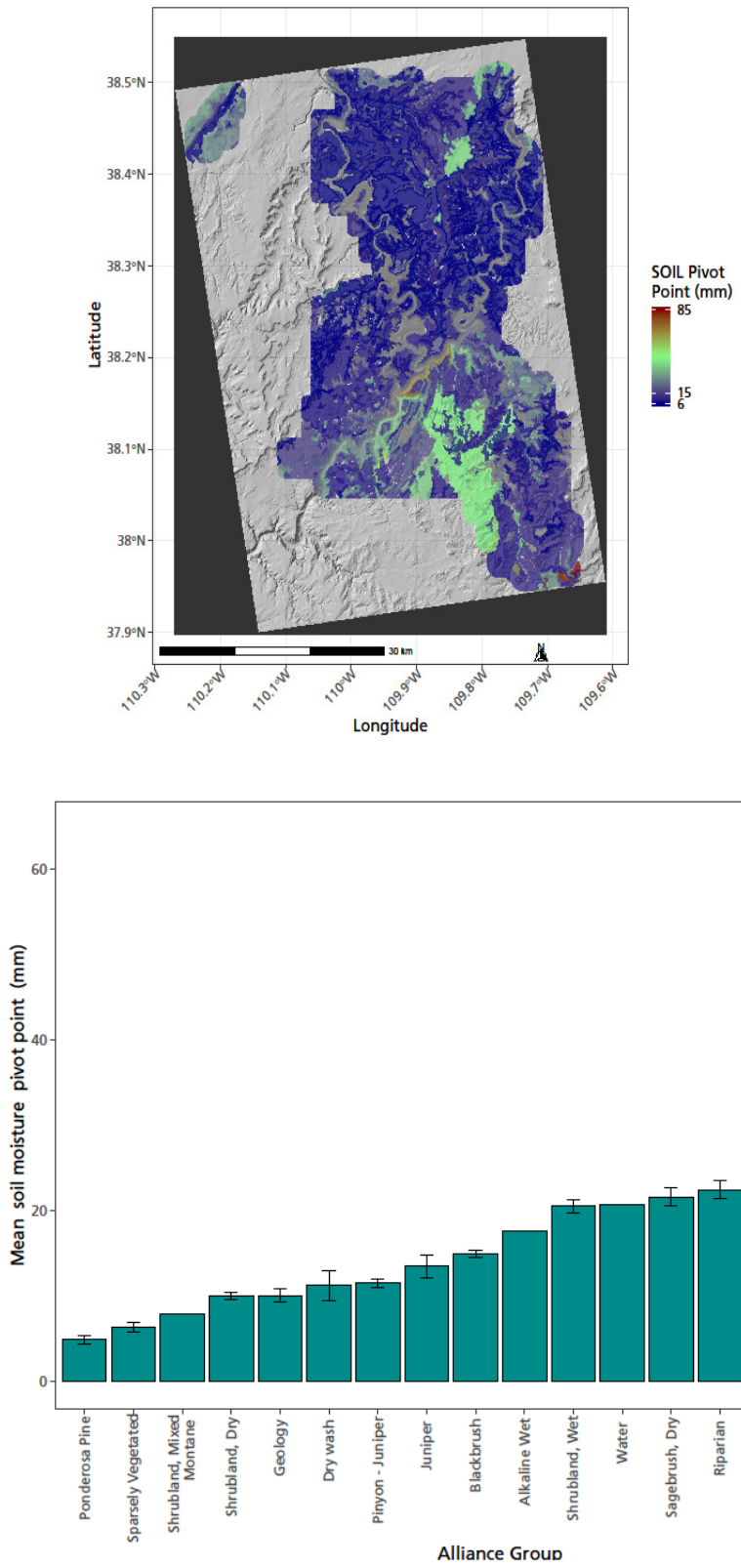

Figure A-2a. Pivot points for polygons where climate variables were significantly related to interannual variation in production (p-value < 0.05). Climate data summarized by water year.

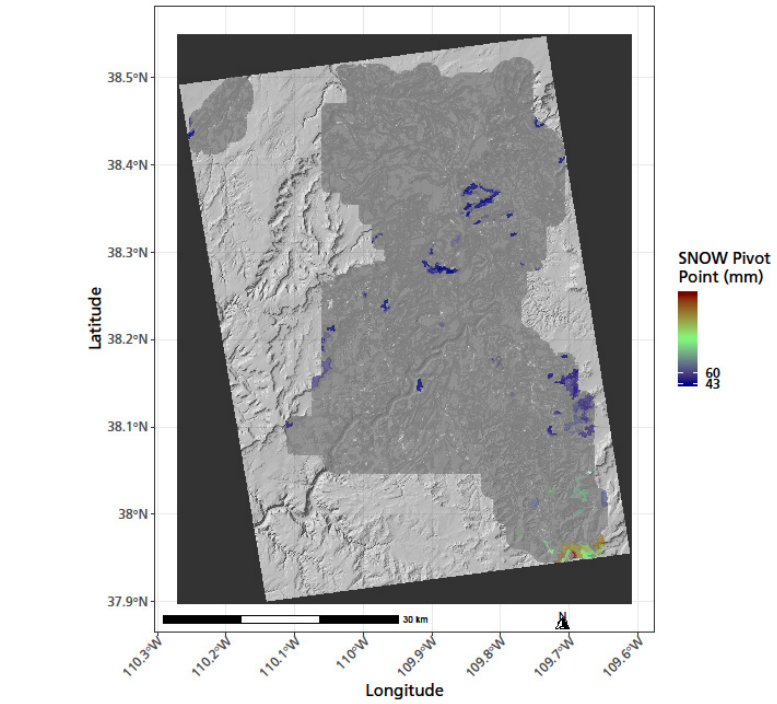

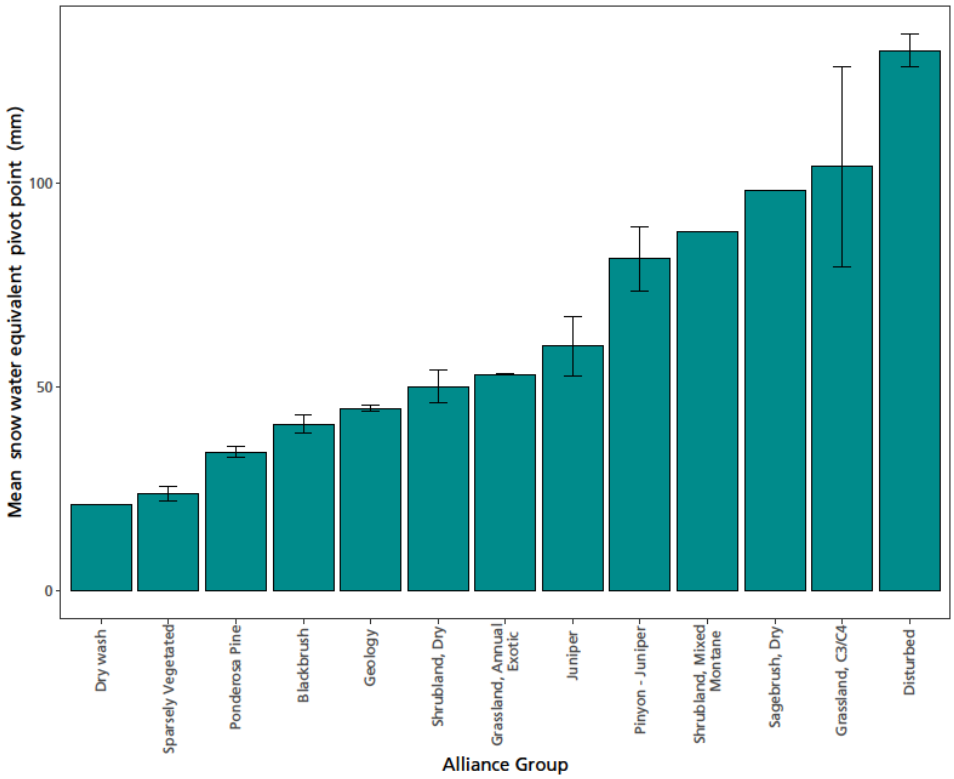

Figure A-2b. Pivot points for polygons where climate variables were significantly related to interannual variation in production (p-value < 0.05). Climate data summarized by water year.

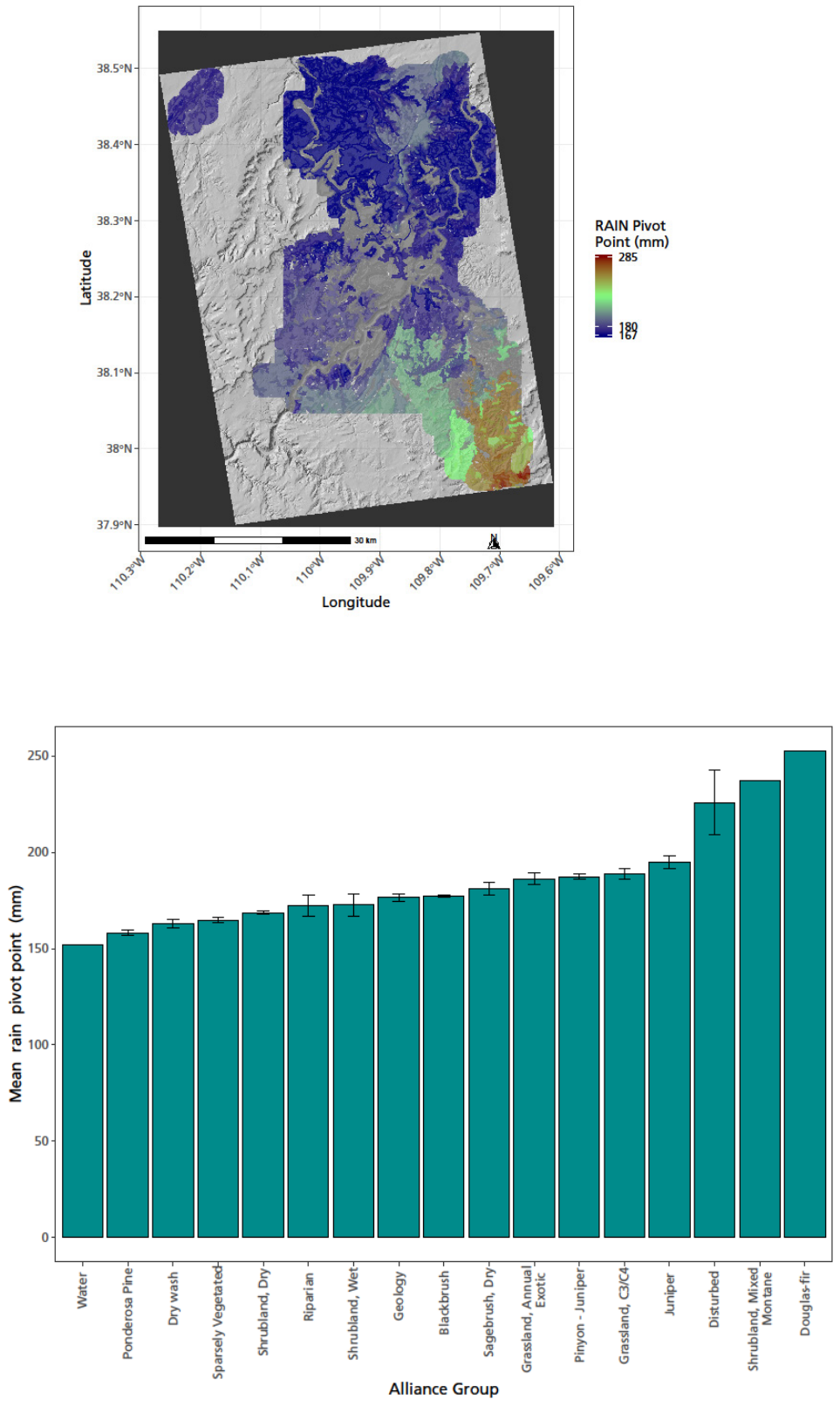

Figure A-2c. Pivot points for polygons where climate variables were significantly related to interannual variation in production (p-value < 0.05). Climate data summarized by water year.

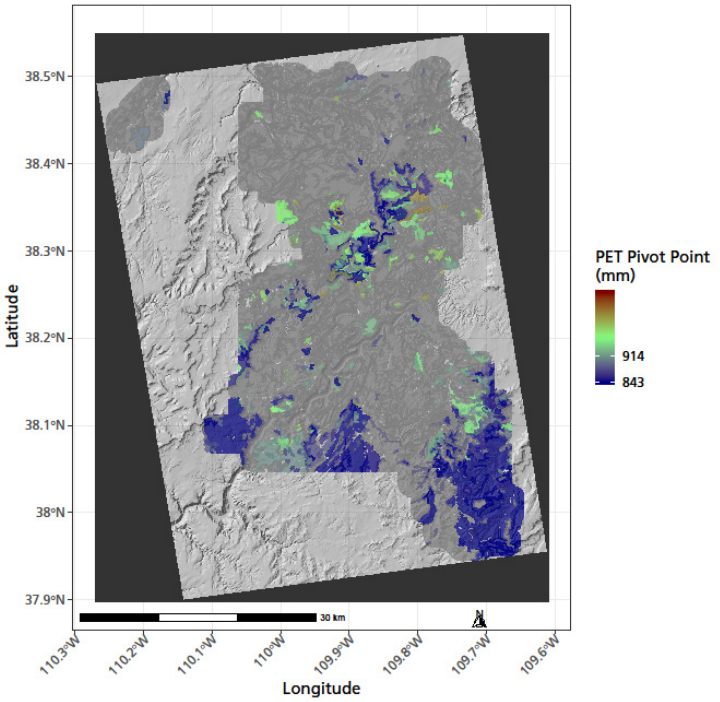

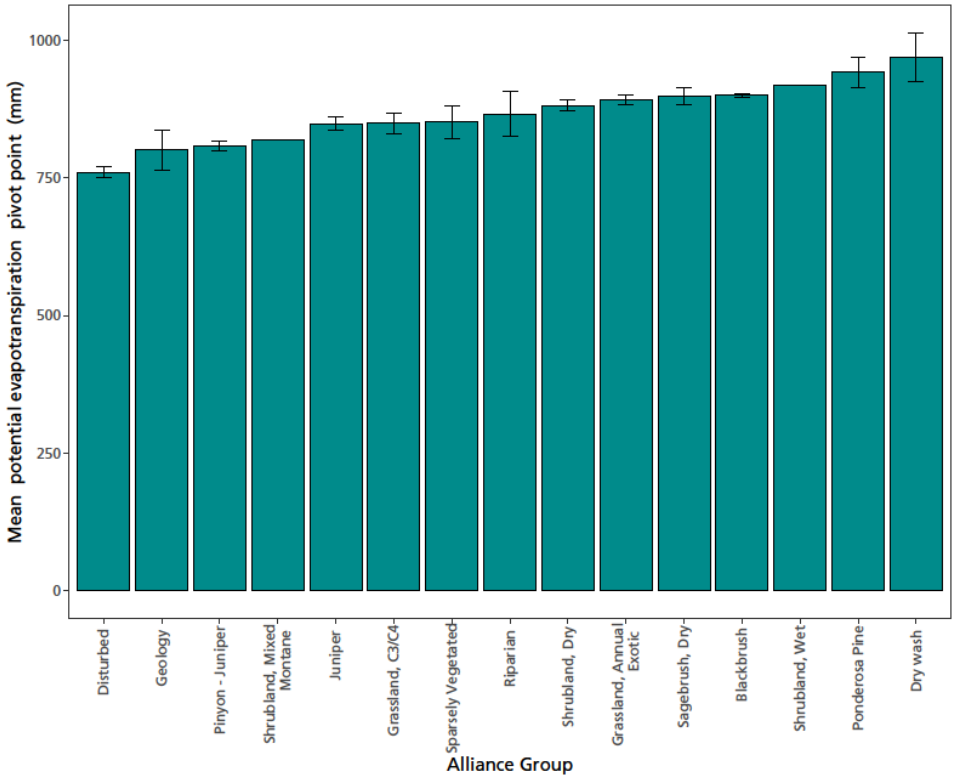

Figure A-2d. Pivot points for polygons where climate variables were significantly related to interannual variation in production (p-value < 0.05). Climate data summarized by water year.

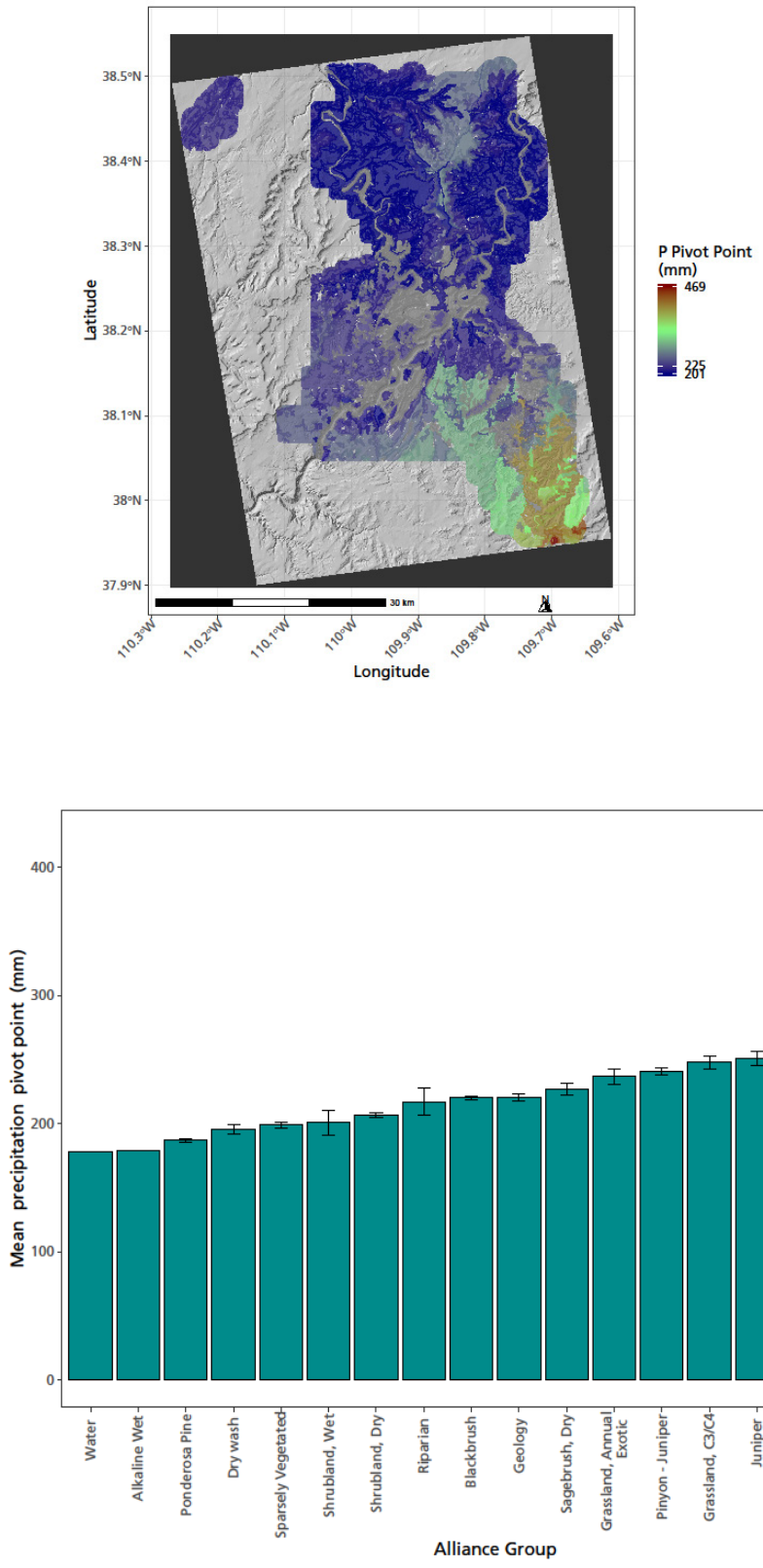

Figure A-2e. Pivot points for polygons where climate variables were significantly related to interannual variation in production (p-value < 0.05). Climate data summarized by water year.

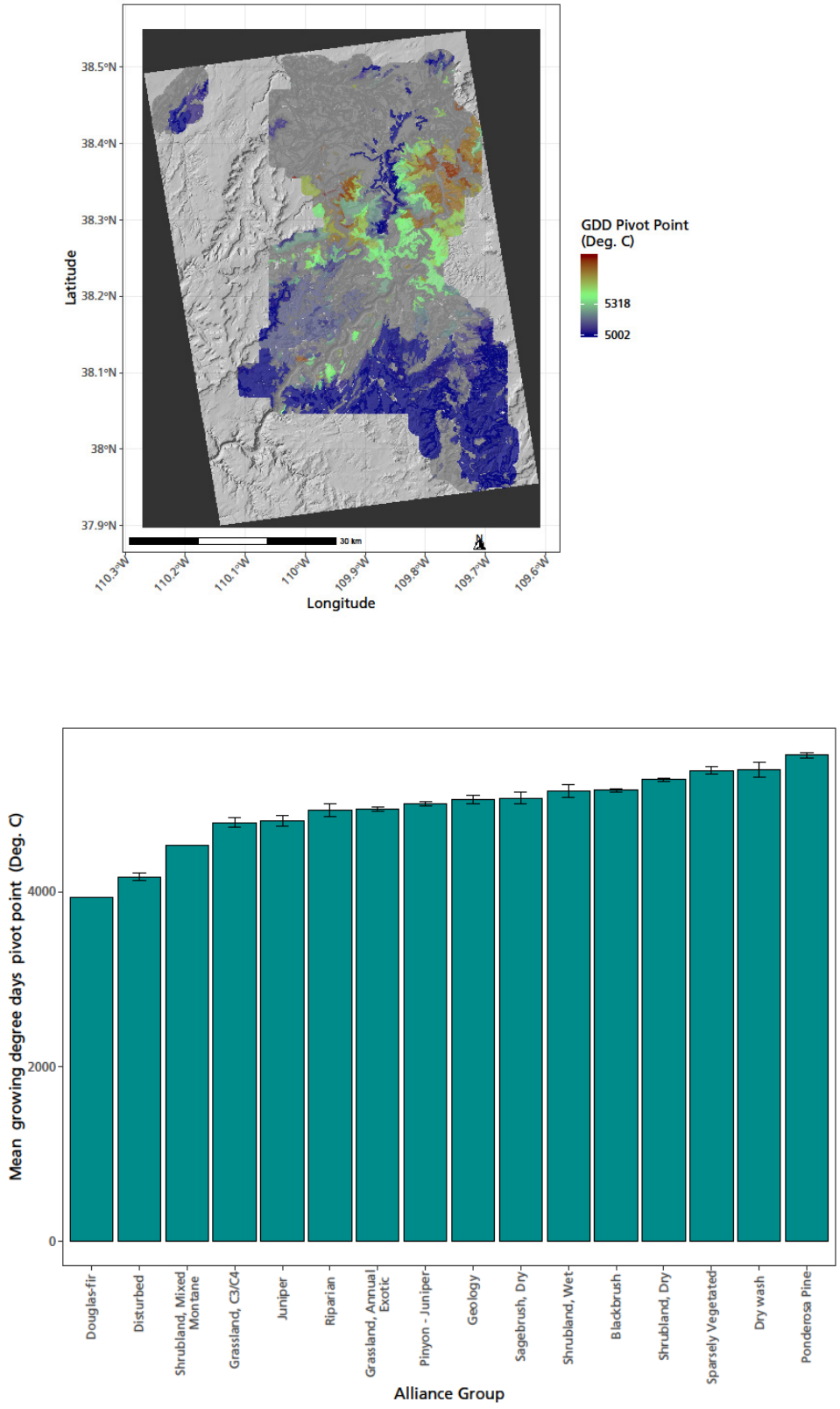

Figure A-2f. Pivot points for polygons where climate variables were significantly related to interannual variation in production (p-value < 0.05). Climate data summarized by water year.

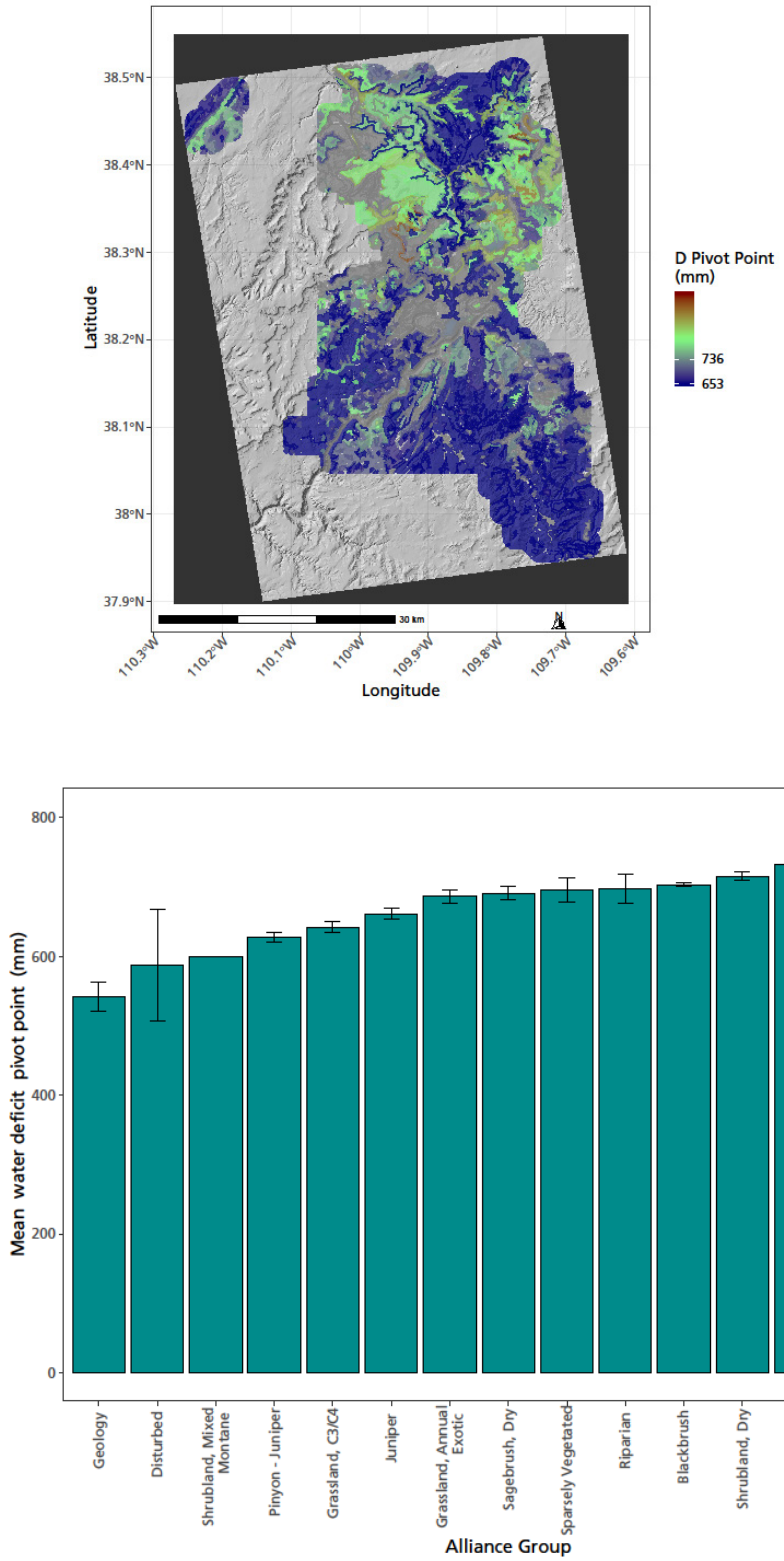

Figure A-2g. Pivot points for polygons where climate variables were significantly related to interannual variation in production (p-value < 0.05). Climate data summarized by water year.

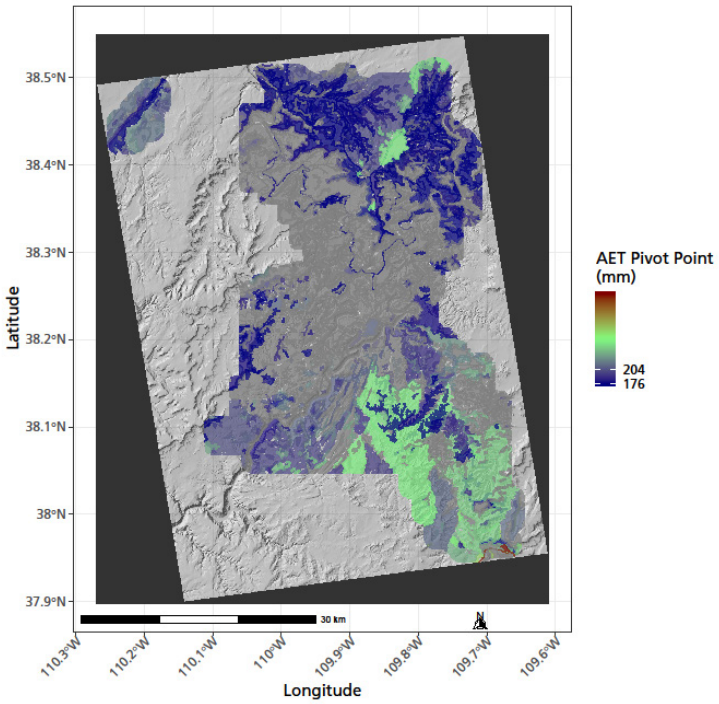

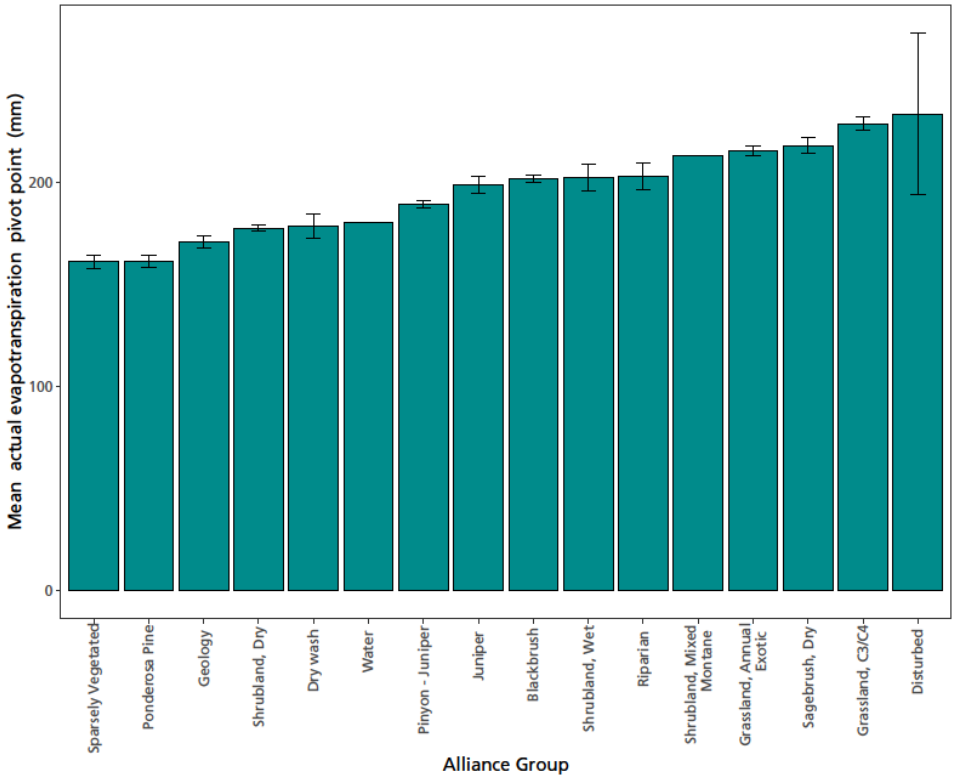

Figure A-2h. Pivot points for polygons where climate variables were significantly related to interannual variation in production (p-value < 0.05). Climate data summarized by water year.

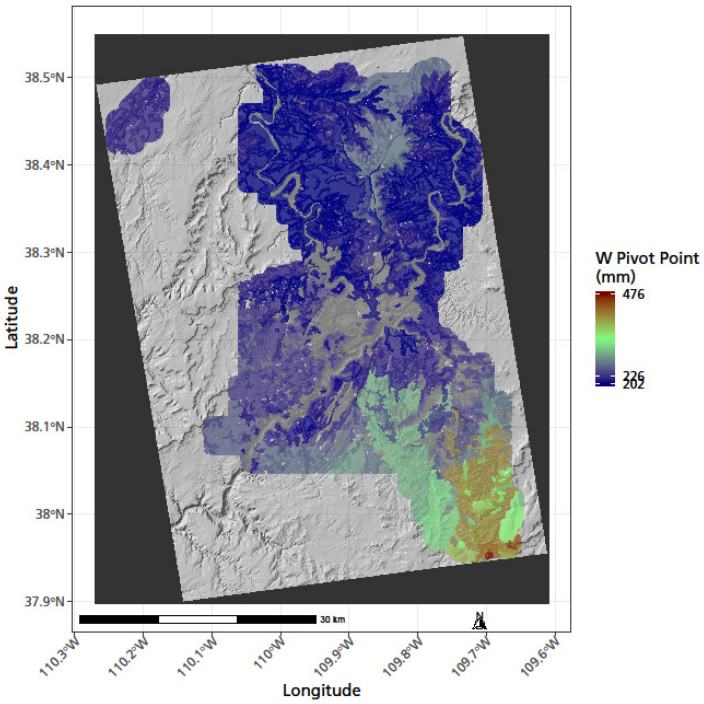

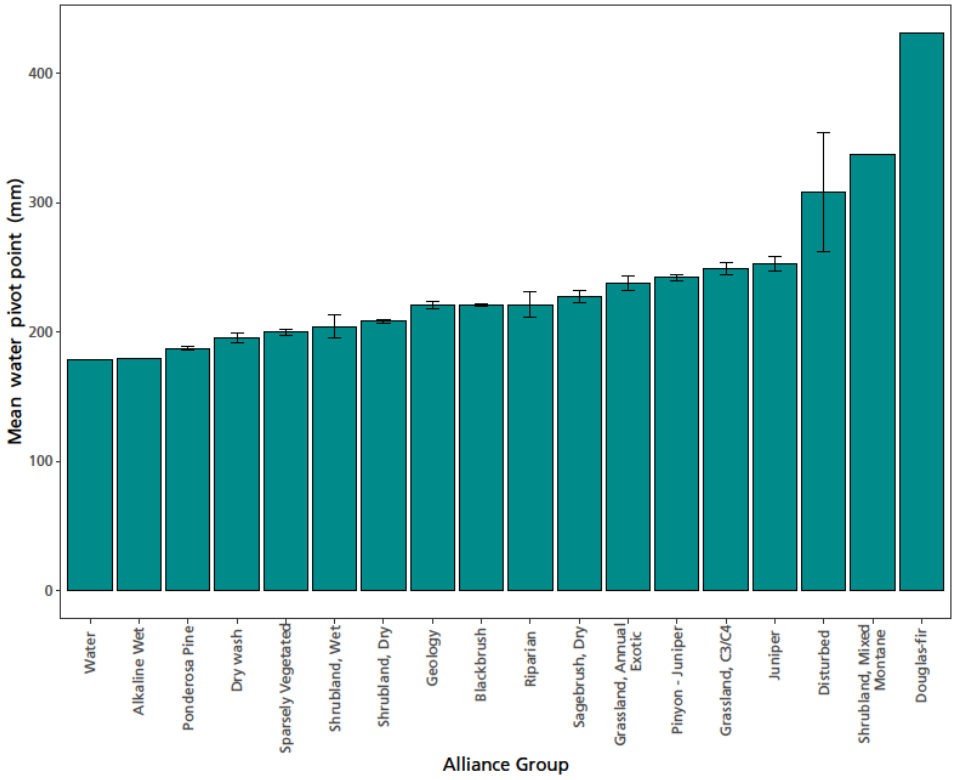

Figure A-2i. Pivot points for polygons where climate variables were significantly related to interannual variation in production (p-value < 0.05). Climate data summarized by water year.

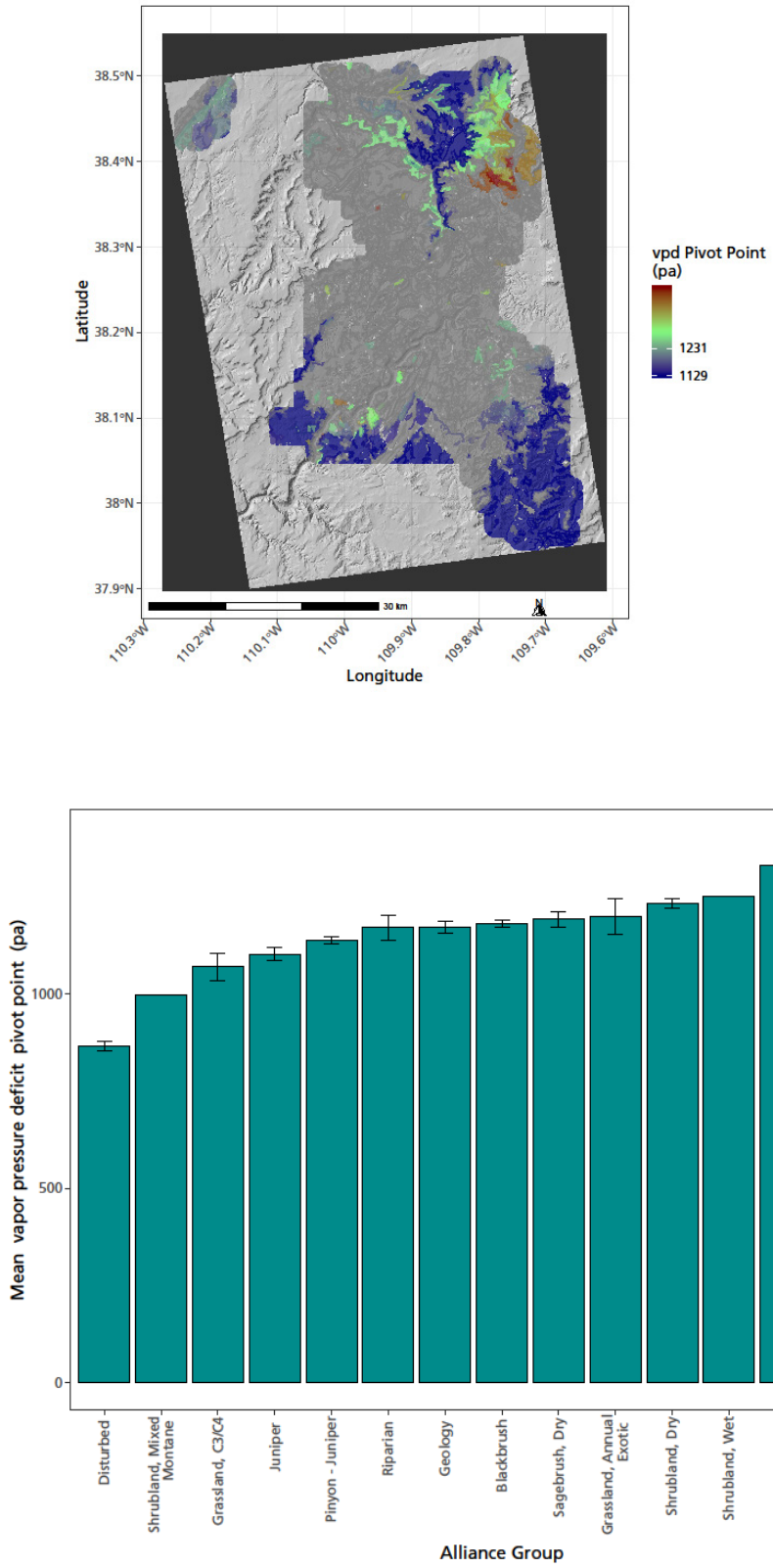

Figure A-2j. Pivot points for polygons where climate variables were significantly related to interannual variation in production (p-value < 0.05). Climate data summarized by water year.

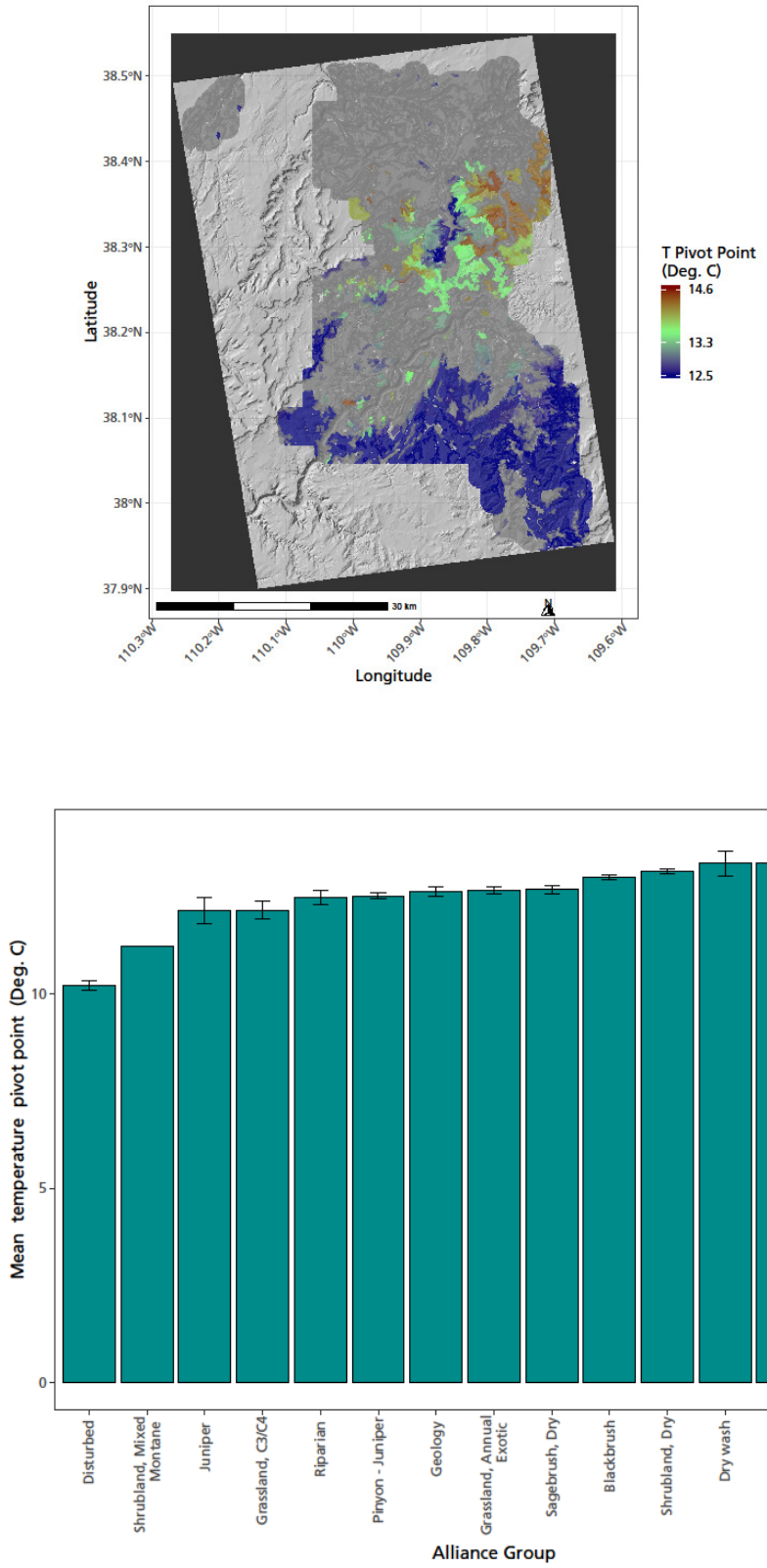

Figure A-2k. Pivot points for polygons where climate variables were significantly related to interannual variation in production (p-value < 0.05). Climate data summarized by water year.

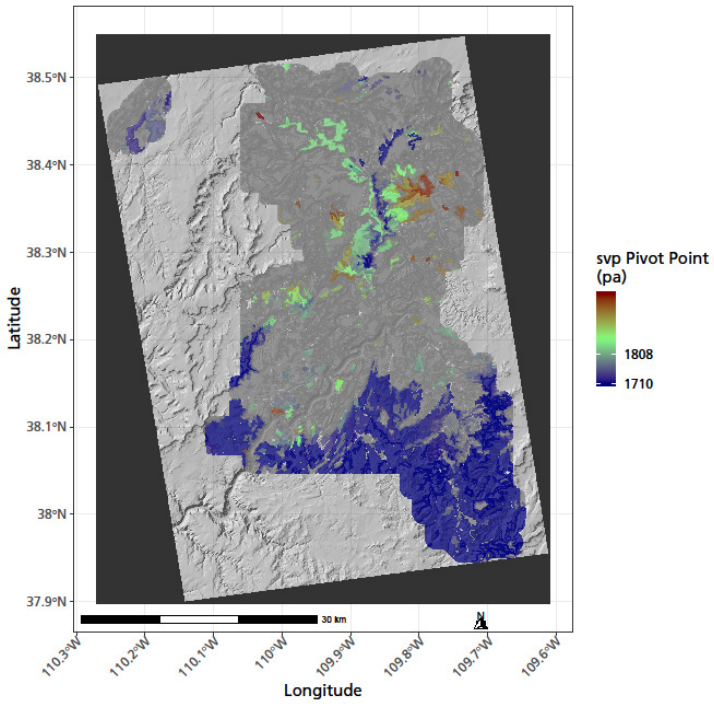

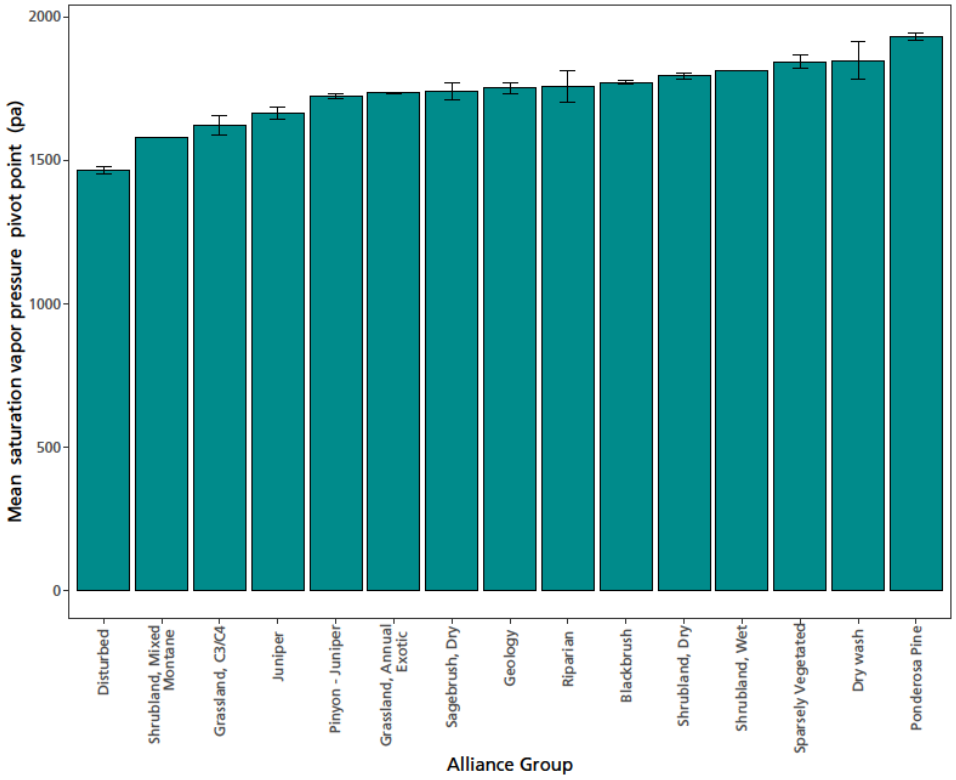

Figure A-2l. Pivot points for polygons where climate variables were significantly related to interannual variation in production (p-value < 0.05). Climate data summarized by water year.

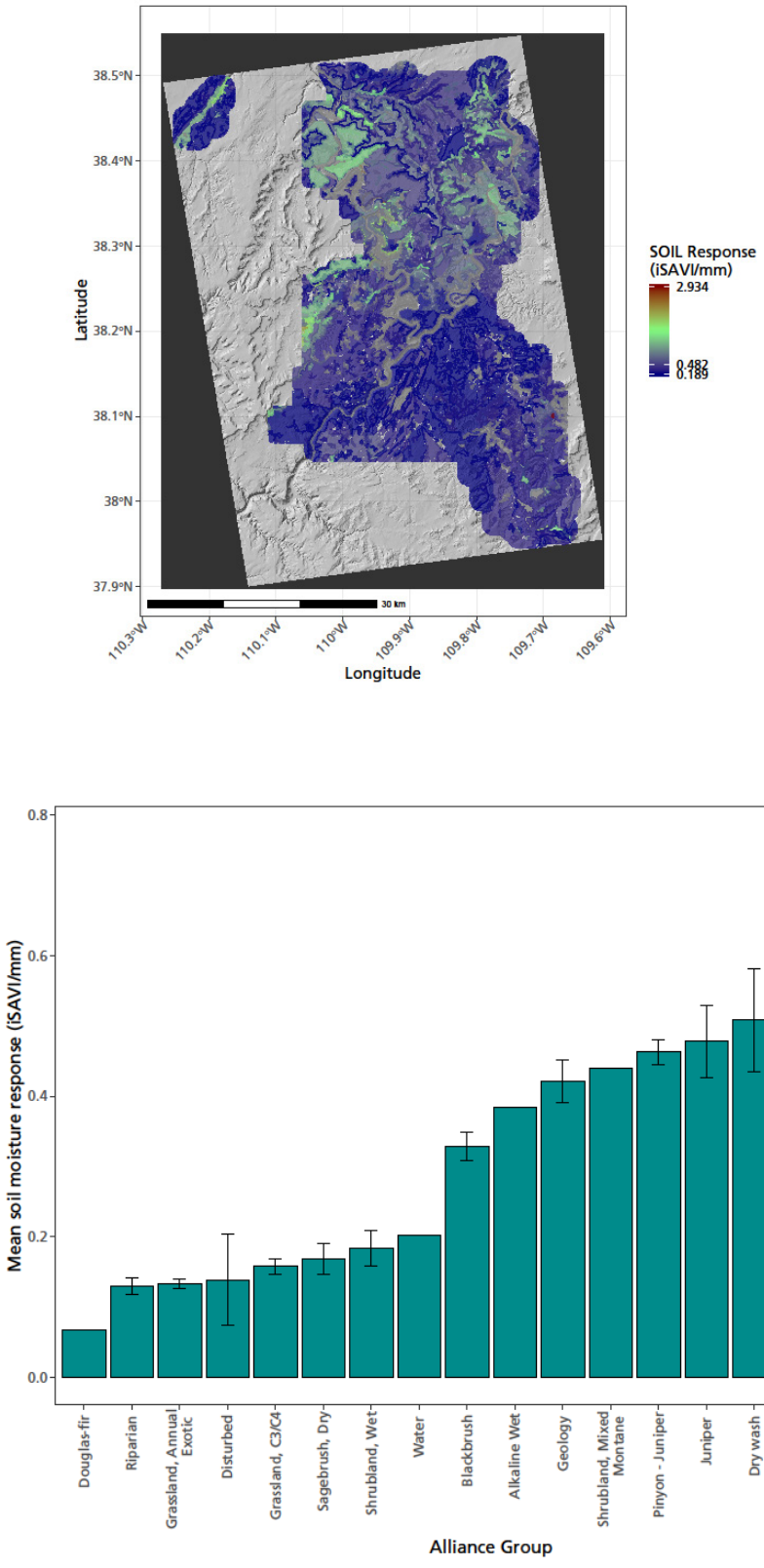

Figure A-3a. Sensitivity of growing season vegetation production to climate variables, where the relationship was significant (p-value < 0.05). Climate data summarized by water year.

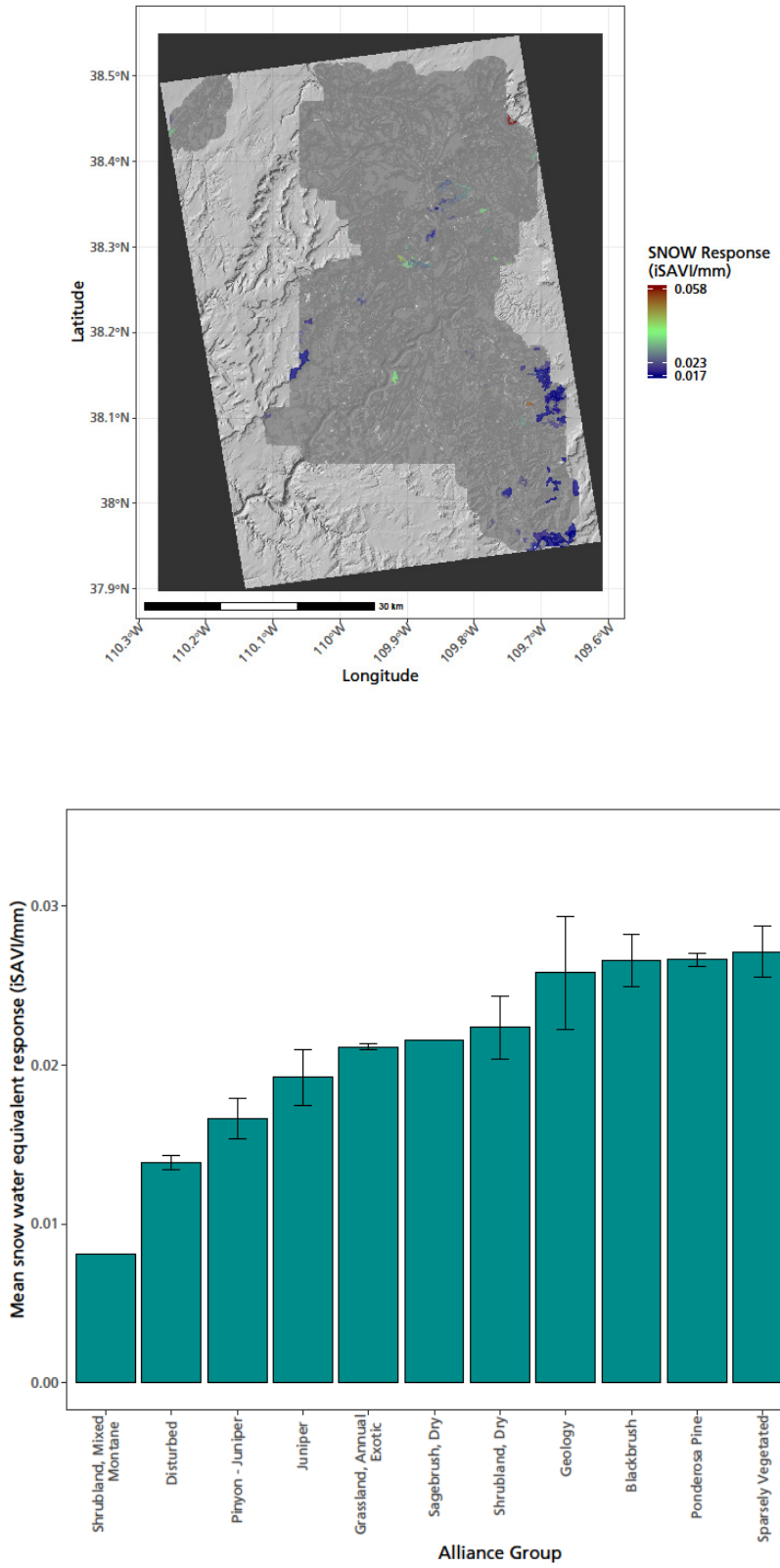

Figure A-3b. Sensitivity of growing season vegetation production to climate variables, where the relationship was significant (p-value < 0.05). Climate data summarized by water year.

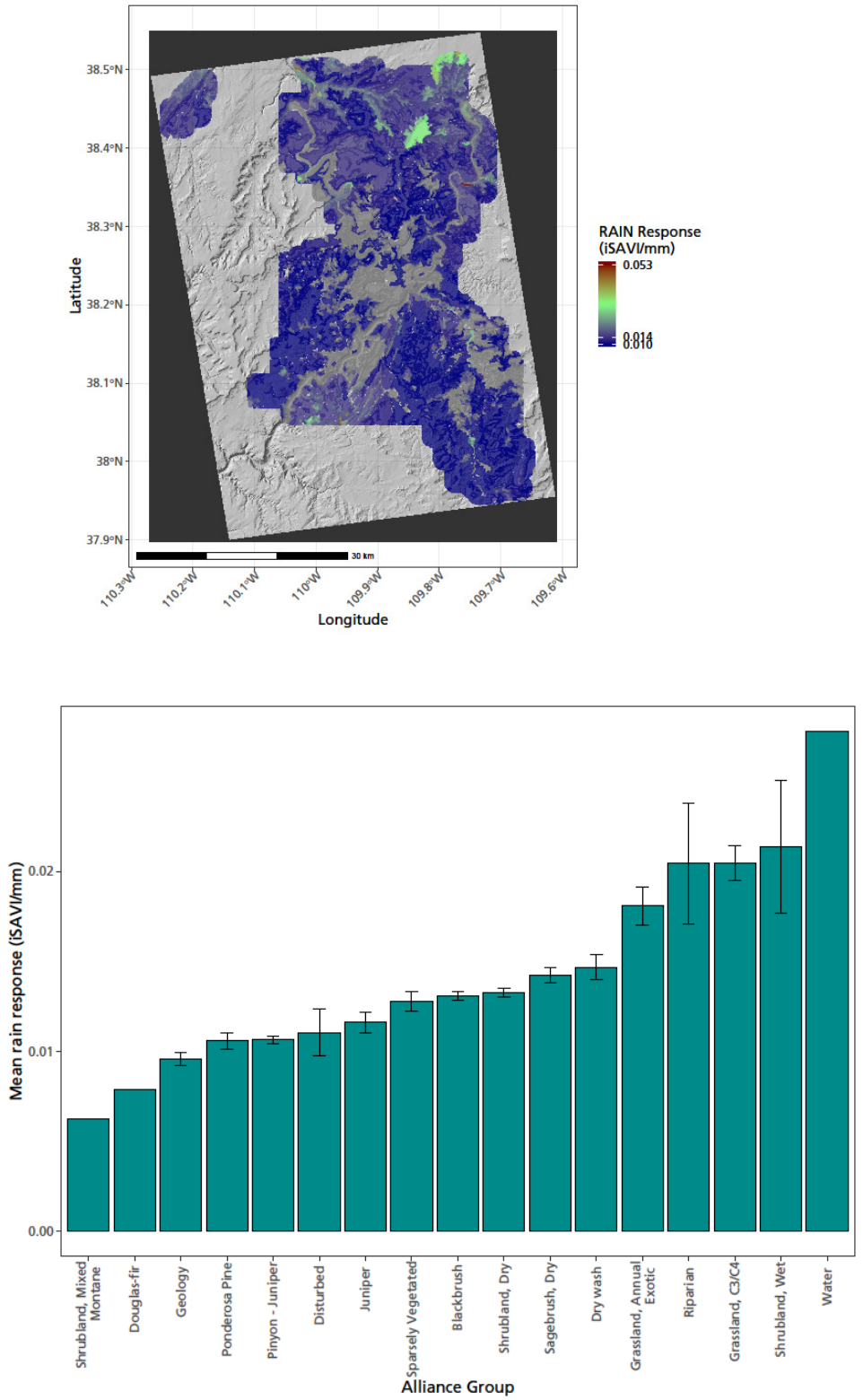

Figure A-3c. Sensitivity of growing season vegetation production to climate variables, where the relationship was significant (p-value < 0.05). Climate data summarized by water year.

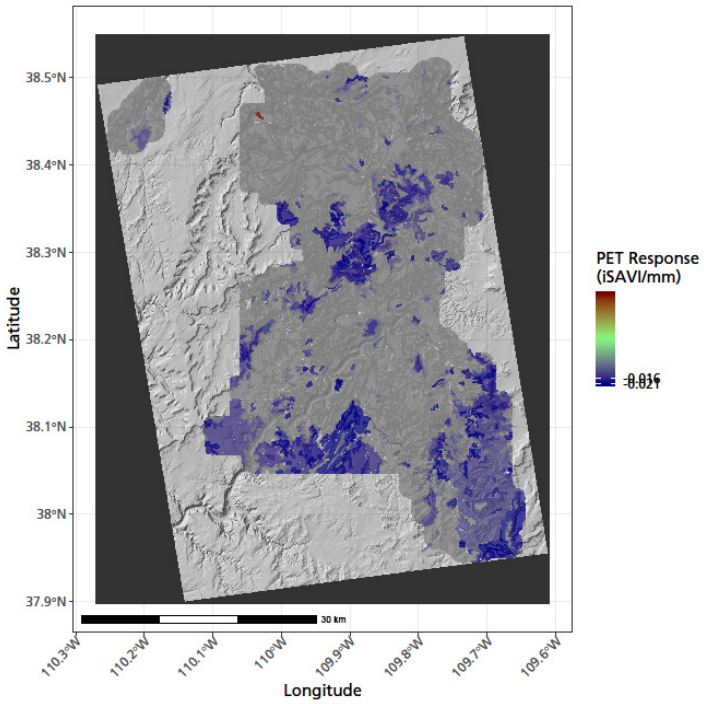

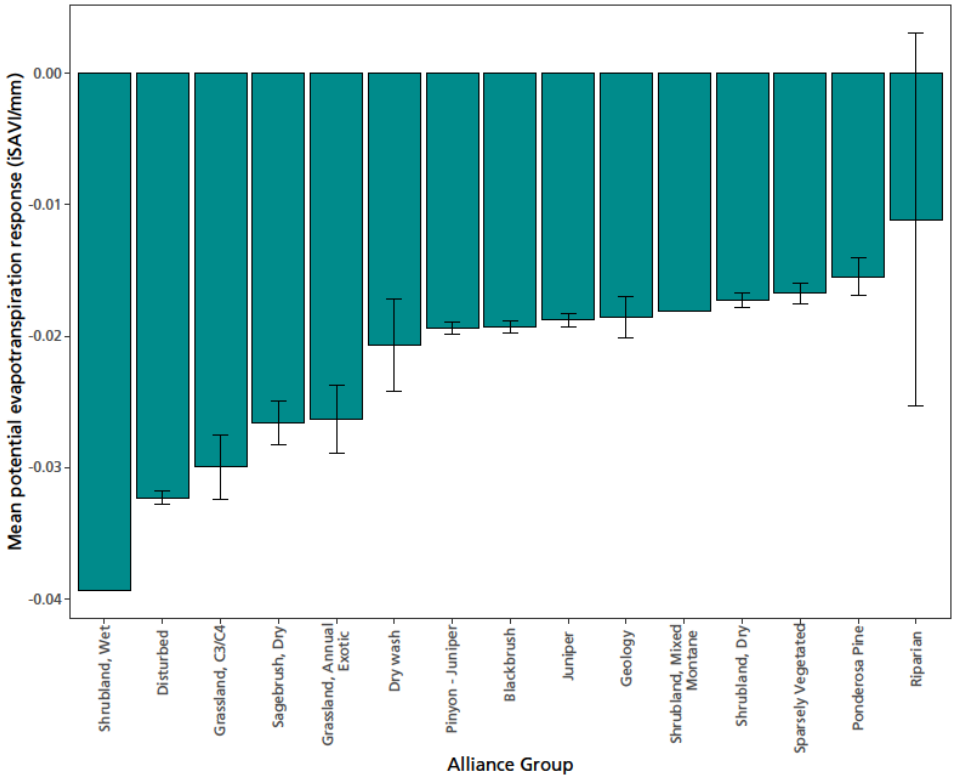

Figure A-3d. Sensitivity of growing season vegetation production to climate variables, where the relationship was significant (p-value < 0.05). Climate data summarized by water year.

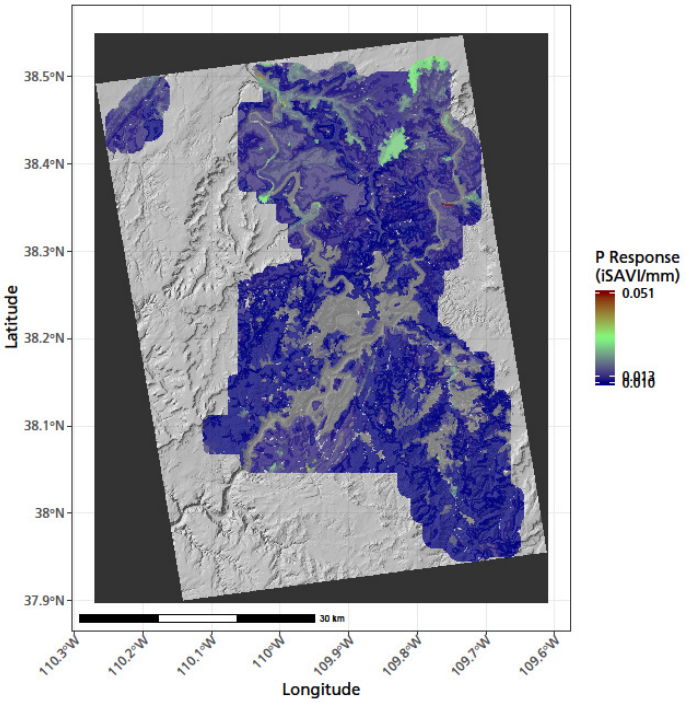

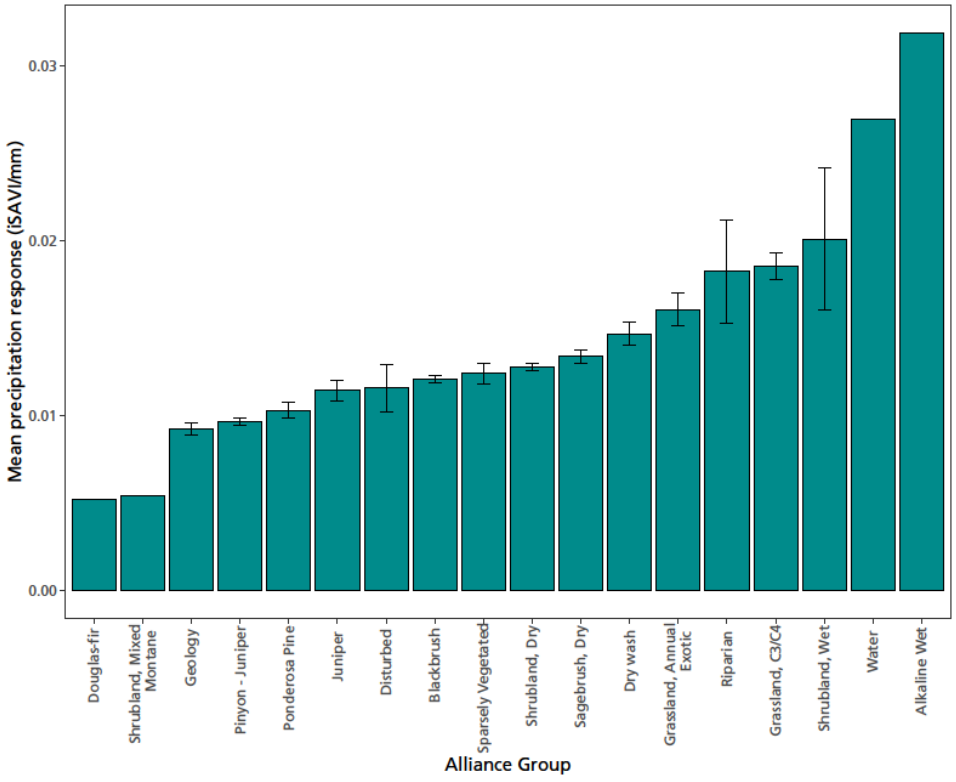

Figure A-3e. Sensitivity of growing season vegetation production to soil moisture where the relationship was significant (p-value < 0.05). Climate data summarized by water year.

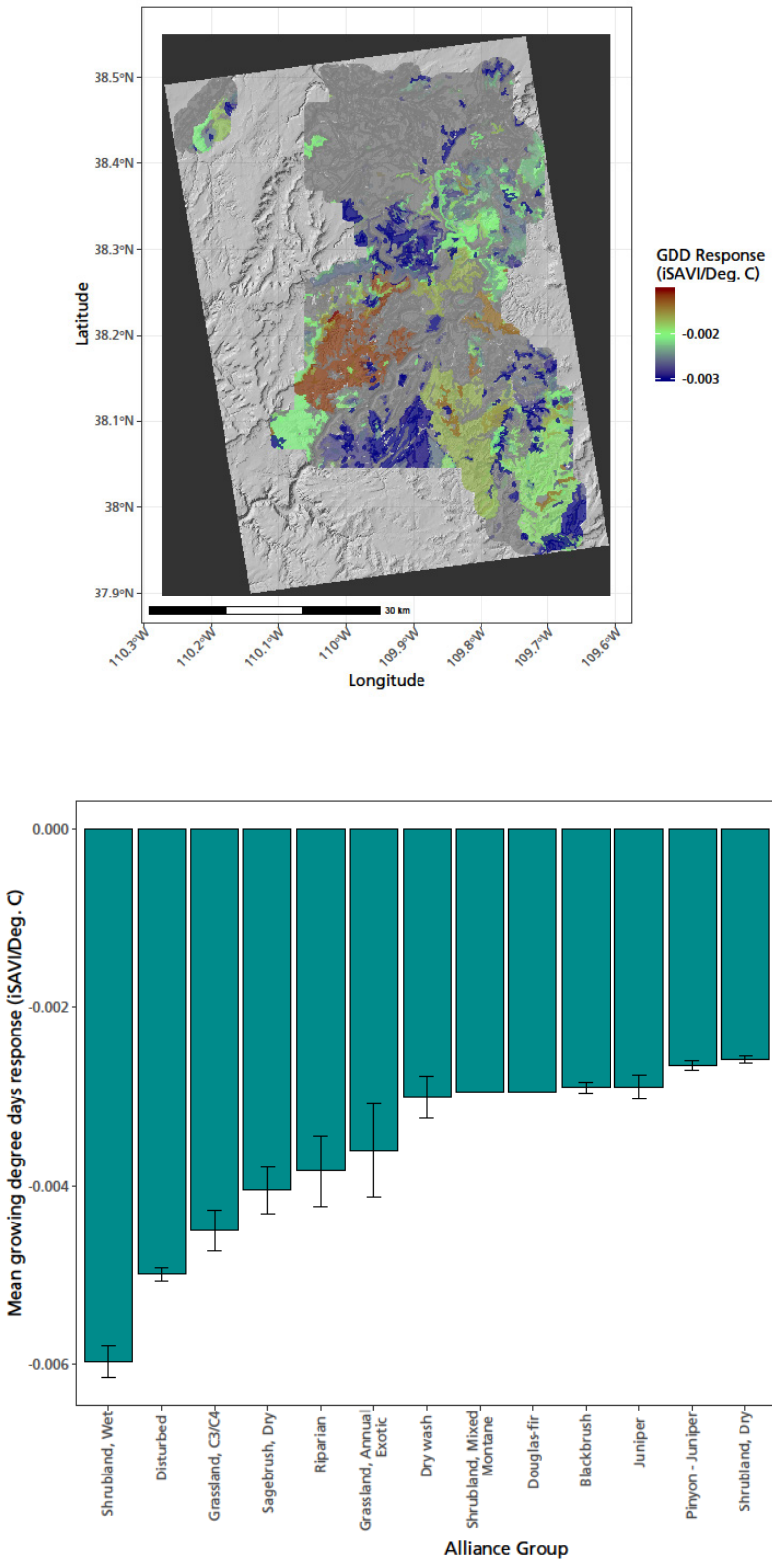

Figure A-3f. Sensitivity of growing season vegetation production to soil moisture where the relationship was significant (p-value < 0.05). Climate data summarized by water year.

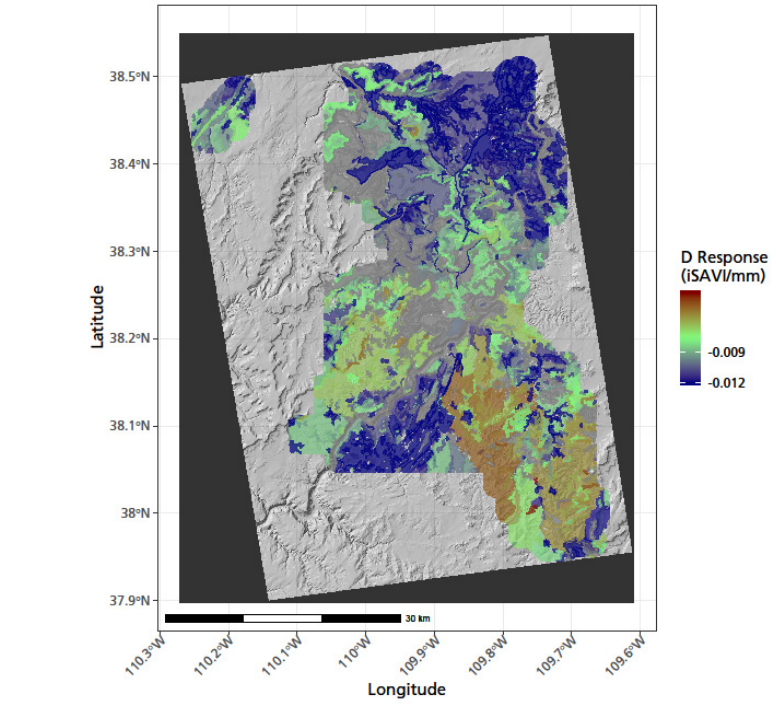

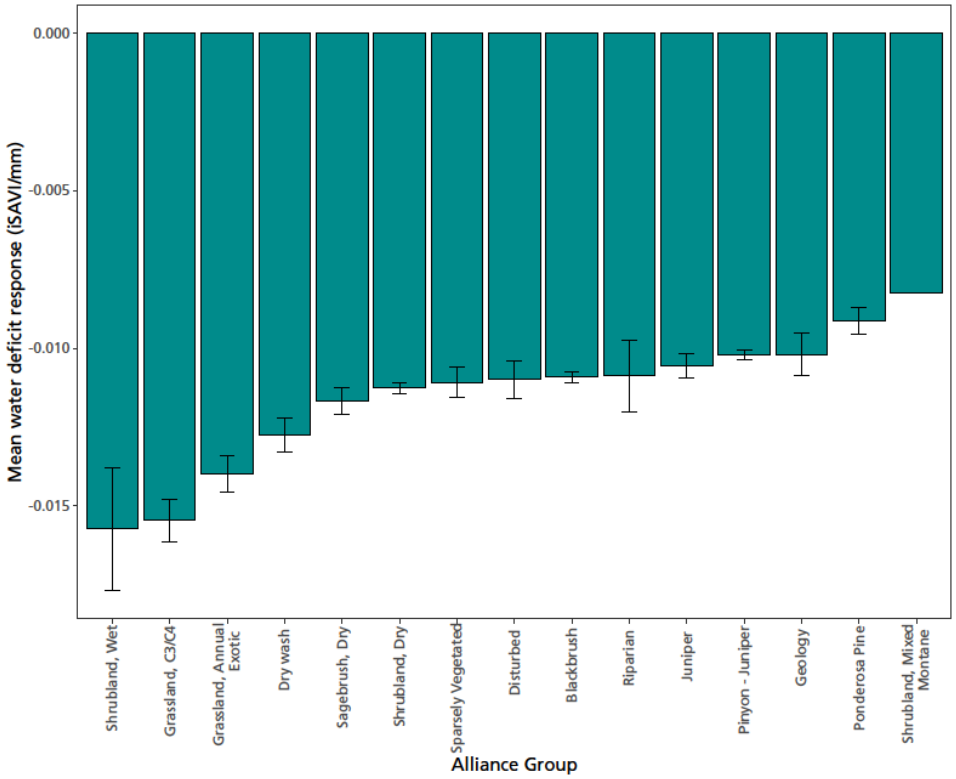

Figure A-3g. Sensitivity of growing season vegetation production to soil moisture where the relationship was significant (p-value < 0.05). Climate data summarized by water year.

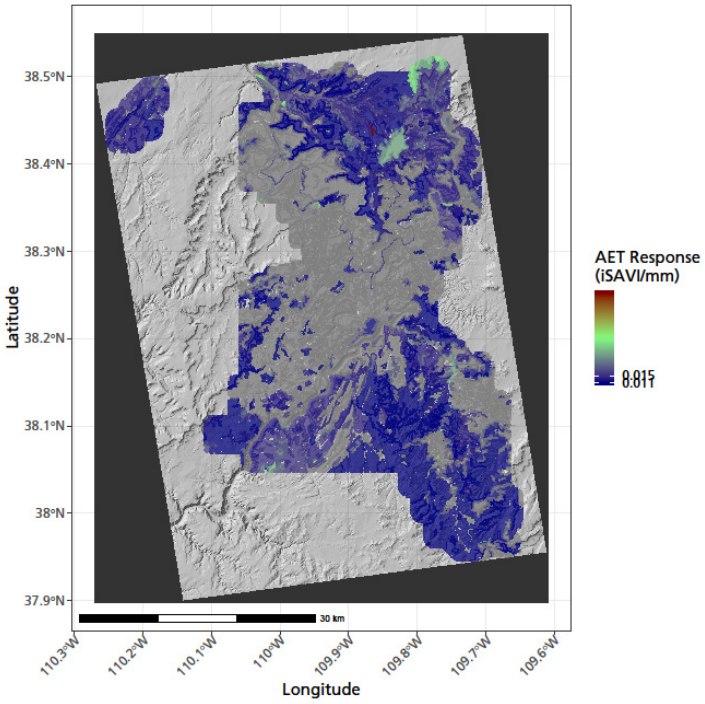

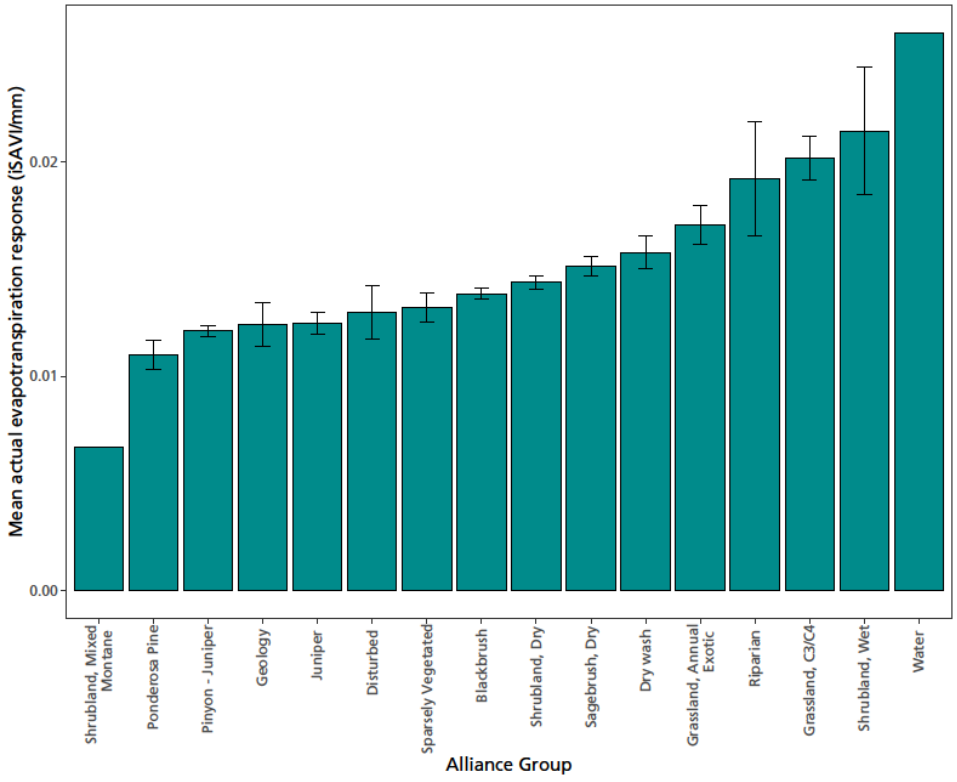

Figure A-3h. Sensitivity of growing season vegetation production to soil moisture where the relationship was significant (p-value < 0.05). Climate data summarized by water year.

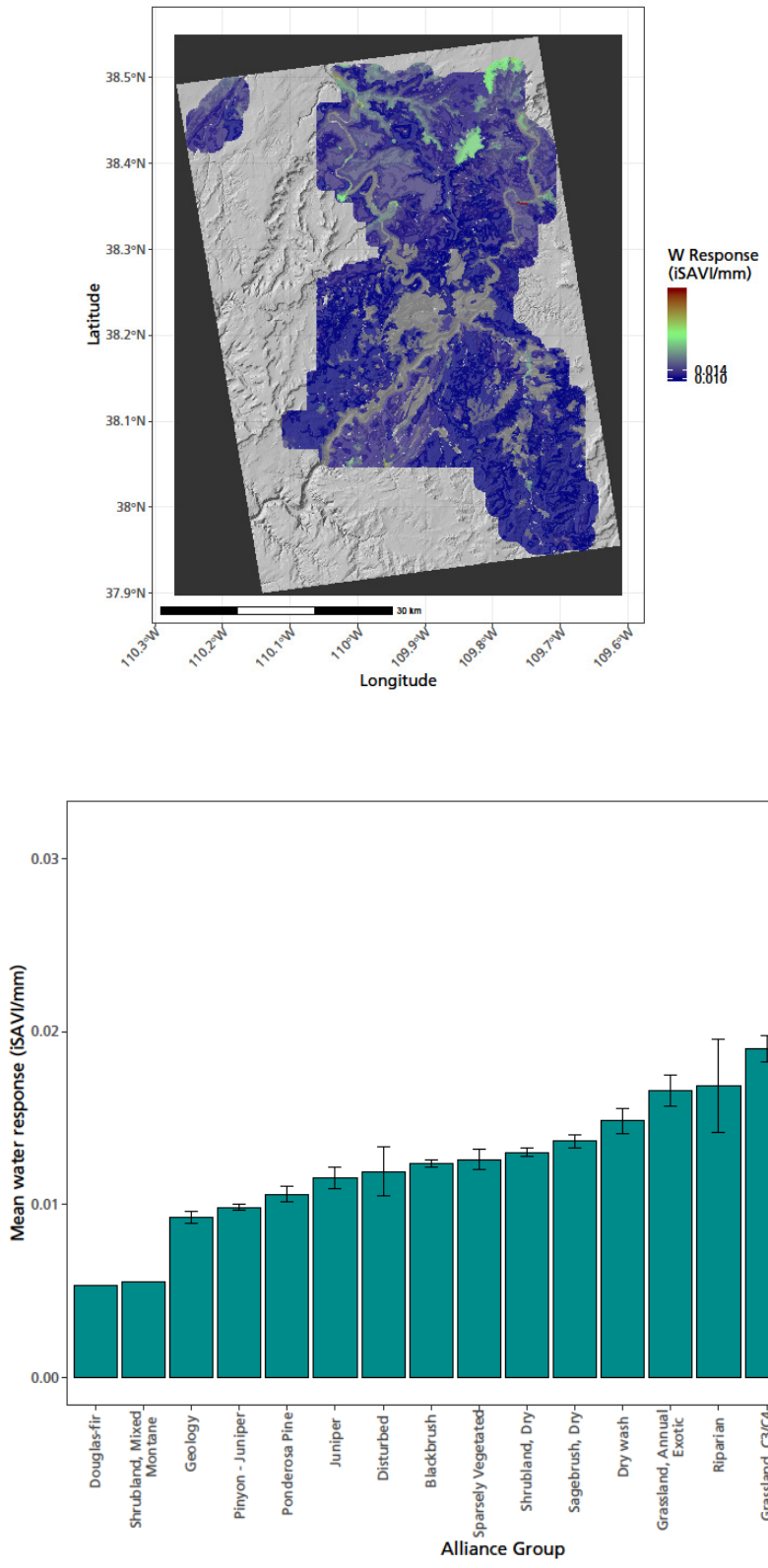

Figure A-3i. Sensitivity of growing season vegetation production to soil moisture where the relationship was significant (p-value < 0.05). Climate data summarized by water year.

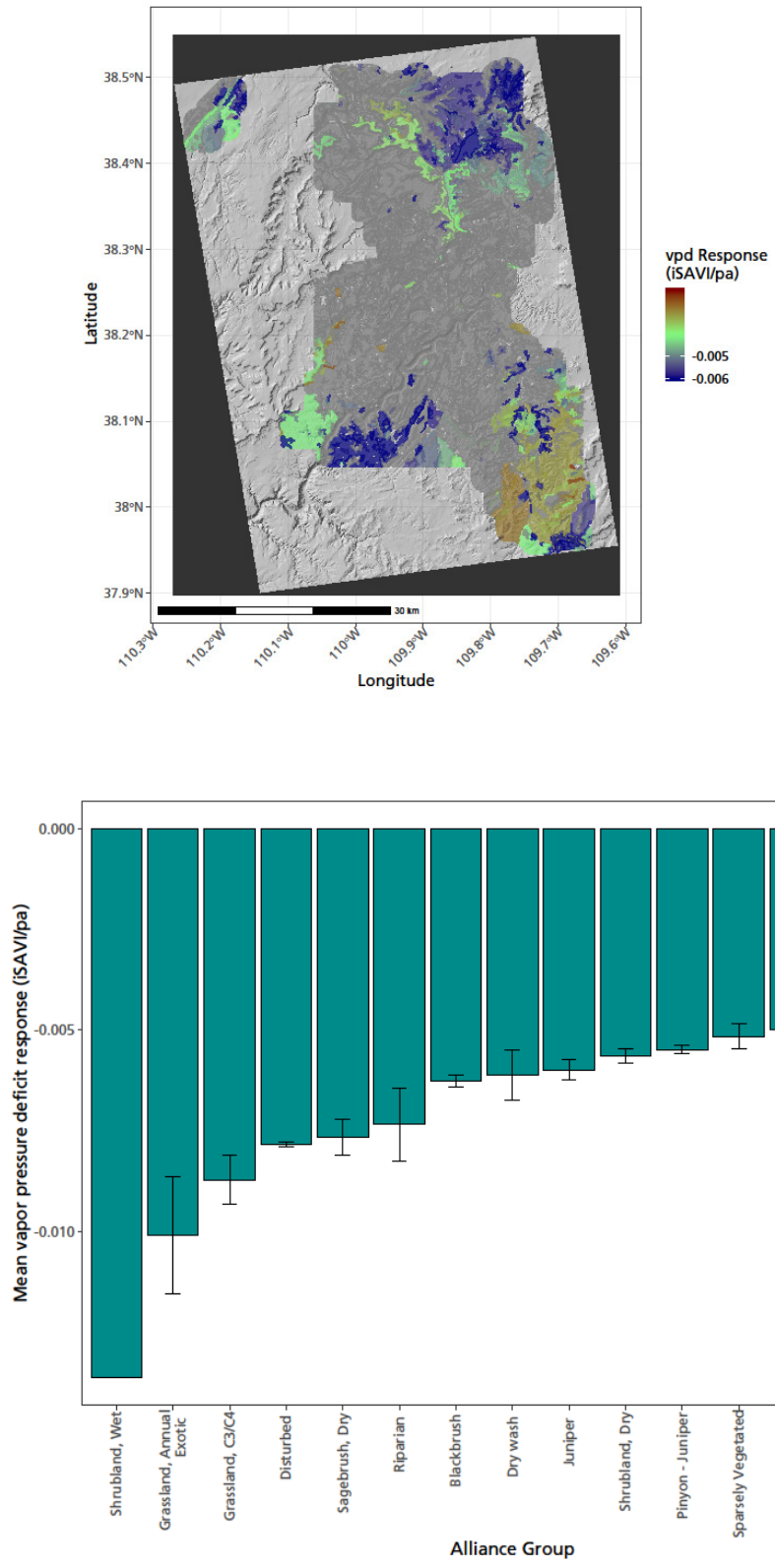

Figure A-3j. Sensitivity of growing season vegetation production to soil moisture where the relationship was significant (p-value < 0.05). Climate data summarized by water year.

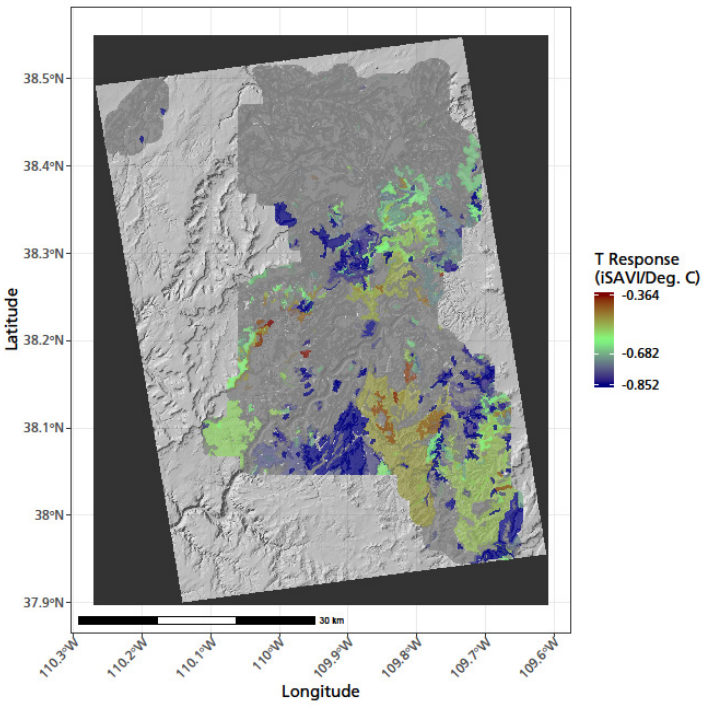

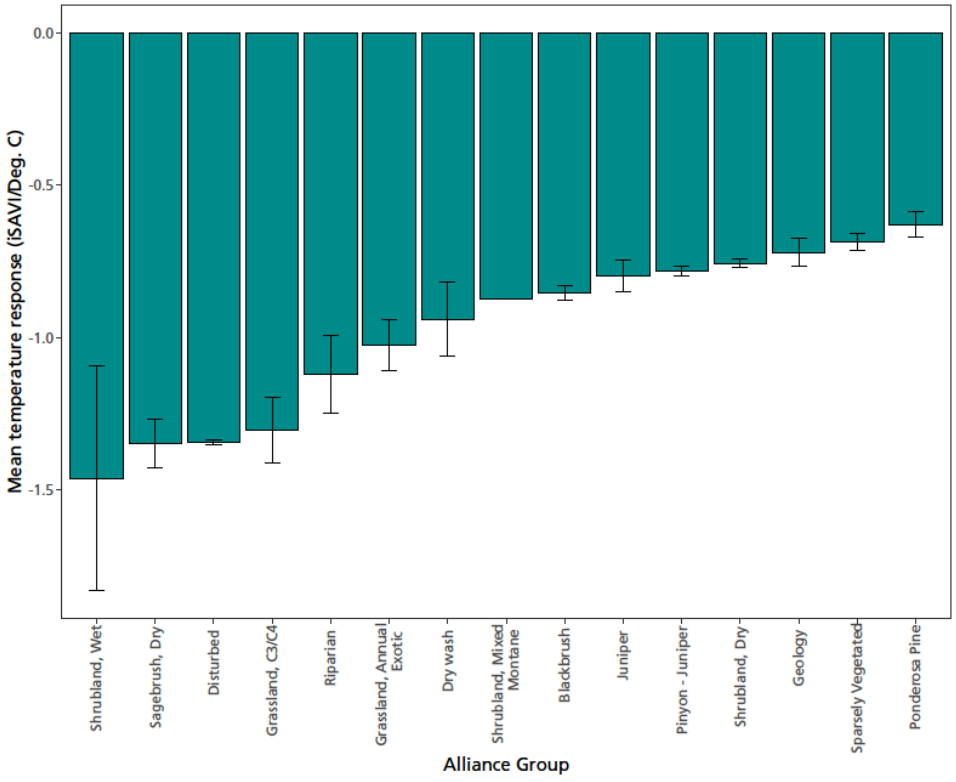

Figure A-3k. Sensitivity of growing season vegetation production to soil moisture where the relationship was significant (p-value < 0.05). Climate data summarized by water year.

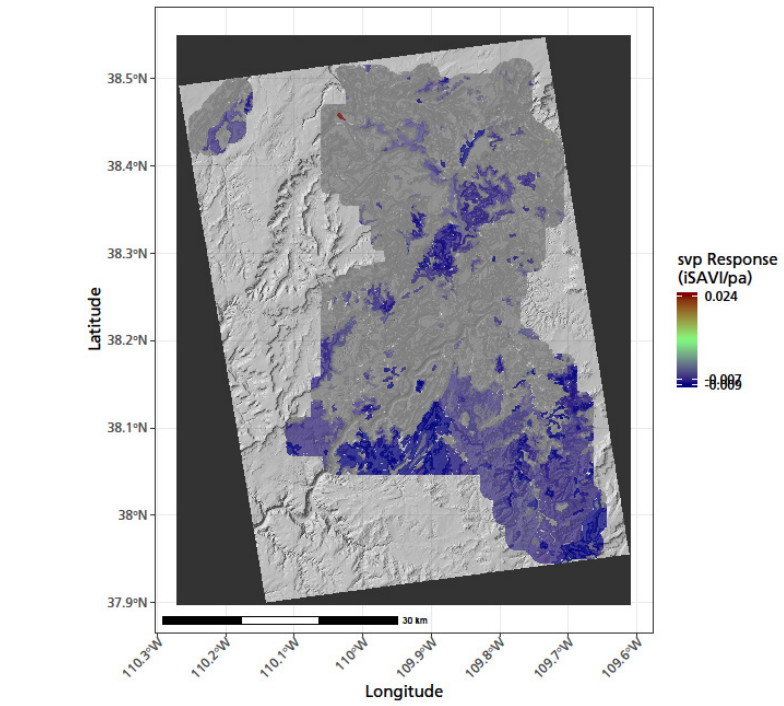

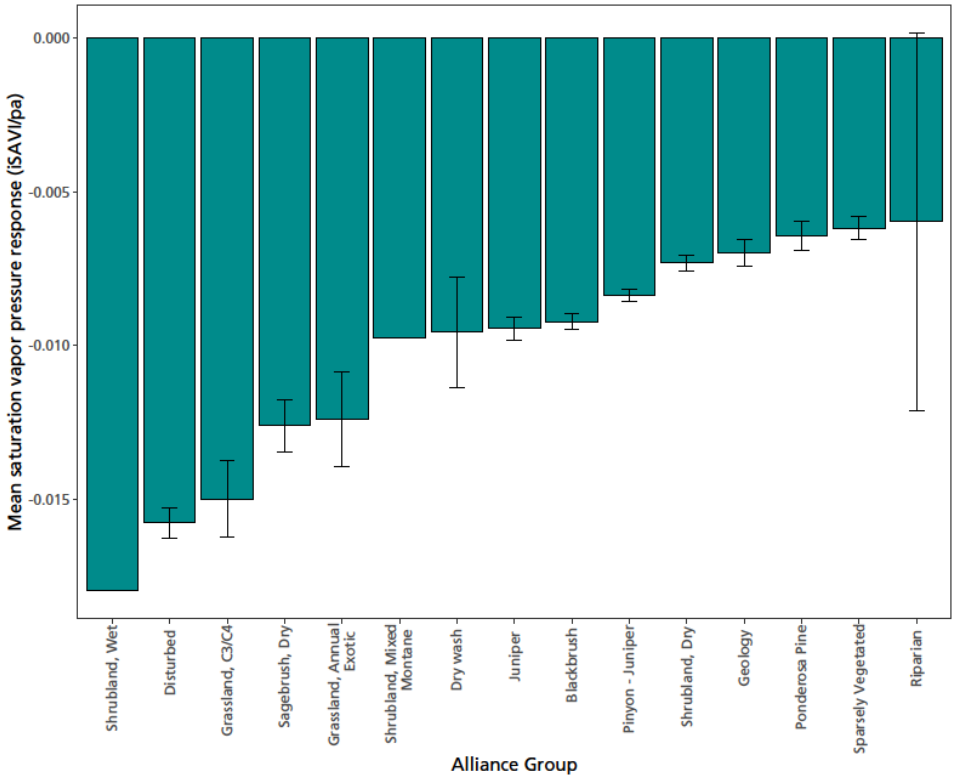

Figure A-3l. Sensitivity of growing season vegetation production to soil moisture where the relationship was significant (p-value < 0.05). Climate data summarized by water year.

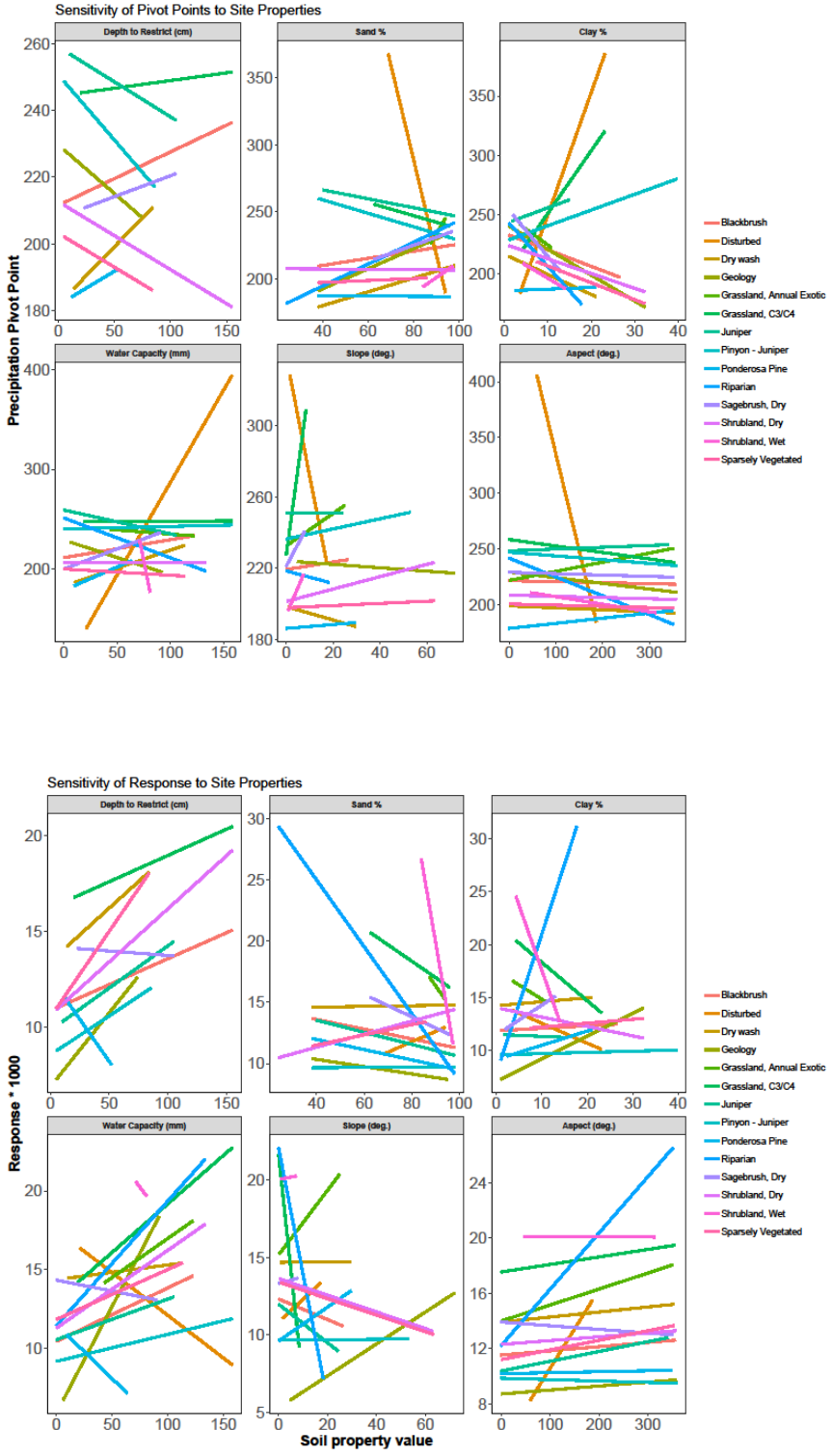

Figure A-4. Variation in (a) precipitation pivot points and (b) responses to precipitation as related to soil and site characteristics. Steeper slopes indicate greater sensitivity of either pivot points or responses to site properties. These site properties are important modifiers of climate because they control water retention and distribution in the soil profile and in the case of site slope and aspect because they affect the heat load on vegetation.

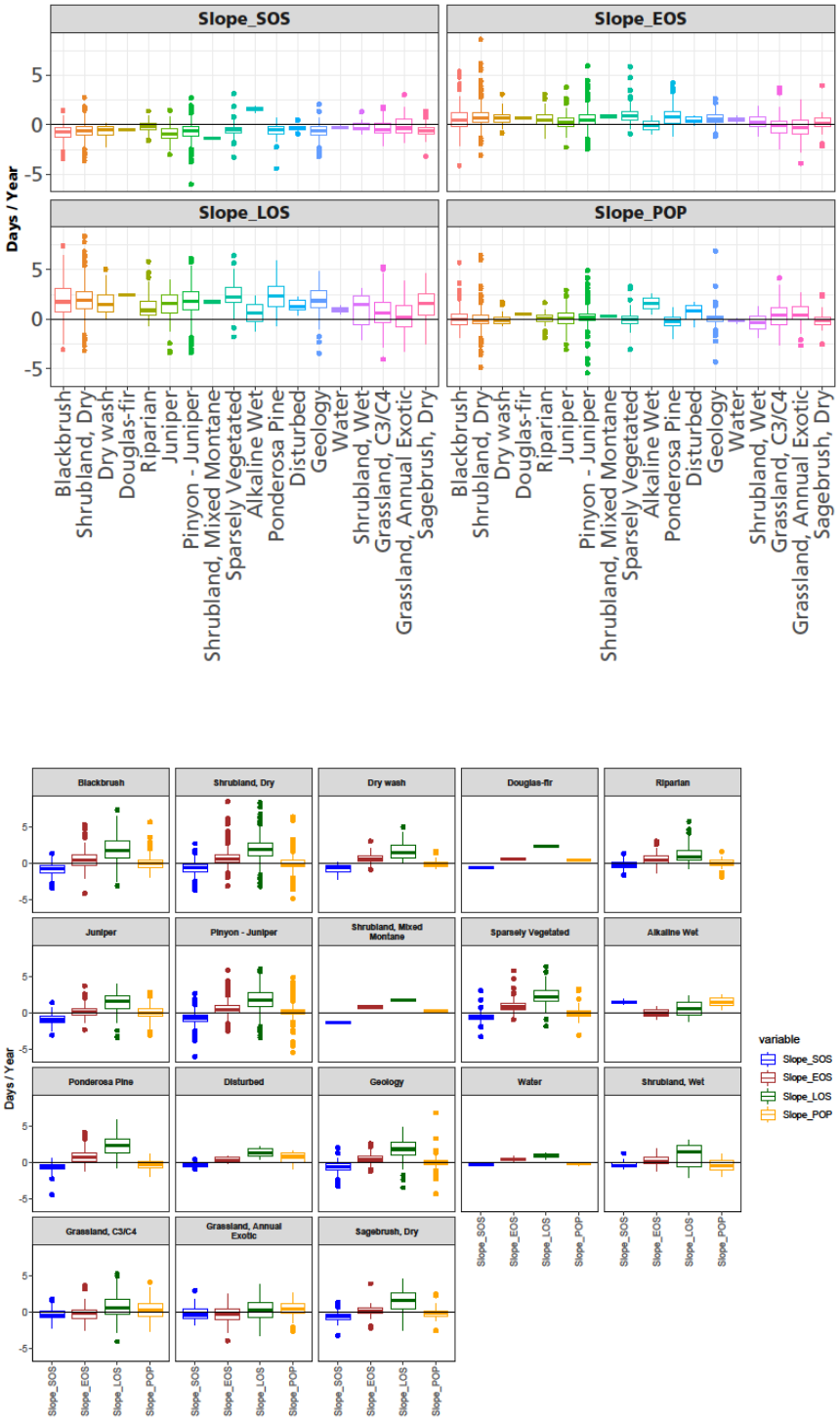

Figure A-5. (a) Direction and magnitude of change rate in land surface phenology metrics determined as +/-days per year for start of season (slope SOS), end of season (slope EOS), length of season (slope LOS) and timing of peak SAVI (slope POP). (b) rates of change in phenology metrics by alliance group. Slope refers to the slope of linear regression of phenology metric versus year for the period 2000–2019.

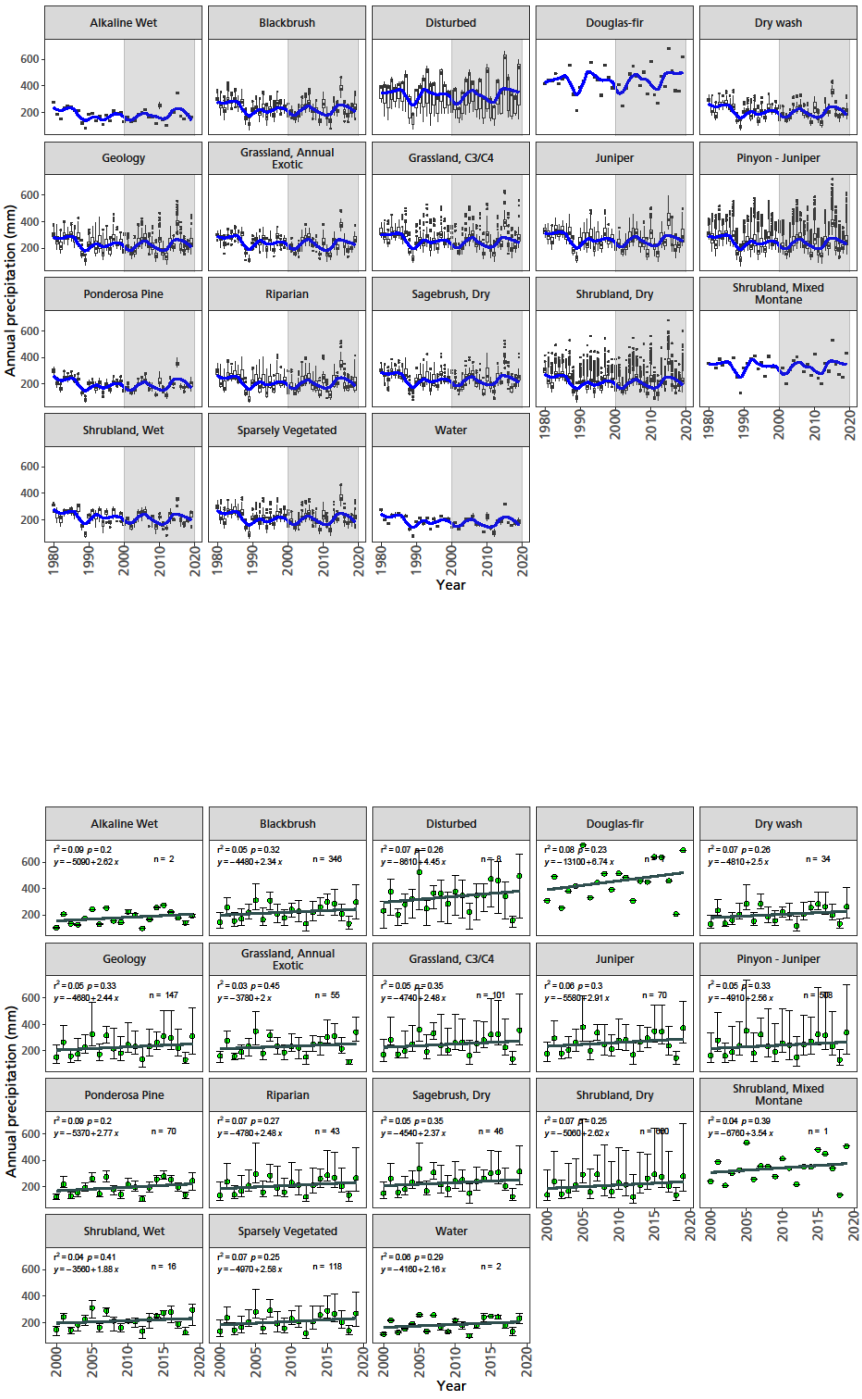

Figure A-6a. Cumulative annual water balance variables over time in vegetation alliance groups. Box plots demonstrate the range of variation within alliance groups by year. The blue line is a loess smooth with a 25 percent span to illustrate multi year patterns. Gray shaded area includes the period investigated for relationships between production and climate when satellite imagery and climate data were both available. In the lower panel, trend over time is shown for the period in gray in the top panel. Bars are standard error.

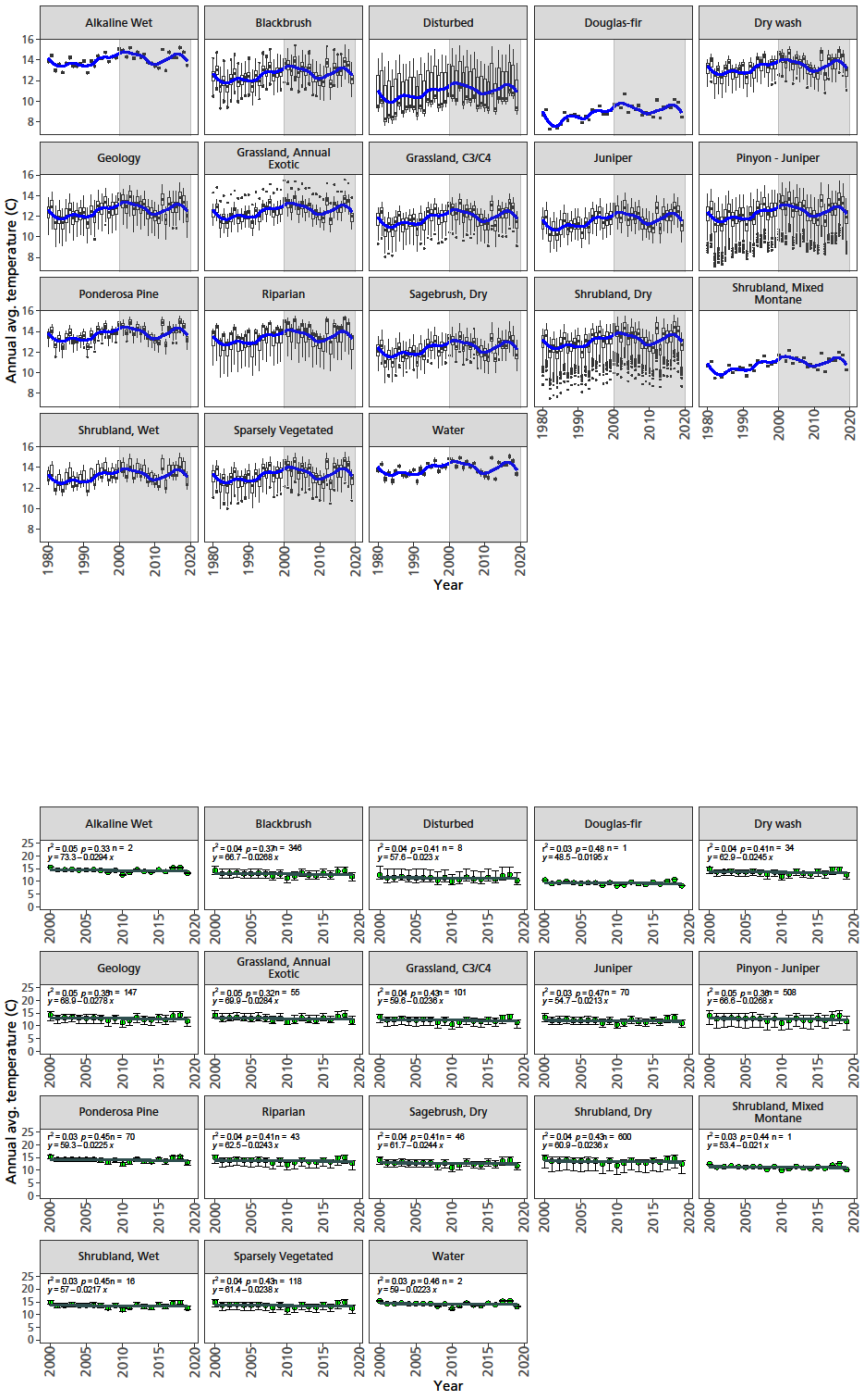

Figure A-6b. Cumulative annual water balance variables over time in vegetation alliance groups. Box plots demonstrate the range of variation within alliance groups by year. The blue line is a loess smooth with a 25 percent span to illustrate multi year patterns. Gray shaded area includes the period investigated for relationships between production and climate when satellite imagery and climate data were both available. In the lower panel, trend over time is shown for the period in gray in the top panel. Bars are standard error.

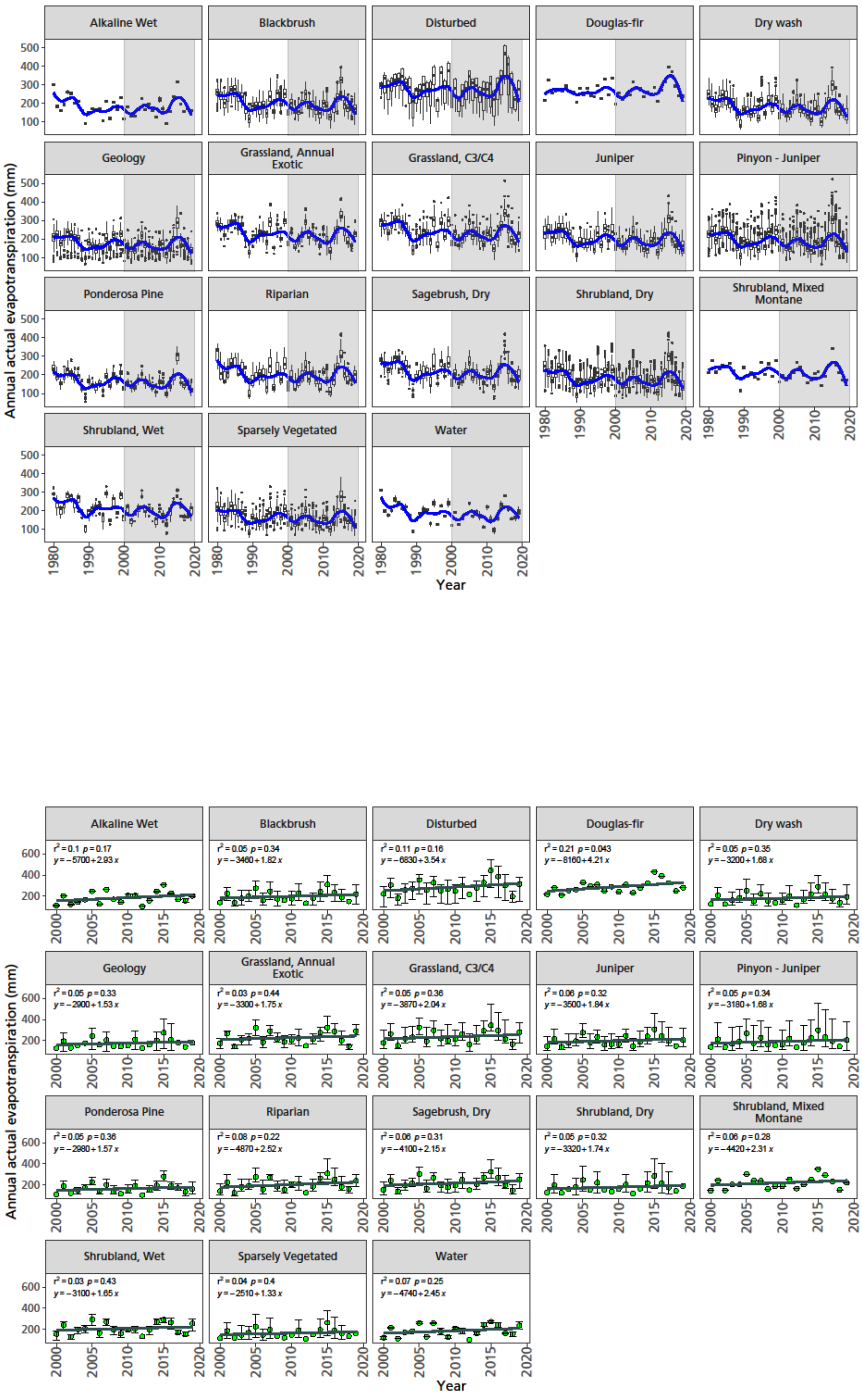

Figure A-6c. Cumulative annual water balance variables over time in vegetation alliance groups. Box plots demonstrate the range of variation within alliance groups by year. The blue line is a loess smooth with a 25 percent span to illustrate multi year patterns. Gray shaded area includes the period investigated for relationships between production and climate when satellite imagery and climate data were both available. In the lower panel, trend over time is shown for the period in gray in the top panel. Bars are standard error.

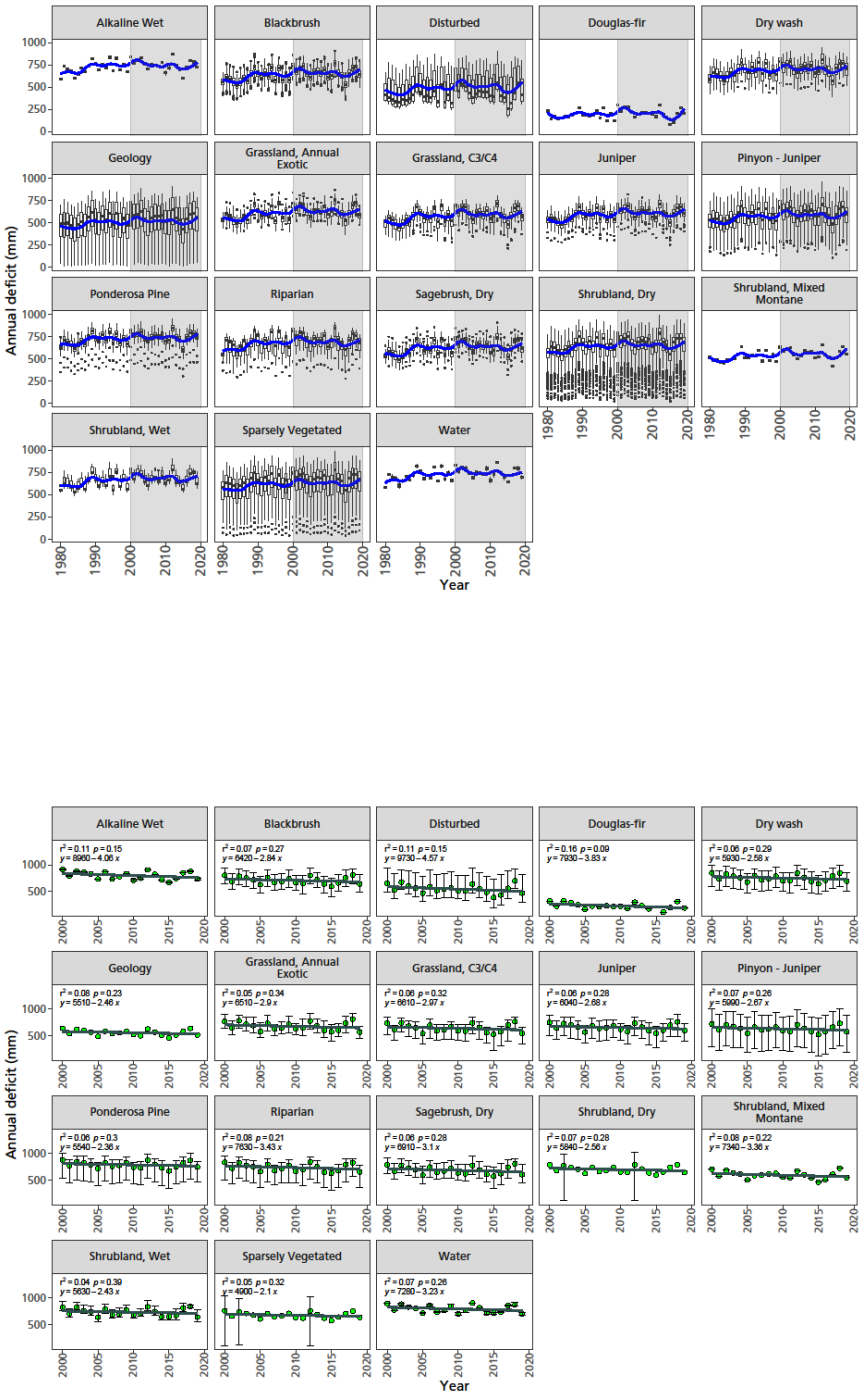

Figure A-6d. Cumulative annual water balance variables over time in vegetation alliance groups. Box plots demonstrate the range of variation within alliance groups by year. The blue line is a loess smooth with a 25 percent span to illustrate multi year patterns. Gray shaded area includes the period investigated for relationships between production and climate when satellite imagery and climate data were both available. In the lower panel, trend over time is shown for the period in gray in the top panel. Bars are standard error.

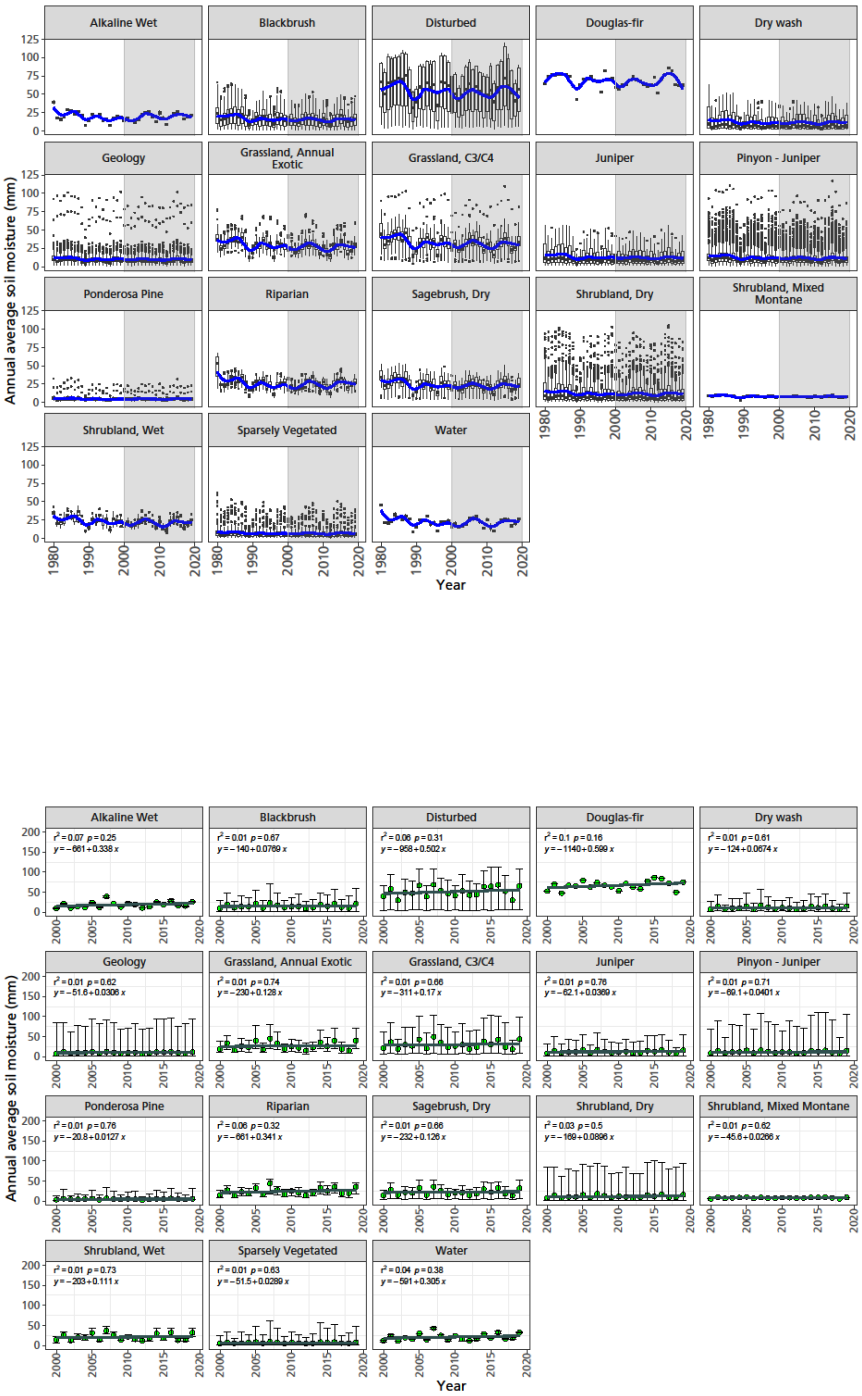

Figure A-6e. Cumulative annual water balance variables over time in vegetation alliance groups. Box plots demonstrate the range of variation within alliance groups by year. The blue line is a loess smooth with a 25 percent span to illustrate multi year patterns. Gray shaded area includes the period investigated for relationships between production and climate when satellite imagery and climate data were both available. In the lower panel, trend over time is shown for the period in gray in the top panel. Bars are standard error.

The Department of the Interior protects and manages the nation's natural resources and cultural heritage; provides scientific and other information about those resources; and honors its special responsibilities to American Indians, Alaska Natives, and affiliated Island Communities.

NPS 164/189628, June 2023

National Park Service
U.S. Department of the Interior

Natural Resource Stewardship and Science
1201 Oak Ridge Drive, Suite 150
Fort Collins, Colorado 80525